THE UNIVERSITY OF CHICAGO

MECHANISM OF ACTION OF A SIGNALING PROTEIN DOCK4 IN MYELODYSPLASTIC SYNDROMES

A DISSERTATION SUBMITTED TO

THE FACULTY OF THE DIVISION OF THE BIOLOGICAL SCIENCES

AND THE PRITZKER SCHOOL OF MEDICINE

IN CANDIDACY FOR THE DEGREE OF

DOCTOR OF PHILOSOPHY

COMMITTEE ON CANCER BIOLOGY

BY

SRIRAM SUNDARAVEL

CHICAGO, ILLINOIS

AUGUST 2019

DEDICATION

To my mentor and well-wisher, Dr. Amittha Wickrema for keeping faith in me, encouraging me and being a guiding light over the past eight years of my research career. My research career would not have been possible without Dr. Wickrema's never-ending, selfless, unconditional support for which I'll be thankful and grateful forever.

TABLE OF CONTENTS

List of Figures…….. x

List of Tables…… xiii

Acknowledgments……..… xiv

Abstract……..…… xvi

CHAPTER 1: BACKGROUND AND SIGNIFICANCE……. 1

a. HEMATOPOIESIS…….……. 2

b. CONTROL OF HEMATOPOIESIS AND LINEAGE COMMITMENT……..…….. 3

c. ERYTHROID DIFFERENTIATION…… 6

d. DEVELOPMENT OF AN *Ex Vivo* PRIMARY HUMAN ERYTHROID DIFFERENTIATION CELL MODEL……..…….. 8

e. MOLECULAR ABERRATIONS IN HEMATOPOIETIC STEM CELLS LEAD TO MALIGNANT DISORDERS…….....…. 10

f. MECHANISMS UNDERLYING MYELODYSPLASTIC SYNDROMES ARE POORLY UNDERSTOOD……..…… 12

g. IDENTIFICATION OF GENES/MECHANISMS MEDIATING PATHOGENESIS OF MYELODYSPLASTIC SYNDROMES.. 13

h. EXPRESSION OF DOCK4 IN HSCs AND TERMINAL STAGES OF ERYTHROID DIFFERENTIATION...……...…. 15

i. DEVELOPMENT OF METHODOLOGIES TO STUDY ERYTHROID DYSPLASIA……..……..…… 17

j. SIGNIFICANCE…….…….. 19

CHAPTER 2: REDUCED EXPRESSION OF *DOCK4* LEADS TO ERYTHROID DYSPLASIA IN MYELODYSPLASTIC SYNDROMES…… 21

a. GOALS..…….. 22

b. INTRODUCTION……..... 22

c. RESULTS……. 24

i. *DOCK4* expression is reduced in -7q MDS stem cells and is associated with adverse prognosis……..… 24

ii. *In vivo* suppression of DOCK4 in zebrafish embryos generates dysplastic erythroid cells……...……. 25

iii. DOCK4 knockdown in human erythroblasts results in disruption of the F-actin skeletal network…..... 29

iv. MDS erythroblasts exhibit disrupted F-actin skeleton... 32

v. Reduced expression of DOCK4 leads to reduction in RAC1 GTPase activity…… 36

vi. Increased phosphorylation of Adducin in DOCK4 deficient erythroid cells……..… 38

vii. Reduced terminal differentiation and abnormal erythroid morphology of DOCK4 deficient erythroid cells……. 39

viii. Reduced DOCK4 expression increases the membrane fragility of erythrocytes……..……. 44

d. CONCLUSION……. 45

CHAPTER 3: LOSS OF FUNCTION OF DOCK4 IN MYELODYSPLASTIC SYNDROMES STEM CELLS IS RESTORED BY INHIBITORS OF DOCK4 SIGNALING NETWORKS…….. 49

a. GOALS..…… 50

b. INTRODUCTION…….. 50

c. RESULTS…….. 52

i. Reduction of DOCK4 increases global tyrosine phosphorylation in HSCs……..…….. 52

ii. DOCK4 regulates the phosphorylation of kinases and phosphatases…… 54

iii. SHIP1 and SHP1 are substrates for LYN kinase…..…. 56

iv. LYN kinase activity is regulated as a result of its interaction with DOCK4……..……... . 60

v. Decreased DOCK4 expression leads to increased HSC migration…… 62

vi. Reduction of LYN, SHIP1 or SHP1 protein levels or their enzyme activity decreases HSC migration…..……..… 65

vii. Inhibitors of LYN, SHIP1 and SHP1 restore normal HSC migratory properties in DOCK4 deficient cells……..….. 67

viii. Inhibition of SHP1 promotes erythroid differentiation in -7/(del)7q MDS samples……..……..…. 68

ix. Increased HSPC mobilization into the peripheral circulation in -7/(del)7q MDS patients…… 72

d. CONCLUSION…….. 73

CHAPTER 4: MATERIALS AND METHODS……. 76

a. HEMATOPOIETIC STEM CELL CULTURE…… 77

b. ZEBRAFISH *dock4a* ANALYSIS……..... 79

c. O-DIANISIDINE STAINING..…… 80

d. HARVESTING CELLS FROM ZEBRAFISH EMBRYOS……... 80

e. siRNA AND LENTIVIRAL TRANSDUCTIONS..……. 81

f. IMMUNOFLUORESCENCE MICROSCOPY…….……. 82

g. FLOW CYTOMETRY……..……. 83

h. MULTISPECTRAL FLOW CYTOMETRY (IMAGESTREAMX^{TM} ANALYSIS)……..... 84

i. Actin disruption quantitation…… 84

ii. Quantifying circular/irregular shaped erythroid cells in zebrafish embryos…… 86

i. RAC1 G-LISA…….……... 87

j. RBC GHOST PREPARATION…….…….. 87

k. IMMUNOBLOT ANALYSIS……..... 87

l. FLUORESCENCE In-situ HYBRIDIZATION (FISH)..…..……... 89

m. QPCR…….. 89

n. RESTORATION OF DOCK4 EXPRESSION IN MDS PATIENT SAMPLES…….. 90

o. OSMOTIC FRAGILITY ASSAY…….. 91

p. NUCLEOFECTION OF CD34+ HSCs…….. 92

q. siRNA SEQUENCES……... 92

r. MASS SPECTROMETRY PHOSPHOPROTEOMICS…….. 93

s. PLASMID TRANSFECTION AND IMMUNOPRECIPITATION 94

t. LYN KINASE ACTIVITY ASSAY (ENDOGENOUS)……. 95

u. LYN KINASE ACTIVITY ASSAY (In vitro)…….…….. 95

v. In vitro BINDING ASSAY……..……..…. 96

w. In vitro KINASE ASSAYS……..…… 96

x. TRANSWELL MIGRATION ASSAYS……... 97

y. DAVID ANALYSIS……..... 98

z. METHYLCELLULOSE COLONY ASSAYS AND HEMOGLOBIN ELISA……..….. 98

aa. STATISTICAL ANALYSIS……... 98

CHAPTER 5: DISCUSSION AND PERSPECTIVES…… 100

a. DISCUSSION…….. 101

b. FUTURE DIRECTIONS…….. 107

i. Delineate the function of DOCK4 in HSC differentiation, localization and mobilization *in vivo*…….. 107

ii. Identify the molecular mechanisms by which DOCK4 regulates LYN/SHIP1/SHP1 signaling axis……..……. 108

iii. Determine the involvement SHP1 in the pathogenesis of anemia associated with DOCK4 reduced MDS…...…… 110

iv. Develop multispectral flow cytometry (ImageStreamX^{TM}) actin disruption assay as an early prediction/diagnostic tool for MDS…..…..…… 113

REFERENCES……..…. 115

LIST OF FIGURES

Figure 1.1	Human CD34+ HSC *ex vivo* erythroid differentiation model..	9
Figure 1.2	Mechanisms causing myelodysplastic syndromes (MDS).....	11
Figure 1.3	Schematic representation of DOCK4 protein with different conserved signaling domains……..…	16
Figure 1.4	Tracking terminal erythroid differentiation by Imagestream multispectral flow cytometry…….....	19
Figure 2.1	Reduced expression of DOCK4 in MDS correlates with anemia phenotype in patients….....	24
Figure 2.2	*In vivo* suppression of *dock4a* in a zebrafish model leads to dysplastic erythroid cells…….....	28
Figure 2.3	*DOCK4* knockdown in primary human erythroblasts disrupts F-actin skeleton..……..	31
Figure 2.4	Analysis strategy to quantify F-actin disruption by Multispectral flow cytometry (ImageStreamX^{TM})…….....	33
Figure 2.5	Quantitation of F-actin disruption in major MDS subtypes by Multispectral flow cytometry (ImageStreamX^{TM})…….…….	35
Figure 2.6	DOCK4 suppression leads to reduction in RAC1 GTPase activity and increased Adducin phosphorylation..…….....	37
Figure 2.7	Abnormal differentiation in DOCK4 deficient erythroid cells..	40
Figure 2.8	Correlation of the extent of erythroid terminal differentiation and the malignant cells in cultured primary MDS erythroblasts…	41

Figure 2.9 Re-expression of DOCK4 in DOCK4 deficient MDS patient samples……. 43
Figure 2.10 Reduced DOCK4 expression increases the membrane fragility of erythrocytes……..……..... 44
Figure 2.11 Schematic of the DOCK4 signaling pathway in erythroblasts. 46
Figure 3.1 Expression of DOCK4 and increased global phosphorylation of proteins in human primary hematopoietic stem cells with reduced DOCK4 levels……... 52
Figure 3.2 Reduced levels of DOCK4 leads to increased phosphorylation of LYN kinase and phosphatases SHIP1 and SHP1……. 55
Figure 3.3 Active LYN kinase phosphorylates SHIP1 (Y1021) and SHP1 (Y536)…….. 57
Figure 3.4 SHIP1 and SHP1 are substrates of LYN kinase in HSCs….. 59
Figure 3.5 LYN kinase and SHIP1 are components of DOCK4 signaling complex..... 61
Figure 3.6 Reduced levels of DOCK4 leads to increased cell migration and cell morphology in HSCs ……..…… 63
Figure 3.7 LYN kinase, phosphatases SHIP1 and SHP1 regulate HSC migration downstream of DOCK4……..……..… 66
Figure 3.8 Inhibition of LYN or SHP1 or SHIP1 activities reverse increased migration exhibited by DOCK4 deficient HSCs….. 68
Figure 3.9 Inhibition of SHP1 activity promotes erythroid differentiation In DOCK4 deficient MDS ……..…….. 70

Figure 3.10 Increased HSPC mobilization into the peripheral circulation in -7/(del)7q MDS patients…….…….. 72

Figure 3.11 Schematic of the DOCK4 signaling pathway in HSCs……... 74

Figure 5.1 DOCK4 is phosphorylated in hematopoietic cells…….. 109

Figure 5.2 SHP1 interacts with multiple proteins in HSCs……..…….. 112

LIST OF TABLES

Table 1.	MDS patient characteristics and summary of results..……	47
Table 2.	Differentially tyrosine phosphorylated proteins in cells with reduced DOCK4 levels ……..……	74
Table 3.	MDS patient characteristics……..……...……	75

ACKNOWLEDGEMENTS

My graduate school journey at The University of Chicago wouldn't have been possible without the support of several people. I like to begin by expressing my gratitude to my PhD advisor Dr. Amittha Wickrema for believing in me and providing me an opportunity to be a part of his research team. I strongly believe meeting Dr. Wickrema was the defining moment which enabled me to embark on an active research career. His patience, support and active mentoring have been a positive influence on my performance throughout my tenure in the Wickrema research laboratory. I wouldn't have been able to get this far without Dr. Wickrema's unconditional support.

I am extremely thankful to my thesis committee members Dr. Barbara Kee, Dr. Geoffrey Greene and Dr. Sandeep Gurbuxani for their scientific and professional mentoring throughout the course of graduate school. Their insightful comments during the thesis committee meetings and other times enabled me to stay focused and complete my PhD in time. In addition, I would like to extend my special thanks to Dr. Kay Macleod for providing me the opportunity to be a part of the Cancer biology PhD program and offering her support throughout.

I thank our close collaborator Dr. Amit Verma (Albert Einstein College of Medicine) for his extensive support with my graduate research and career development. Furthermore, I thank Dr. Todd Evans (Weill Cornell Medical College), Dr. Alan List (Moffitt Cancer Center), Dr. Michelle LeBeau, Dr. John Crispino (Northwestern University), Dr. Andrew Artz and Dr. Ulrich Steidl (Albert Einstein College of Medicine) for their valuable research and career support.

During the course of my tenure at the University of Chicago, I have collaborated with many colleagues for whom I have great regard, and I wish to extend my warmest thanks to all those who have helped me with my work. My research would not have been possible if not for the support of the Wickrema research and clinical cell therapy teams. Research team: Hui Liu, Wen Kuo, Jong Jeong and other past lab members. Clinical cell therapy team: Lauren Frehr, Guadalupe Martinez and others.

I thank my friends/classmates, Alex Ling, Anastasia Hains, Kyle Delaney, Logan Poole and Matthew Krause for their support. The social events organized by them helped overcome challenging and stressful times. I also thank my friend/mentor Payal Tiwari for her immense support throughout. In addition, I thank all the students of the CCB for all their support and making graduate school fun. I also thank Laura Negrete and other present and past cluster office members for their administrative support.

Next, I would like to thank my family who has supported me throughout my graduate career. Particularly, I would like to thank my fiancé Rashika Rangaraj for her continuous support and encouragement as I pursued my PhD.

Finally, I would like to acknowledge and thank all the funding sources which supported me to pursue my graduate education and conduct my research: International student fellowship (2015-2016), University of Chicago Comprehensive Cancer Center Women's Board Fellowship (2016-2017), Goldblatt research scholarship (2016-2017), NIH-NCI F99/K00 (CA223044) Pre-doctoral to Post-doctoral career transition award (2017-2023), Biological Sciences Division graduate fellowship (2017-2019), Biological Sciences Division travel award (2018) and Ben May department of cancer research Dr. Frank Fitch travel award (2018).

ABSTRACT

Refractory anemia and erythroid dysplasia remain as one of the common clinical presentations and predominant causes of morbidity in patients with the blood malignancy, myelodysplastic syndromes (MDS). Better understanding of mechanisms underlying ineffective erythropoiesis in MDS is critically needed to develop novel therapeutic strategies. Reduced levels of the adaptor protein Dedicator of Cytokinesis 4 (DOCK4) is frequently observed in MDS patients due to epigenetic silencing and/or chromosomal deletions and is associated with dismal prognosis. In this dissertation, I investigated the functional and signaling role of DOCK4 during red blood cell development from a hematopoietic stem cell (HSC). Firstly, my studies have determined that reduced levels of DOCK4 results in erythroid dysplasia. Furthermore, re-expression of DOCK4 in MDS patient samples lacking DOCK4, partially reversed the observed erythroid defects suggesting that re-activation of the DOCK4 pathway might be therapeutically beneficial in MDS patients harboring DOCK4 defects. Secondly, as a means to reactivate the DOCK4 pathway in MDS, I identified targetable signaling networks downstream of DOCK4 by performing unbiased phosphoproteomics using HSCs expressing reduced levels of DOCK4. Finally, I demonstrate avenues for restoring the DOCK4 functions by targeting signaling elements downstream of DOCK4. Specifically, pharmacological inhibition of one of the identified candidates; PTPN6, is capable of relieving the differentiation block along the erythroid lineage in MDS patients expressing reduced levels of DOCK4. In summary, my work has uncovered novel functions and signaling networks regulated by DOCK4 that can be targeted to reverse the aberrant phenotypes arising due to reduced expression of DOCK4 in hematopoietic

cells. Most importantly, my work has identified PTPN6 as a potential therapeutic target to alleviate anemia in MDS.

CHAPTER 1 - BACKGROUND AND SIGNIFICANCE

BACKGROUND AND SIGNIFICANCE

The hematopoietic system regulates critical functions in the body such as i) carrying oxygen and nutrients to various tissues, ii) clearance of metabolic wastes, iii) fighting foreign pathogens by providing immunity, iv) regulating body temperature and so on. Hematopoietic system is comprised of different types of blood cells broadly classified as erythroid (red), myeloid and lymphoid (white) cells. This chapter gives a brief overview about the various factors controlling the production of blood cells and their fate/characteristics under normal as well as malignant conditions.

1. a). Hematopoiesis

Hematopoiesis is defined as the process by which different types of blood cells are generated in the body. This is a very tightly regulated process which maintains a fine balance between the number of primitive pluripotent hematopoietic stem cells (HSCs) and mature differentiated cells (Orkin and Zon 2008; Wickrema and Kee 2009; Jagannathan-Bogdan and Zon 2013). HSCs are defined by their capacity to reconstitute the entire hematopoietic system in the recipient. These are rare cells which represent 0.01% of nucleated cells in the bone marrow (Challen et al. 2009). While the HSCs are long-lived (van Galen et al. 2014), the mature cells produced by them are relatively short lived and there is always a constant need to replenish the supply of hematopoietic cells. HSCs remain at the apex of the hematopoietic hierarchy which not only undergo self-renewal through symmetric divisions but also give rise to lineage committed

progenitor cells through asymmetric divisions. Lineage committed progenitors then proliferate and differentiate into mature erythroid, myeloid and lymphoid cells (Lodish et al. 2010). Hematopoiesis occurs in multiple waves during development in vertebrates and the initial wave of blood generation in the mammalian yolk sac is called as primitive hematopoiesis. The primary function of the primitive hematopoiesis is generation of red blood cells (RBCs) which facilitate tissue oxygenation to the rapidly growing embryo. The hallmark feature of the primitive erythroid cells is expression of embryonic globin (ε and γ globin) proteins (Orkin and Zon 2008). The primitive hematopoietic system is transient and rapidly replaced by adult-type hematopoiesis that is termed as definitive hematopoiesis. Definitive hematopoiesis in the embryo begins with the emergence of the first identifiable HSCs in the aorto-gonado-mesonephros (AGM) region. Subsequently, hematopoiesis shifts to the fetal liver, and thereafter to the bone marrow, where HSCs will reside throughout the life span of the mammalian organism (Ng and Alexander 2017). Within the bone marrow, the HSCs reside within specialized zones/microenvironment called stem cell niche which regulates self-renewal and differentiation (Morrison and Scadden 2014).

1. b). Control of hematopoiesis and lineage commitment

Research performed over the past two decades have demonstrated that the optimal maintenance of HSCs and production of different hematopoietic lineages is controlled by concerted regulation of several cell extrinsic and intrinsic factors such as cytokines/growth factors in the bone marrow microenvironment, signaling proteins and transcription factors (Zhu and Emerson 2002). Cytokines in the bone marrow are

predominantly secreted by various critical HSC niche component cells such as osteoblasts, vascular and stromal cells (Orkin and Zon 2008). Two such cytokine that are critical for HSC maintenance are thrombopoietin (TPO) and stem cell factor (SCF) which are secreted by osteoblasts and stromal cells respectively. Studies using prospectively isolated mouse HSC have shown that the cognate receptors for both TPO and SCF (c-Kit and c-Mpl) are expressed in high levels on HSCs, and genetic ablation of either TPO or c-Mpl leads to reduction of HSC. Consistent with this information, cytokines SCF and TPO support survival and proliferation of purified human and mouse HSCs under serum-free culture conditions. In addition to the classical hematopoietic cytokines, developmental signaling pathways such as Wnt signaling, notch signaling pathway, transforming growth factor β (TGFβ) and bone marrow morphogenetic protein (BMP) signaling have also been implicated in maintaining the quiescence of HSCs (Zhang and Lodish 2008; Seita and Weissman 2010).

Transcription factors (TFs) are critical cell intrinsic molecules which are essential for maintaining hematopoiesis. These TFs are comprised of virtually all classes of DNA-binding proteins, rather than belonging to a specific family. Growing body of literature has indicated that several TFs have been found to play critical roles in HSC physiology, including SCL (stem cell leukemia hematopoietic transcription factor), GATA-2 (GATA-binding factor 2), RUNX1 (Runt-related transcription factor 1) and LMO2 (LIM domain only 2), which are essential for primitive and definitive hematopoiesis. Genetic deletion of these TFs results in abrogation of blood cell development. While these TFs are absolutely critical for the survival and proliferation of HSCs, TFs such as HOXB4 (Homeobox protein B4), IKZF1 (Ikaros family zinc finger 1) and NOTCH1 (Notch

homolog1, translocation associated) are involved in HSC maintenance and self-renewal (Orkin and Zon 2008).

In order to generate mature blood cells with distinct functions, the HSCs undergo lineage commitment, a multistep process during which these cells become progressively more specified in their potential. Lineage commitment is a stepwise process which forms the basis of the hematopoietic hierarchy and establishes a paradigm for studying cellular development, differentiation, and malignancy. The concerted action of TFs and growth factors has been shown to control cell differentiation, and play instructive roles in lineage specification. Growth factors such as SCF, Fms-related tyrosine kinase-3 ligand (FLT3-L), thrombopoietin (TPO), interleukin-3 (IL3), interleukin-6 (IL-6), Granulocyte-colony stimulating factor (G-CSF), Granulocyte-macrophage colony stimulating factor (GM-CSF), erythropoietin (EPO) and TFs such as GATA-1, IKZF1, PU.1 (Transcription factor PU.1), C/EBPα (CCAAT/enhancer-binding protein alpha) promote the proliferation and differentiation of HSCs into myeloid and erythroid cells (Orkin and Zon 2008). The growth factors and cytokines exert their action on HSCs by binding to their cognate cell surface receptors and initiating downstream signaling cascades which activate the master lineage TFs eventually leading to lineage specific gene expression programs (Zon 2008). For example, EPO binds to erythropoietin receptor (EPOR) on the surface of hematopoietic stem/progenitor cells (HSPCs) and activates the EPO signaling pathway. This process activates the downstream Janus kinase 2 (JAK2) - Signal transducer and activator of transcription 5 (STAT5) pathway (Wickrema et al. 1999b) which eventually leads to the expression of erythroid specific transcription factors such as GATA-binding factor 1

(GATA1) and erythroid kruppel like factor 1 (EKLF1). Expression of GATA1 and EKLF1 gene expression programs promote the lineage commitment and differentiation of hematopoietic stem/progenitor cells (HSPCs) into the red blood cell (RBC) lineage (Yoshimura and Arai 1996; Kuhrt and Wojchowski 2015; Jeong et al. 2019).

1. c). Erythroid differentiation

RBCs are the most abundant cell type in the body with about 2 million RBCs entering the circulation from the bone marrow every second (Higgins 2015). They are characterized by the presence of hemoglobin, the oxygen carrying protein. RBCs have unique morphology; these are biconcave, disc shaped cells devoid of nucleus and have a life span of about 120 days in circulation. This unique structure enables these cells to access various parts of the body through tiny capillaries and venules. Research performed over the past two decades have indicated that erythropoiesis (generation of RBCs) occurs in two waves during development. The first wave is the primitive erythropoiesis which occurs in the yolk sac and the second wave is the definitive erythropoiesis which occurs in the bone marrow (Lodish et al. 2010). Definitive erythropoiesis is characterized by the suppression of embryonic globins and expression of adult globin (β-globin) genes. During definitive erythropoiesis in the bone marrow, the stem cells undergo several distinct stages prior to forming a mature RBC. The first stage is the blast forming unit – erythroid (BFU-E)/proerythroblast stage where the HSPCs commit into the erythroid lineage. The next stage is the proliferative stage where the committed cells go through a series of distinct sub-stages namely basophilic, polychromatic and orthochromatic stages. These stages are characterized by

progressive decrease in cell size, nuclear condensation and increase in hemoglobin expression. The third stage is the enucleation stage where the condensed nucleus and organelles are extruded from the cells to form a reticulocyte. The reticulocytes become a fully mature RBC in circulation (Lodish et al. 2010; Hattangadi et al. 2011; Dzierzak and Philipsen 2013).

Recent studies have highlighted the roles of several distinct molecular mechanisms which regulates erythropoiesis. In addition to signaling pathways regulating erythroid specific gene expressions, key mechanisms such as microRNAs (miR), long non-coding RNAs (lncRNA) and DNA epigenetic modifications have been identified as regulators of erythroid differentiation (Zhao et al. 2010; Zhang et al. 2012; Alvarez-Dominguez et al. 2014; Zhang and Hu 2016; Li et al. 2018). Particularly, our lab has recently described the stage specific roles of DNA epigenetic modifications, methyl cytosine (mC) and hydroxyl-methyl cytosine (hmC) in facilitating differentiation of erythroid cells from HSCs. DNA cytosine methylation and hydroxyl-methylation at gene promoters are associated with repressed and activated transcriptional states respectively. We have demonstrated that there is a decrease in global DNA cytosine methylation (DNA methylation) during erythropoiesis suggesting that downregulation of DNA methylation is critical for erythroid commitment and differentiation (Yu et al. 2013). On the other hand, DNA cytosine hydroxyl-methylation (DNA hydroxymethylation) is dynamic throughout erythropoiesis and is absolutely critical for commitment of HSCs into erythroid lineage (Madzo et al. 2014). In hematopoiesis/erythropoiesis, DNA methylation and hydroxymethylation is facilitated by enzymes DNMT3A (DNA methyltransferase 3 alpha) and TET2 (Ten eleven translocase 2) respectively.

1. d). Development of an *ex vivo* primary human erythroid differentiation cell model

Human erythropoiesis is a complex multistep process which involves the differentiation of lineage uncommitted HSC into enucleated RBCs. To study the impact of a gene in contributing to aberrant/dysplastic erythropoiesis, appropriate model systems are required. Previous studies have been performed using malignant and/or healthy hematopoietic cell lines; however, these cell lines do not robustly differentiate capturing all the distinct stages of erythroid differentiation. To overcome these caveats, the Wickrema lab has developed and used the primary human CD34+ hematopoietic stem cells (CD34+ HSCs) as a model system to study different aspects of erythroid differentiation over the past twenty five years (Wickrema et al. 1992; Wickrema et al. 1999b; Uddin et al. 2004; Yu et al. 2013; Madzo et al. 2014) (Figure 1.1).

This *ex vivo* model is unique because it is driven solely by physiological cytokines (EPO, SCF and IL3) and without added glucocorticoids faithfully recapitulates the normal human erythroid differentiation program in the bone marrow, yielding large number of reticulocytes. The use of human serum for differentiation facilitates synchronous differentiation and also mimics the process that occurs in the human bone marrow. This model also has a distinct advantage over murine models in that human differentiation occurs over a much longer period of time (14-18 days as opposed to 3 days in mice) giving us the opportunity to dissect specific cellular events without overlapping of multiple functions in a very short time span, which occurs in the case of mouse models.

In this model, the first erythroid lineage-committed cells (burst forming unit-erythroid; *BFU-E*) are observed by day 3 of culture of CD34+ HSPCs, and they continue to grow and reach proerythroblast/basophilic erythroblast stage by day 7. These basophilic erythroblasts continue to proliferate and by day 10 reach the orthochromatic stage of maturation. From the time of lineage commitment until very late stages of differentiation, the cells continue to transcribe globin genes and other erythroid-specific genes that ultimately characterize cells of red blood cell origin. In addition, these primary human cells are capable of extruding their nuclei during the terminal phase of differentiation to give rise to reticulocytes (40-50% of cells enucleate).

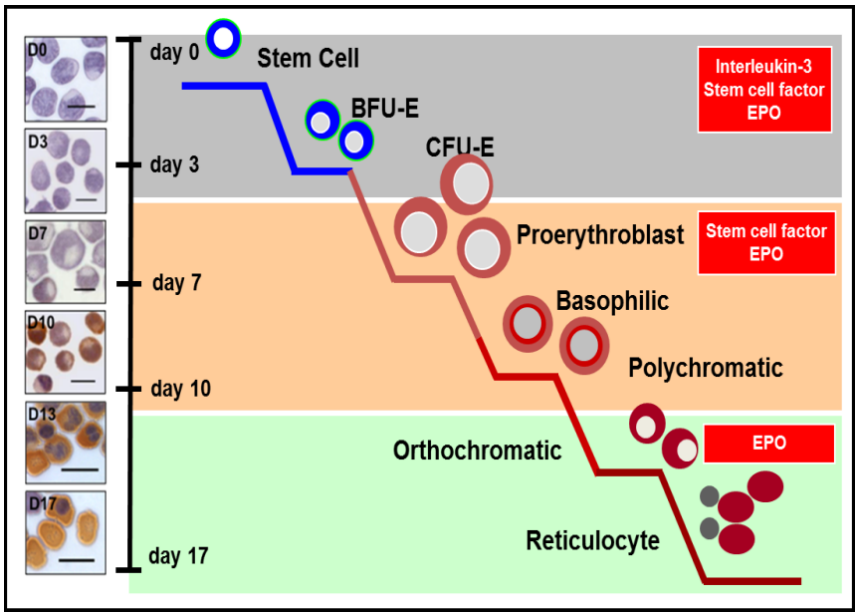

Figure 1.1: Human CD34+ HSC *ex vivo* erythroid differentiation model. HSCs are cultured under a defined cytokine regimen for 17 days to promote differentiation along the erythroid lineage (adapted from (Wickrema and Crispino 2007)). Cytospin images of cells during different stages of erythroid differentiation are depicted.

We have previously published utilizing this model to elucidate specific roles of DNA methylation and hydroxymethylation during normal erythropoiesis. Apart from

studying molecular events regulating erythropoiesis, I have also used the CD34+ HSCs to study various aspects of stem cell biology under stem cell expansion conditions as well as used HSCs to differentiate into myeloid and megakaryocyte lineages (Yu et al. 2013; Madzo et al. 2014). Taken together this amenable *ex vivo* model will provide a unique opportunity to study the functional and mechanistic aspects of any gene in normal and malignant hematopoiesis in a context/stage specific manner.

1. e). Molecular aberrations in hematopoietic stem cells lead to malignant disorders

In pre-leukemic conditions like myelodysplastic syndromes (MDS), the tight control of hematopoiesis is lost and results in aberrant hematopoiesis which is the key feature of these pathogenic conditions. MDS are a group of heterogeneous, clonal hematopoietic disorders originating from the hematopoietic stem cells and are characterized by cytopenias caused by ineffective hematopoiesis (Heaney and Golde 1999). MDS have been categorized into different subtypes by the World Health Organization (WHO) each of which has different characteristics of the disease and mechanisms by which it contributes to the disease pathogenesis. Even though about a third of MDS patients progress to acute myeloid leukemia (AML), majority of the MDS patients experience morbidity due to low red blood counts and peripheral cytopenias (Bejar et al. 2011a). Furthermore, the blood cells produced in these patients often harbor abnormal morphologies (dysplasia) and are unable to function properly. Even though MDS patients can exhibit dysplasia in multiple lineages, dysplasia in the erythroid cells is predominant.

Over the past decade scientists have studied and mapped out different mechanisms by which MDS are caused. The results of these studies identify a variety of cell intrinsic mechanisms such as chromosomal aberrations, somatic mutations or epigenetic deregulations and cell extrinsic mechanisms such as changes in bone marrow microenvironment as the underlying causes of MDS etiology (Figure 1.2).

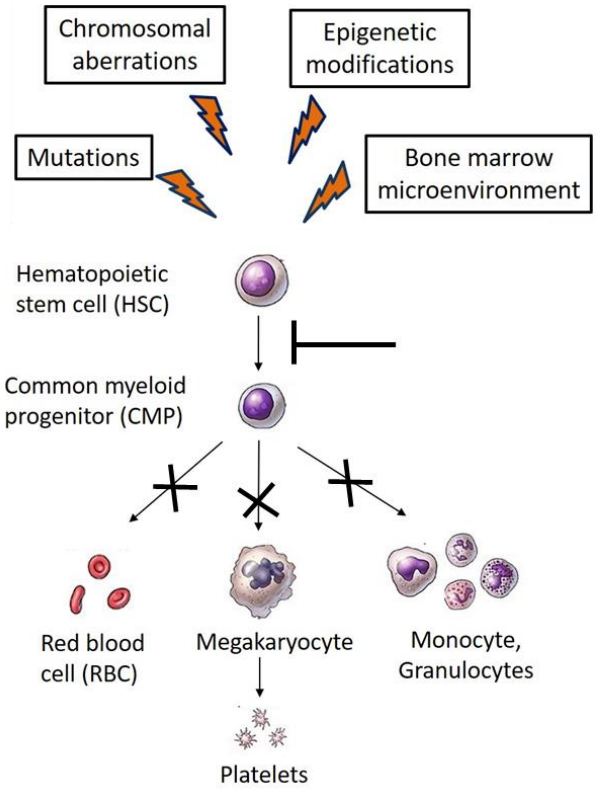

Figure 1.2: Mechanisms causing myelodysplastic syndromes (MDS). Schematic diagram depicting different mechanisms involved in pathogenesis of MDS leading to differentiation block along the myeloid lineage.

Clonal heterogeneity has been the greatest hindrance in treating MDS. Drugs such as lenalidomide and hypomethylating agents (Decitabine and Azacytidine) are used generally in the treatment of MDS but their effects are generally modest and do not result in complete cure. HSC transplantation remains the best treatment for these

patients; however, complications such as graft versus host disease or patient ineligibility due to old age (median age at MDS diagnosis is 71), limits the application of this treatment modality (Bejar et al. 2012). Therefore, there is a dire need to study the molecular mechanisms of myelodysplasia so that it may facilitate development of novel therapies for these patients.

1. f). Mechanisms underlying myelodysplastic syndromes are poorly understood

There are more than 200 chromosomal translocations and mutations reported in MDS although there are few commonly occurring translocations and mutations (Sekeres and Gerds 2014). With the advances in genomic efforts, recent studies have identified about 50 genes that are recurrently mutated in MDS. Even though the numbers of genes recurrently mutated is large, functionally these genes can be categorized as splicing factors, epigenetic regulators, transcription factors, signaling proteins, cohesins and DNA repair (Kennedy and Ebert 2017). For example, mutations in DNA hmC regulator TET2 is observed in 20% of MDS patients and DNA mC regulator DNMT3A is observed in about 12% of MDS patients. Mutations in these genes result in aberrant DNA epigenetic profiles in MDS which eventually results in altered gene expression programs. Similarly, mutations in splicing factor SF3B1 are observed in about 28% of MDS patients which are associated with the formation of ring sideroblasts (Bejar and Steensma 2014).

In addition to gene mutations, chromosomal abnormalities are also frequently observed in MDS. Some of the recurrent ones are chromosome 5q deletions (-5q, 15% of MDS), chromosome 7/7q deletions (-7/(del)7q, 11% of MDS), trisomy 8 (+8, 8% of MDS) and others (Garcia-Manero). These chromosomal aberrations are observed not

only as isolated events but also in combination with other chromosomal aberration and/or gene mutations. The identified gene mutations and chromosomal abnormalities serve as prognostic/predictive biomarkers of response to therapy. For example, MDS patients with mutations in TET2 or SF3B1 have better prognosis whereas patients with mutations in TP53, ASXL1, SRSF2, ETV6, RUNX1 and EZH2 mutations have poor prognosis (Kennedy and Ebert 2017). Similarly, patients with chromosome 5q deletions have good prognosis but patients with chromosome 7 deletions tend to have a worse clinical outcome. Mechanistic studies to uncover the MDS driver mechanisms and functions of the recurrently mutated/deleted genes under normal hematopoiesis are critically needed.

1. g). Identification of genes/mechanisms mediating pathogenesis of myelodysplastic syndromes

Following the identification of recurrent molecular aberrations in MDS, recent research efforts have focused on identifying the molecular mechanisms by which these aberrations promote MDS development. For example, genetic loss of *Tet2* in mouse models led to increased self-renewal of stem cells and myeloproliferation similar to what is observed in human MDS. Tet2 is a α-ketoglutarate- and Fe^{2+}-dependent dioxygenase (α-KGDDs) which catalyze the conversion of mC to hmC on DNA (Moran-Crusio et al. 2011) and loss of Tet2 results in DNA hypermethylation due to failure in hydroxymethylation of DNA. Recent work has shown that restoration of Tet2 function genetically or pharmacologically through administration of Vitamin C (a co-factor for α-KGDDs) can reverse aberrant self-renewal of stem cells (Cimmino et al.

2017). In a similar fashion, mechanistic studies performed on other recurrently mutated genes (DNMT3A, ASXL1, SF3B1 and RUNX1) in MDS have led to a better understanding of the disease pathogenesis (Challen et al. 2012; Ichikawa et al. 2013; Obeng et al. 2016; Nagase et al. 2018).

While investigating the mechanisms underlying recurrently mutated genes has been relatively straight-forward, the identification of pathogenic genes in chromosomal abnormalities has been challenging. This is due to the fact that these deletions are usually large and contain a large number of genes. In a breakthrough for the field, an elegant study recently identified *RPS14* as a candidate pathogenic gene in the commonly deleted region (CDR) of chromosome 5q. The 5q CDR contains 40 genes and in this study, the authors performed a short hairpin RNA (shRNA) screen targeting each of the 40 genes. Reduction of RPS14 to 50% levels (mimicking haploinsufficiency observed in MDS patients) in cord blood CD34+ HSPCs phenocopied the erythroid defects observed in 5q MDS and re-expression of RPS14 in 5q MDS patient HSPCs rescued the observed erythroid defects (Ebert et al. 2008). Following this, several groups reported other candidate driver genes on 5q namely CSNK1A1, CDC25C, TIFAB and others (McNerney et al. 2017).

Similar to 5q deletions, about 10-15% of MDS patients harbor deletions of entire or parts of chromosome 7. These deletions are extremely large in comparison with 5q and are associated with poor prognosis. The precise mechanisms by why -7/(del)7q contribute to MDS pathogenesis is poorly understood (Inaba et al. 2018). To identify potential mechanisms, the search for the pathogenic genes in the CDR of chromosome 7 has been ongoing for many decades. In 2011, our group reported dedicator of

cytokinesis 4 (*DOCK4*) as a candidate pathogenic gene on chromosome 7 (Zhou et al. 2011b). Following our initial report, several groups reported other candidate driver genes on chromosome 7 such as *CUX1*, *MLL3*, *EZH2*, *SAMD9*, *SAMD9L*, *HIPK2*, *ATP6V0E2* and *LUC7L2* (McNerney et al. 2013; Chen et al. 2014; Kotini et al. 2015; McNerney et al. 2017).

1. h). Expression of *DOCK4* in HSCs and terminal stages of erythroid differentiation

DOCK4 belongs to a large family (CED5/DOCK180/MYOBLAST CITY class) of unconventional guanidine exchange factors (GEFs) that is well conserved in mammals (Hasegawa et al. 1996; Wu and Horvitz 1998; Nolan et al. 1998). DOCK4 is one of the members of the eleven DOCK super family proteins. Based on the sequence homology, the DOCK4 proteins are divided into four sub families and DOCK4 belong to the DOCK-B sub family. DOCK4 is a large protein of ~225 kilo Daltons (KDa) with several signaling/protein-protein interaction domains such as Src-homology 3 (SH3), DOCK homology region 1 (DHR1), DOCK homology region 2 (DHR2) and proline rich (Pro-rich) domains (Laurin and Côté 2014) (Figure 1.3). DOCK4 acts as signaling intermediate and provide docking sites for many other signaling molecules. One of the well-described functions of DOCK4 is its ability to activate GTPases, such as ras-related C3 botulinum toxin substrate 1 (RAC1) and Ras related protein 1(RAP1), in many cell types. The DHR2 domain is responsible for the GEF activity which facilitates the exchange of the GTP in small GTPases such as RAC1 and RAP1 through direct interaction (Côté and Vuori 2002; Yajnik et al. 2003). Even though GEF activation is a

classical function of DOCK4, recent studies have identified GEF-independent functions of DOCK4. For example, DOCK4 has been shown to regulate Wnt signaling by interacting with APC, Axin, GSK3β (Upadhyay et al. 2008) and receptor tyrosine kinase signaling by interacting with EGFR and PDGFR (Kawada et al. 2009; Erdem-Eraslan et al. 2015).

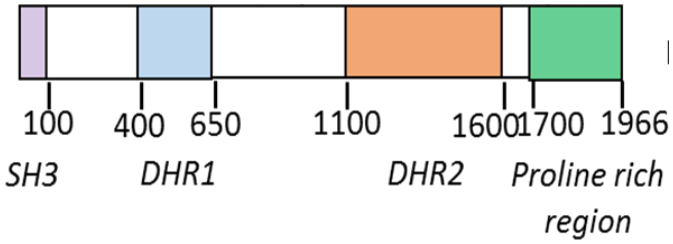

Figure 1.3: Schematic representation of DOCK4 protein with different conserved signaling domains.

DOCK4 functions across multiple tissue types in maintaining tissue homeostasis and recent studies have identified *DOCK4* as a tumor suppressor. DOCK4 mutations/deletions/amplification are detected in wide range of cancers such as lung, breast, brain and blood (Kjeldsen and Veigaard 2013; Yu et al. 2015; Abraham et al. 2015; Debruyne et al. 2018). *DOCK4* resides in chromosome 7 of humans which are commonly deleted in 10-15% of MDS patients. In addition to deletions, DOCK4 is also targeted by mutations and/or hyper-methylation in MDS (Zhou et al. 2011b). Even though it has been established that DOCK4 is targeted in malignant hematologic disorders, the specific functions of DOCK4 within the hematopoietic compartment are unknown. In hematopoietic system, *DOCK4* expression is dynamic during the differentiation of HSCs into erythroid lineage. High expression of DOCK4 detected during early stem cell stage and terminal stages of erythroid maturation which suggests

the possibility of DOCK4 facilitating stage specific functions. This is a valid hypothesis because recent studies have highlighted DOCK4 to function both as a GEF as well as a signaling intermediate downstream of cell surface receptor tyrosine kinases. Therefore, to uncover the functions of DOCK4 during hematopoiesis, in this dissertation, I investigated the roles played by of *DOCK4* in normal differentiating erythroblasts, early stem/progenitor cells as well as in CD34+ clonal MDS cells isolated from patient blood and marrow samples. The focus of the work was identifying signaling networks regulated by DOCK4 and functional outcomes when these signaling pathways were disrupted due to reduced expression of DOCK4.

1. i). Development of methodologies to study erythroid dysplasia

Dysplastic morphologies of erythroid cells are hallmark features in MDS. Erythroid dysplasia is commonly diagnosed through bone marrow (BM) sections and peripheral blood (PB) smears from MDS patients (Zini 2017). The inter-observer agreement for specific subtypes such as ringed sideroblasts (marked by the presence of iron loaded mitochondria visualized by Prussian blue staining) is good and reproducible whereas inter-observer agreement for other forms of erythroid dysplasia is poor and inconsistent. In most cases this leads to bias in diagnosis of erythroid dysplasia (Della Porta et al. 2006).

Recent efforts have focused on developing methodologies to quantify erythroid dysplasia in an unbiased manner using flow cytometry approaches. This is achieved by analyzing the expression profiles of key erythroid differentiation markers such as CD71,

CD105, cytosolic H-ferritin (HF), L-ferritin (LF) and mitochondrial ferritin (MtF) in MDS diagnostic BM specimens. These studies have demonstrated that MDS patients with erythroid dysplasia expressed high levels of CD105, HF and low levels of CD71. MtF was specifically highly expressed in MDS with ringed sideroblasts compared to other MDS (Della Porta et al. 2006; Eidenschink Brodersen et al. 2015; Westers et al. 2017). While the flow cytometry approach is reproducible and reliable in 95% of the cases, this approach completely ignores the morphological features of the cells. An ideal methodology might be one in which expression levels of erythroid markers as well as morphological features of the cells can be analyzed simultaneously.

Multispectral flow cytometry (ImageStreamX) combines flow cytometry with immunofluorescent microscopy which enables the analysis of expression of specific proteins and spatial organization simultaneously (Zuba-Surma et al. 2007; Zuba-Surma and Ratajczak 2011). Imagestream enables analysis of cells which is not possible by standard histology or flow cytometry approaches alone. The ImageStreamX instrument comes with built-in software which enables the user to be creative and develop novel analysis strategies. We and others have used this technology to analyze terminal differentiation of erythroid cells (McGrath et al. 2008; Konstantinidis et al. 2012). Using the built-in delta centroid feature, I quantitated the percentage of enucleating cells during the late stages of the erythroid differentiation process (Figure 1.4A-C). In addition to analyzing enucleation, I also applied Imagestream technology to develop novel assays to quantitate dysplastic morphologies of erythroid cells such as cell shape changes and F-actin disruption in this study.

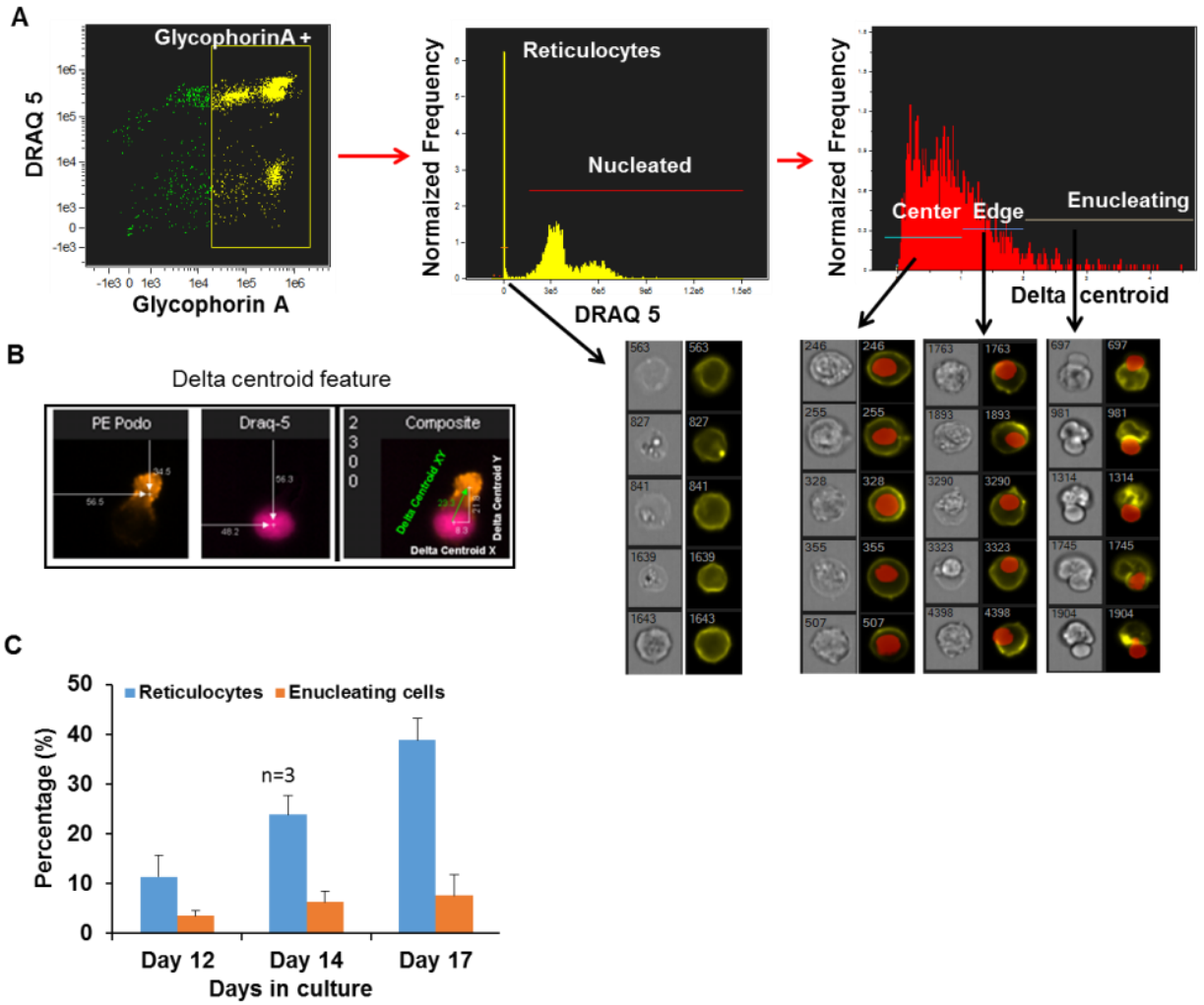

Figure 1.4. Tracking terminal erythroid differentiation by Imagestream multispectral flow cytometry. (A) Sequential analysis plots and representative images of different stages of erythroblasts enucleation. (B) Pictogram describing the delta centroid features built-in to the Imagestream analysis software (IDEAS). (C) Percentage of reticulocytes and enucleating cells at days 12, 14 and 17 during the erythroid differentiation as analyzed by Imagestream.

1. j). Significance

Myelodysplastic syndromes are the common causes of anemia in the elderly and are characterized ineffective hematopoiesis(Heaney and Golde 1999; Bejar et al. 2011a; Bejar et al. 2012). Drugs such as lenalidomide and hypomethylating agents are used generally in the treatment of MDS but most patients do not respond to the drug

and therefore there is an utmost need to develop new treatment strategies. The anemia in these patients is generally unresponsive to erythropoietin and MDS patients require frequent blood transfusions as supportive therapy. Overall survival of these patients is also impacted by excess iron deposits in liver and heart, leading to improper functioning, in addition to multiple other comorbidities (Malcovati et al. 2007). Although hematopoietic stem cell transplant is the best option available for these patients, majority of the patients are not eligible to receive a transplant due to factors such as advanced age and lack of matching donor cells. Even though a third of patients with MDS can transform to acute leukemias, a majority of patients experiences mortality due to complications of cytopenias. Since most of the morbidity experienced by such patients is due to low red blood counts, studies on the molecular pathogenesis of dysplastic erythropoiesis are critically needed. I have identified DOCK4 as a novel silenced gene in MDS and show that its downregulation leads to disruptions in erythropoiesis. Furthermore, in the same study, I also showed that reduced DOCK4 expression was an independent adverse prognostic factor (Zhou et al. 2011b). The studies performed in this thesis dissertation identify and establish the different components of the DOCK4 signaling pathway establishing the molecular imprint of DOCK4 signaling and interacting network. Identification of specific elements of the DOCK4 signaling cascade is of high clinical relevance, as it may lead to the ultimate development of potent and specific therapeutic approaches for the treatment of MDS, by targeting of distinct downstream effectors. In addition, my work will provide a roadmap for studying other genes that are often deleted or expressed in reduced amount due to epigenetic silencing in MDS and leukemia.

CHAPTER 2 - REDUCED EXPRESSION OF *DOCK4* LEADS TO ERYTHROID DYSPLASIA IN MYELODYSPLASTIC SYNDROMES

REDUCED EXPRESSION OF *DOCK4* LEADS TO ERYTHROID DYSPLASIA IN MYELODYSPLASTIC SYNDROMES

Majority of the sections of this chapter has been adapted from: Sundaravel S., Duggan R., Bhagat T., Ebenezer D. L., Liu H., Yu Y., Bartenstein M., Unnikrishnan M., Karmakar S., Liu T.-C., Torregroza I., Quenon T., Anastasi J., McGraw K. L., Pellagatti A., Boultwood J., Yajnik V., Artz A., Le Beau M. M., Steidl U., List A. F., Evans T., Verma A. and Wickrema A. 2015. Reduced DOCK4 expression leads to erythroid dysplasia in myelodysplastic syndromes. *Proceedings of the National Academy of Sciences of the United States of America*, 112(46), pp. E6359-68. doi:10.1073/pnas.1516394112.

2. a). Goals

The key goals of this chapter are to:

- Delineate the functional roles of DOCK4 during terminal stages of erythroid differentiation.
- Identify the molecular mechanisms involved in DOCK4 mediated signaling.
- Determine the involvement of DOCK4 in the pathogenesis of anemia associated with MDS.

2. b). Introduction

Anemia is the most common clinical manifestation in MDS and most of the morbidity experienced by MDS patients is due to low RBC counts. Dysplastic erythropoiesis in MDS leads to production of red cells that are deformed, macrocytic, and exhibit nuclear cytoplasmic dissociation thus suggesting defects during the terminal stages of erythropoiesis when the membrane skeleton and morphology are being established. This is further reinforced by the fact that membranes of MDS erythrocytes

are less deformable (Athanassiou et al. 1992). In a previous study (Zhou et al. 2011b), we had observed dedicator of cytokinesis 4 (*DOCK4*) as a gene which was deleted, mutated or epigenetically silenced in MDS. In addition, mutations or reduced expressed of *DOCK4* can lead to malignancies in prostate, breast, lung, brain and blood tissues as well as solid tumor metastasis (Kjeldsen and Veigaard 2013; Yu et al. 2015; Abraham et al. 2015; Debruyne et al. 2018)..

DOCK4 is a multi-domain protein and is a part of the DOCK superfamily of 11 unconventional GEFs, characterized by the presence of DHR1 and DHR2 (DOCK homology regions 1 and 2) domains. DOCK4 can activate the GTPases RAP1 and RAC1 (Yajnik et al. 2003; Hiramoto et al. 2006) and previous studies have indicated that these GTPases perform critical functions in regulating erythrocyte morphology, cell membrane integrity and differentiation (Kalfa et al. 2006). Based on this information, I hypothesized that DOCK4 is an important signaling protein that is instrumental in maintaining erythroblast membrane homeostasis and cell shape. Furthermore, I hypothesized that aberrant silencing of DOCK4 is responsible for ineffective erythropoiesis in MDS. In this study, I tested this hypothesis by determining the functional role of DOCK4 depletion in RBC formation by using a zebrafish model (Traver et al. 2003) and an *ex vivo* model of human erythropoiesis that recapitulates the erythroid differentiation program.

2. c). Results

i) *DOCK4* expression is reduced in -7q MDS stem cells and is associated with adverse prognosis

In order to determine whether DOCK4 is downregulated in MDS, I examined expression levels of *DOCK4* in a large gene expression dataset obtained from bone marrow CD34+ cells isolated from 183 MDS patients (Pellagatti et al. 2010). Analysis of *DOCK4* expression in the various subtypes of MDS found that *DOCK4* expression is significantly reduced in MDS CD34+ samples that had deletion of chromosome 7/7q or belonged to Refractory Anemia (RA) subtype when compared to healthy controls (Figure 2.1A).

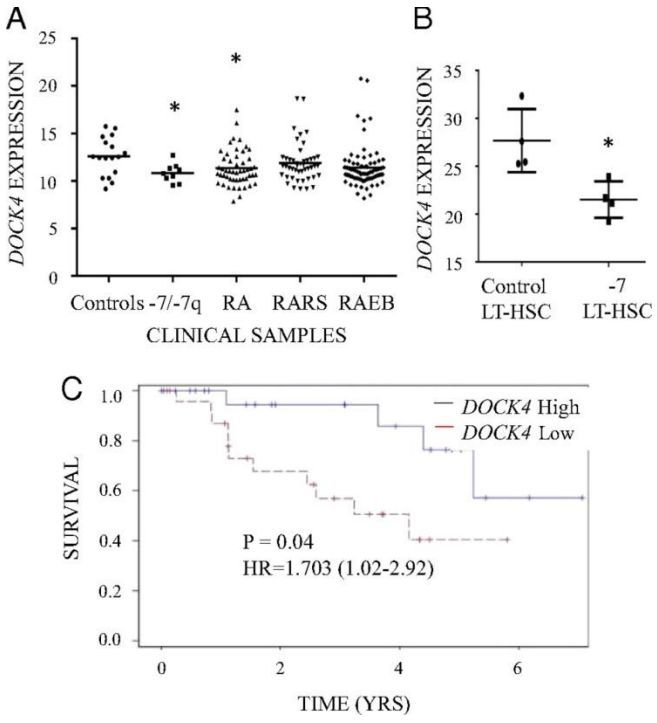

Figure 2.1. Reduced expression of DOCK4 in MDS correlates with anemia phenotype in patients (A) Expression of *DOCK4* is significantly reduced in -7/del(7q) MDS (n=9), Refractory Anemia (RA) (n=55) subtype of MDS. Gene expression profiles were generated from CD34+ cells from MDS patients and controls (n=17). Refractory anemia with excess of blasts (RAEB)

Figure 2.1, continued: Reduced expression of DOCK4 in MDS correlates with anemia phenotype in patients. (n=74) and Refractory anemia with ringed sideroblasts (RARS) (n=48) are other subtypes of MDS. (*, *P* value<0.05, Student's *T* test). (B) Comparison of gene expression data from sorted AML/MDS bone marrow samples (N=4) with -7 to healthy controls (N=4) revealed significantly decreased *DOCK4* expression in Long-Term Hematopoietic Stem Cells (LT-HSC), (P Value= 0.01). (C) Within the RA patients, lower expression of *DOCK4* is significantly associated with worse overall survival. (log Rank *P* value=0.045. Hazard ratio =3.744 (1.1- 12.2). (Low expression <Median, High > Median Expression).

Determination of *DOCK4* expression in an transcriptomic study (Will et al. 2012) from an independent set of purified primitive hematopoietic stem cells ($CD34^+$,$CD90^+$, Lin^-, $CD38^-$) also revealed significantly reduced levels in MDS/AML samples with deletion of chromosome 7 (Figure 2.1B). Furthermore, the patients with low expression of *DOCK4* within the refractory anemia (RA) subgroup of MDS had a significantly worse prognosis with hazard ratio=3.744 (1.1- 12.2) on univariate analysis (Log Rank P Value =0.02. On multivariate analysis after adjusting for clinically relevant prognostic factors (International prognostic scoring system, IPSS) (Bejar et al. 2011b) reduced expression of *DOCK4* was also determined to be an independent adverse prognostic factor (HR=1.703; (1.02-2.91); P value= 0.045) (Figure 2.1C). Since, RA patients present predominantly with anemia, this prompted us to examine the precise role played by *DOCK4* in the pathogenesis of reduced erythropoiesis in MDS.

ii) *In vivo* suppression of DOCK4 in zebrafish embryos generates dysplastic erythroid cells

To determine the impact of *DOCK4* knockdown *in vivo,* in collaboration with the Todd Evans laboratory, I depleted Dock4 protein during zebrafish embryogenesis.

Bioinformatic analysis indicated the presence of two duplicated orthologs of human *DOCK4* in the zebrafish genome. In collaboration with Evans laboratory, I used *in situ* hybridization to compare the expression patterns of the two zebrafish *dock4* genes. I found that *dock4a* maternal transcripts are present at the one-cell stage, and that the gene is widely expressed during gastrulation, decreased in levels during early somitogenesis, but then again widely expressed from 24-48 hours post fertilization (hpf, Figure 2.2A). Since *dock4a* appeared to encode the predominant embryonic isoform, in collaboration with Evans laboratory, I generated both translation-blocking (TB) and splice-blocking (SB) morpholinos (MOs) to target the depletion of Dock4a expression. Titration of the SB MO showed that 5ng was sufficient to deplete most of the normal message at 24 hpf (Figure 2.2B). Injection of 5-10ng of either the TB or SB MO generated embryos with similar morphant phenotypes at 48 hpf, with a predominant pericardial edema and a lack of blood circulation, with blood pooling on the yolk sac (Figure 2.2C). Expression of markers of early erythroid transcriptional regulator *gata1* appeared normal (Figure 2.2D).

Although erythropoiesis appeared to initiate normally, when *dock4a* morphants were stained with o-Dianisidine to visualize hemoglobin-staining cells, erythroid cells were missing from the circulation, and the morphants were relatively depleted of red cells in the yolk sac sinus compared to control injected embryos (Figure 2.2E). To better quantify erythropoiesis in the *dock4a* morphants, I utilized a transgenic *gata1: dsred* reporter strain in which red blood cells (RBCs) and erythroblasts express a red fluorescent protein (RFP) and can be quantified by flow cytometry. When Dock4a was depleted in this model using either SB or TB MOs, the resulting embryos had

approximately 28% fewer erythroblasts/erythrocytes compared to the controls (Figure 2.2F).

I next focused on examining the morphology of erythroid cells in zebrafish embryos that were injected with either *dock4a* or control MOs by two approaches. First, I examined the overall morphology of benzidine and hematoxylin positive cells to identify erythroid cells on cytospun slides. I observed that erythroid cells from zebrafish embryos injected with *dock4* MOs showed a large number of irregular shapes, whereas uninjected embryos or those that received control MOs contained mostly cells that were circular in shape (Figure 2.2G). I then developed a novel assay to distinguish cells with irregular shape from cells that were circular and to quantify the percentages of each population using multispectral flow cytometry (ImageStreamX^{TM}). In developing this assay, I first examined Gata1+ erythroid cells (RFP+) from zebrafish embryos injected with *dock4* MOs to capture cells with circular shape and irregular shape to identify the two different cell morphologies of interest (Figure 2.2H). Applying these data to the ImageStreamX algorithm for circularity, I was able to differentiate between circular and irregular shaped cells (described in detail in chapter 4) to segregate the RFP+ erythroid cell compartment systematically based on the circularity feature (Figure 2.2I). I utilized both bright-field and fluorescent channels, providing two independent measures of the circularity in our cell populations. The data from such an analysis showed increased numbers of irregular shaped cells in *dock4a* morphants samples (Figure 2.2I). I performed four independent experiments using zebrafish embryos depleted for Dock4a, along with three control replicates, and found that *dock4a* knockdown resulted in increased numbers of dysplastic erythroid cells in zebrafish embryos (Figure 2.2J).

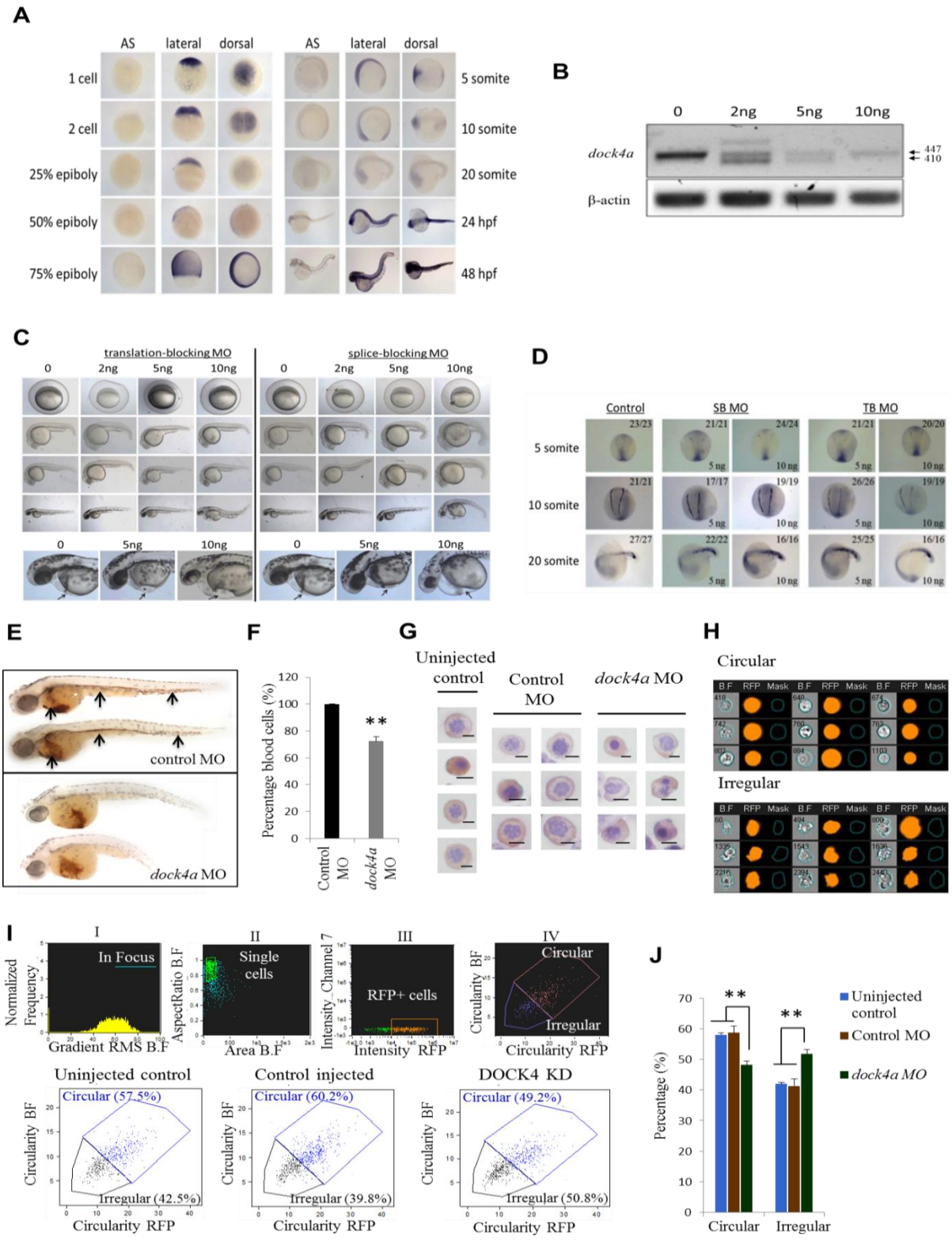

Figure 2.2. ***In vivo*** **suppression of** ***dock4a*** **in a zebrafish model leads to dysplastic erythroid cells**. (A) *Dock4a* gene expression was determined using *in situ* hybridization.

Figure 2.2, continued: *In vivo* suppression of *dock4a* in a zebrafish model leads to dysplastic erythroid cells. Wild-type zebrafish embryos were harvested and fixed at the stages indicated, from the 1-cell stage to 48 hpf. Embryos were hybridized to either a sense (control) probe or an antisense digoxygenin labeled RNA probe. Embryos were photographed with lateral or dorsal views as indicated (sense is a lateral view). (B) Embryos were injected at the 1 cell stage with 0, 2.5, 5 or 10 ng of the *dock4a* TB MO. Embryos were harvested at 24 hpf and RNA extracted. The *dock4a* transcript levels were assessed using semi-quantitative RT-PCR. The expected normal transcript is 447 nt, and the SB MO causes some accumulation of a mis-spliced 410 nt transcript. (C) Wild-type zebrafish embryos were injected at the one cell stage with 0, 2, 5, or 10 ng TB (left panels) or SB (right panels) morpholino. Shown are representative embryos (n>100). Panels below are higher magnification views demonstrating a pericardial edema and the location of blood pooling in the ventral part of the embryo (arrows). (D) Wild-type zebrafish embryos were injected with 0 (control), 5 ng, or 10 ng of the *dock4a* SB morpholino. The embryos were harvested and fixed in 4% PFA at the 5, 10, or 20 somite stage. *Gata1*transcript patterns were detected using an antisense digoxygenin labeled RNA probe, seen initially as two stripes in the lateral mesoderm, converging at the intermediate cell mass in the tail. (E) Shown are representative embryos following staining at 48 hpf with o-Dianisidine to detect hemoglobin (red stain). Embryos were injected with 5 ng of standard control MO (top panel). Arrows indicate blood circulation through the caudal hematopoietic tissue, cardinal vein, and heart with substantial staining in the sinus venosus on the yolk sac. Embryos were injected with 5 ng of the *dock4a* splice-blocking MO (lower panel) and at 48 hpf lack blood circulation and appear relatively pale with less blood in the yolk sac. For both panels n=30 embryos. (F) Relative percentages of erythroid cells in zebrafish embryos were determined by flow cytometry comparing *dock4a* knockdown with control samples (the later set to 100%). Use of *gata1:dsred* transgenic zebrafish embryos allowed direct assessment of erythroid cells in samples of dissociated whole embryos blood (n=4 independent experiments, at minimum 200 embryos per experiment). (G) Photomicrographs of benzidine and hematoxylin positive erythroid cells from cytospins prepared using cells from dissociated zebrafish embryos (Scale bar, 5μm). (H) Bright field and fluorescence images of RFP expressing erythroid cells depicting circular and irregular shaped morphology harvested from embryos with reduced expression of Dock4. (I) Quantitation of RFP positive embryonic zebrafish blood cells that are circular or irregular in shape based on analysis of bright field and RFP images using the ImageStreamX^{TM} instrument. (J) Percentages of circular and irregular shaped erythroid cells harvested from dissociated zebrafish embryos 48 hours post injection of dock4a SB MO or control MO or from uninjected embryos. (**, *P* value <0.005, Student's *t* test)

iii) DOCK4 knockdown in primary human erythroblasts results in disruption of the F-actin network

I next used an established *ex vivo* human HSPC culture system to determine the mechanism by which *DOCK4* depletion causes the generation of dysplastic erythrocytes

that are observed in MDS patient samples and in our *in vivo* zebrafish knockdown studies. The *ex vivo* human primary cell model uses cultured human CD34+ stem/early progenitors to promote lineage commitment and terminal differentiation into reticulocytes. The culture conditions are regulated by a strict cytokine feeding regimen at precise time intervals, allowing the cells to go through every major stage in the erythroid differentiation program yielding large numbers of hemoglobinized reticulocytes by day 17 (Figure 2.3A). These cells acquire glycophorin A and CD71, two key surface markers that are highly up-regulated as the cells reach the reticulocyte stage (Figure 2.3B). Using this dynamic model, I determined that *DOCK4* is expressed throughout the differentiation program and a gradual up-regulation occurs as the cells become terminally differentiated (Figure 2.3C).

In order to determine the functional significance of *DOCK4* during erythroid differentiation, I knocked down its expression using high-titer lentiviral particles (with GFP reporter) carrying shRNA against *DOCK4* and examined the cell morphology and levels of glycophorin A and CD71. These experiments revealed that knockdown of *DOCK4* resulted in large number of late-stage erythroblasts (day 15) with multinucleate morphology compared to the control mock transduced cells (Figure 2.3D). Furthermore, I performed flow cytometry analysis on day 10 of culture, which showed reduced levels of glycophorin A/CD71 expression in *DOCK4* depleted cells compared to mock transduced cells suggesting that DOCK4 is important in promoting terminal differentiation of erythroblasts (Figure 2.3E).

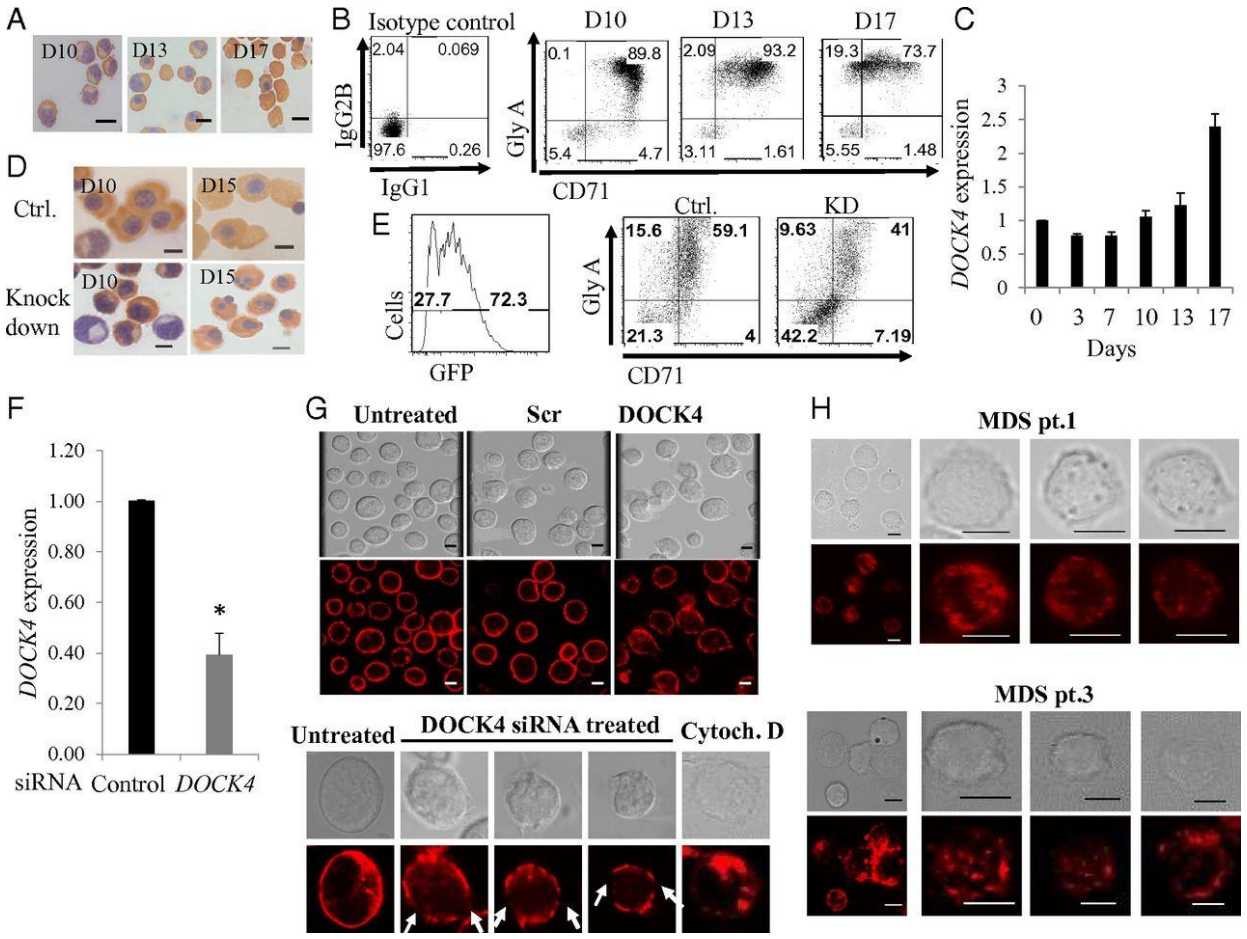

Figure 2.3. *DOCK4* knockdown in primary human erythroblasts disrupts F-actin skeleton. (A) Photomicrographs depicting differentiating human primary erythroblasts on various days stained with benzidine and hematoxylin. D3; day 3 committed erythroid progenitors. D7; day 7 basophilic erythroblasts. D10; day 10 polychromatic erythroblasts. D13; day 13 orthochromatic erythroblasts. D17; day 17 reticulocytes. (B) Flow cytometry analysis of differentiating human primary erythroid progenitors for transferrin receptor (CD71) and glycophorin A, showing gradual acquisition of surface markers that signify the erythroid program. (C) Quantitative RT-PCR (qRT-PCR) showing relative expression levels of *DOCK4* transcripts during pre-lineage commitment (day 0) and post committed terminal differentiation into reticulocytes (*, *P* value<0.05, Student's *T* test, n=3). (D) Photomicrographs of differentiating human erythroblasts on various days stained with benzidine and hematoxylin following DOCK4 knockdown with shRNA against DOCK4 depicting multinucleated cells. (E) Flow cytometry analysis depicting the efficiency of DOCK4 knockdown (fist panel) and impeded differentiation as measured by the levels of glycophorin A/CD71 levels. (F) qRT-PCR showing the extent of DOCK4 knockdown by siRNA on day 8 erythroblasts. (G) Top panel; Immunofluorescence microscopy analysis showing disrupted actin filaments on day 8 erythroblasts after *DOCK4* knockdown. Photomicrographs also depict cells that were treated with scrambled or left untreated with siRNAs along with corresponding DIC images. Bottom panel; depicts individual cells at high magnification showing gaps in the F-actin skeleton in a sample treated with *DOCK4* specific siRNA and a sample treated with the actin disrupting agent cytochalasin D as a positive control.

Figure 2.3, continued: *DOCK4* knockdown in primary human erythroblasts disrupts F-actin skeleton. A cell from an untreated sample was used as the negative control. (H) DIC and immunofluorescence micrographs of day 10 (orthochromatic erythroblasts) derived from MDS patients showing disrupted F-actin skeleton. (Scale bars, 5μm)

Previous work had identified DOCK4 as a signaling intermediate capable of modulating RAC GTPase activity (Yajnik et al. 2003; Upadhyay et al. 2008). Since RAC-1 GTPases are known to regulate the actin cytoskeleton in erythroid cells (Konstantinidis et al. 2012), I reasoned that lack of *DOCK4* expression might affect the F-actin skeleton in differentiating erythroblasts. Indeed, I found that suppression of *DOCK4* resulted in disruption of F-actin skeleton as determined by immunofluorescence microscopy using Texas-red-conjugated phalloidin for detection (Figure 2.3F, G). *DOCK4* siRNA-treated cells clearly exhibited gaps in the F-actin skeleton similar to when these cells were treated with cytochalasin D, an actin depolymerizing agent (Figure 2.3G, bottom panel). Examination of erythroblasts derived from CD34+ cells from two MDS patients with -7/(del)7q lacking one allele of *DOCK4* and found a phenotype similar to when I knocked down *DOCK4* in control cells, where the F-actin skeleton was disrupted at numerous locations within the actin skeleton (Figure 2.3H).

iv) MDS erythroblasts exhibit disrupted F-actin skeleton.

Although immunofluorescence microscopy enabled us to assess F-actin disruption, this approach did not provide us the means to assess the level of disruption objectively in a quantitative fashion, especially when using large number of patient samples. To this end, I developed a novel assay capable of objectively quantifying the

extent of F-actin disruption using multispectral flow cytometry (ImageStreamX^{TM}). In order to quantify the extent of F-actin disruption in erythroblasts from -7/(del)7q MDS patients lacking *DOCK4* expression, I purified CD34+ cells from bone marrow and/or blood samples obtained from ten patients that included multiple subtypes of MDS (RA; refractory anemia, RAEB; refractory anemia with excess blasts and RCMD; refractory cytopenia with multilineage dysplasia). CD34+ cells were cultured for ten days and erythroblasts (polychromatic stage) were used to quantify the extent of F-actin disruption in these MDS samples. The multispectral flow cytometry assay I developed entailed first staining the cells for F-actin with fluorescently labeled phalloidin and using the ImageStreamX^{TM} instrument to capture single cells in focus that were positive for actin (Figure 2.4-i - iii). Using algorithms available on the IDEAS 6.0 software, I defined the cortical F-actin continuity index taking into account the fluorescence staining of actin filaments (Figure 2.4-iv) (details described in chapter 4).

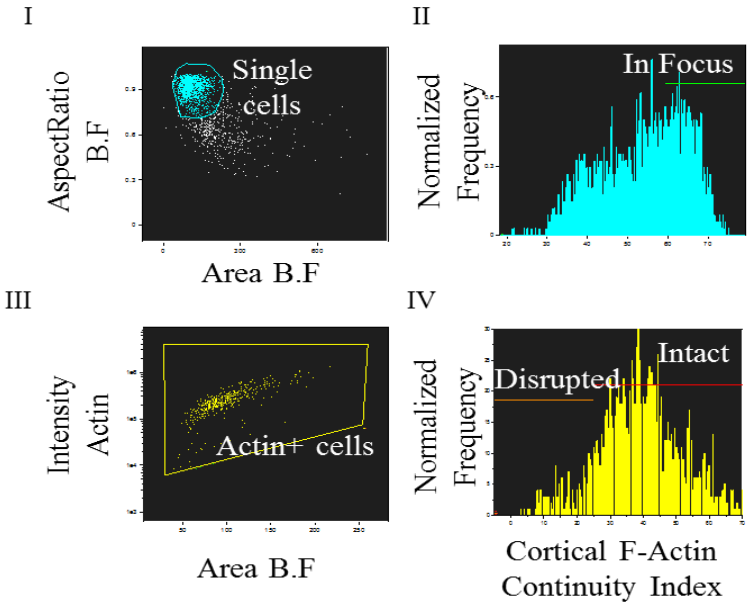

Figure 2.4. Analysis strategy to quantify F-actin disruption by Multispectral flow cytometry (ImageStreamX^{TM}). Day 10 erythroblasts (orthochromatic stage) from human

Figure 2.4, continued: Analysis strategy to quantify F-actin disruption by Multispectral flow cytometry (ImageStreamX^{TM}). primary cultured cells were labeled using fluorescently tagged phalloidin and used for the analysis (I-IV) Strategy used to develop the cortical F-actin continuity index for analysis and quantitation of actin filament disruption. BF; bright field.

Using this assay, I quantified the extent of intact and disrupted F-actin skeleton in erythroblasts from healthy individuals as well as MDS patient samples (Figure 2.5A-E). As positive controls I used samples from healthy donors treated with cytochalasin D or a RAC1 inhibitor (NSC23766) (Figure 2.5B, C). Both positive controls and -7/(del)7q MDS patient samples exhibited a clear pattern of major gaps in actin staining or complete absence of cortical actin staining as seen in the image gallery for each sample, which was quantified by the histograms as depicted (Figure 2.5A-E). On the other hand, erythroblasts from healthy individuals or a non-MDS anemia patient with chronic kidney disease (anemia) did not exhibit disrupted actin filaments (Figure 2.5A, F). Our earlier work had shown that DOCK4 can also be epigenetically silenced by aberrant DNA methylation in MDS (Zhou et al. 2011b). I examined MDS marrow samples without deletion of chromosome 7 and determined that reduced expression of DOCK4 can be seen in some samples and that this correlates with actin filament disruption seen in erythroid cells generated from these samples (Figure 2.5G-I). Taken together, these analyses reveal that MDS erythroblasts with reduced expression of *DOCK4* had disrupted cortical actin filaments compared to those from healthy individuals (Figure 2.5I).

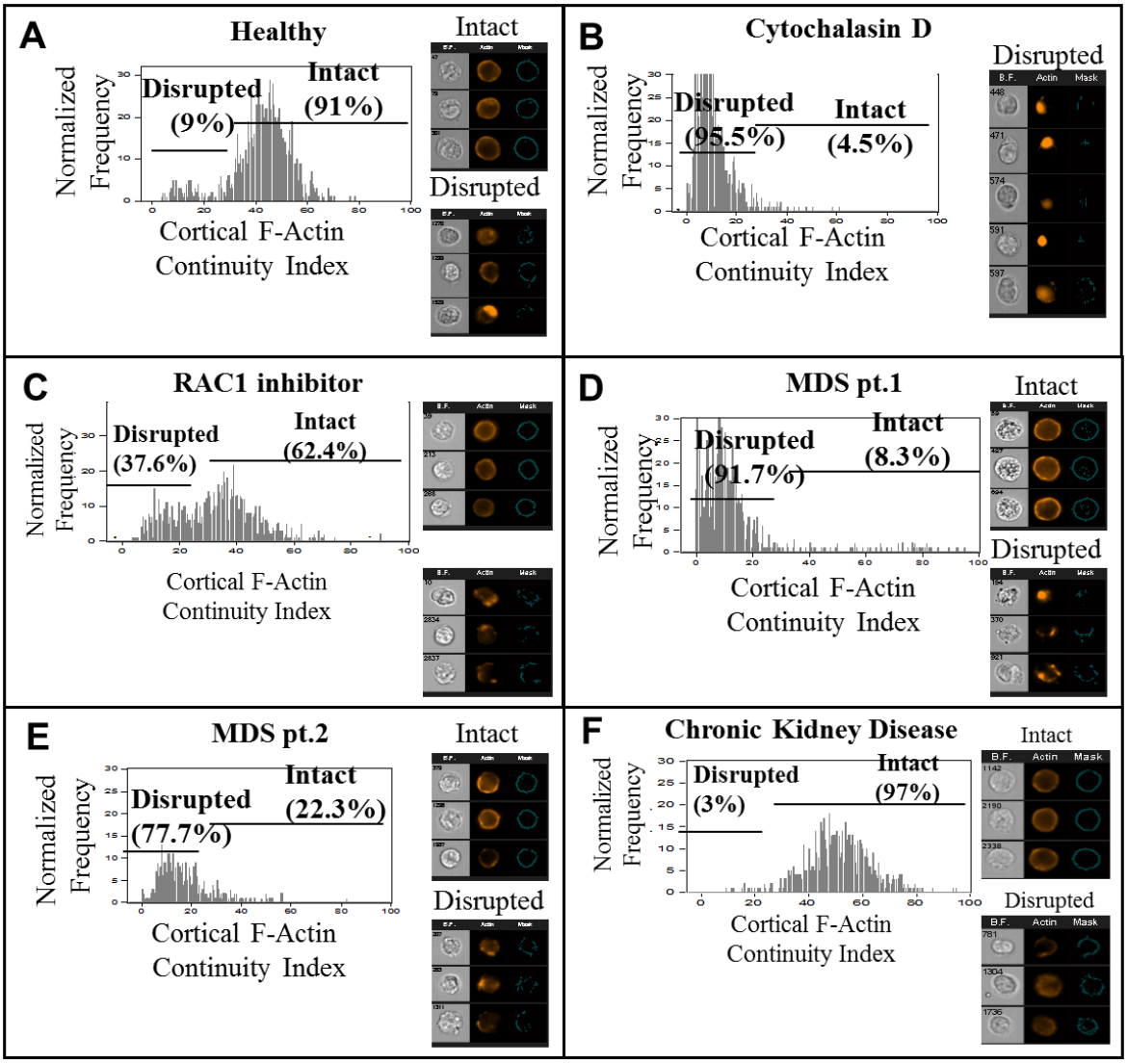

G

MDS pt.	Cytogenetics	Rx	% Actin disruption from Imagestream	DOCK4 IHC
13	Normal	MDS	75.4	0
3	CMML	CMML	73.1	0
10	Normal	UA	63.1	0
12	Normal	MDS	62.9	0
1	Trisomy 20	MDS	59.7	1
2	UA	UA	40.8	1
4	UA	UA	14.7	2
5	Normal	MDS	10.5	2

H

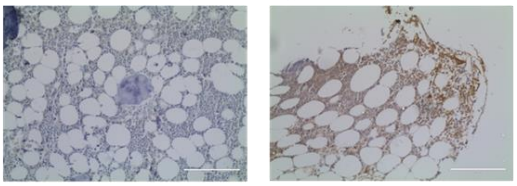

DOCK4 IHC 0 DOCK4 IHC 2+

I

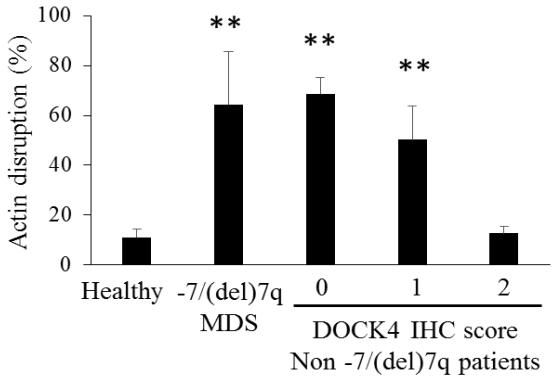

Figure 2.5. Quantitation of F-actin disruption in major MDS subtypes by Multispectral flow cytometry (ImageStreamX™). Day 10 erythroblasts (orthochromatic stage) from human

Figure 2.5, continued: Quantitation of F-actin disruption in major MDS subtypes by Multispectral flow cytometry (ImageStreamX^{TM}). primary cultured cells were labeled using fluorescently tagged phalloidin and used for the analysis (A) Histogram and image gallery of erythroblasts from a healthy individual showing percentages of intact and disrupted F-actin. (B) Histogram and image gallery of erythroblasts from a healthy individual after exposure to cytochalasin D used as a positive control. (C) Histogram and image gallery of erythroblasts from a healthy individual after exposure to RAC1 inhibitor used as a positive control. (D) Histogram and image gallery of erythroblasts from a MDS (RCMD) patient showing percentages of intact and disrupted F-actin. (E) Histogram and image gallery of erythroblasts from a MDS (RA) patient showing percentages of intact and disrupted F-actin. (F) Histogram and image gallery of erythroblasts from a chronic kidney disease patient with anemia showing percentages of intact and disrupted F-actin. (G) Table showing actin disruption (by ImageStream analysis) and DOCK4 expression (by IHC) in MDS patients without deletion of chromosome 7. (H) Representative IHC images showing low and high expression of DOCK4 in the marrow of MDS patients. (I) Extent of actin disruption as measured by the cortical F-actin continuity index quantified from healthy (n=5), MDS patients (n=10) with reduced or absence of *DOCK4* expression and non -7/7q deletion patients with DOCK4 IHC score 0 (n=4), 1 (n=2) and 2 (n=2). (**, *P* value <0.00005, *, *P* value <0.005 Student's *t* test).

v) Reduced expression of DOCK4 leads to reduction in RAC1 GTPase activity

DOCK4 is a known guanine exchange factor for the RAC GTPases (Yajnik et al. 2003). RAC1 and RAC2 are critical for maintaining proper actin filament length that is pivotal for maintaining membrane stability, strength and deformability of erythrocytes. Moreover, because actin is involved in the extrusion of nuclei during enucleation of late-stage erythroblasts, inhibition of RAC GTPase activity leads to reduction in reticulocyte formation (Ji et al. 2008; Konstantinidis et al. 2012). Therefore, I investigated whether knockdown of *DOCK4* in our *ex vivo* culture model reduced RAC1 GTPase activity. I infected human CD34+ early hematopoietic cells with high-titer lentiviral particles carrying shRNA against *DOCK4* and selected with puromycin until day six of culture to select for cells (Figure 2.6A) that had suppressed *DOCK4* expression (Figure 2.6B).

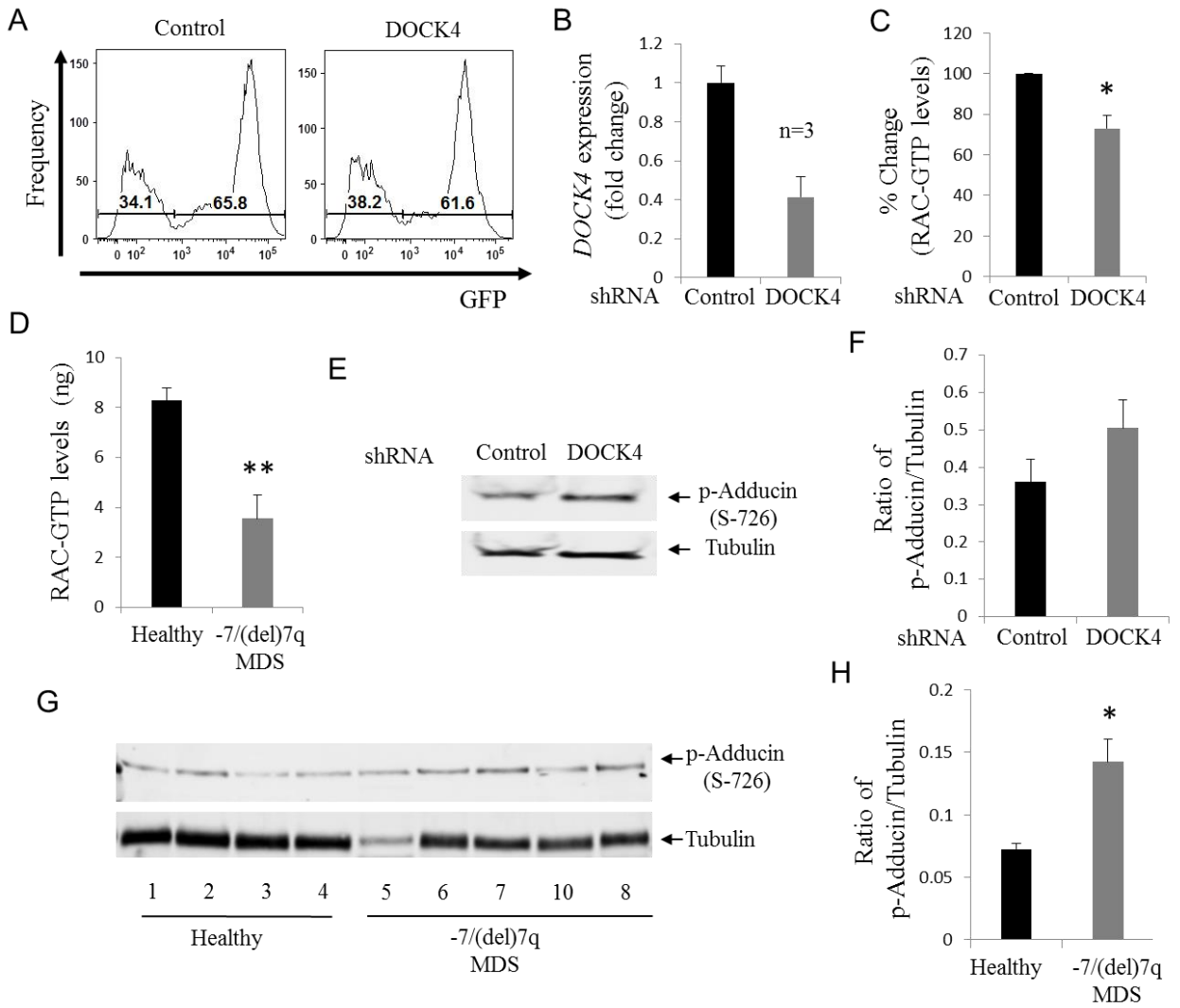

Figure 2.6. DOCK4 suppression leads to reduction in RAC1 GTPase activity and increased Adducin phosphorylation. Day 0 CD34+ cells were infected with lentiviral vector driven shRNAs for knockdown of DOCK4 and selected on puromycin. (A) Flow cytometry analysis on day 6 erythroblasts to evaluate for lentiviral infection efficiency. (B) Q-PCR showing fold reduction of DOCK4 mRNA expression compared to cells infected with control shRNA. (C) Levels of RAC1 GTPase activity were determined by ELISA in day 6 primary erythroblasts after suppression of *DOCK4* expression. Percentage reduction of RAC1 GTPase activity is shown compared to samples infected with control shRNAs. The data are mean of five biological replicates. (D) Levels of RAC1 GTPase activity in mature RBC ghosts prepared from blood samples of healthy donors and MDS patients. The data are mean of seven biological replicates. (E) Immunoblot analysis showing increased phosphorylation of Adducin in day 6 erythroblasts after suppression of *DOCK4* expression. Tubulin was used as a loading control. (F) Quantitation of the levels of phospho-Adducin after suppression of *DOCK4* expression (n=3). (G) Immunoblot (all lanes were run on the same gel but were noncontiguous.) analysis showing phosphorylation of Adducin in cultured human primary day 10 erythroblasts from healthy donors and MDS patients. Tubulin levels were used as a loading control. (H) Shows quantitation of the

Figure 2.6, continued: DOCK4 suppression leads to reduction in RAC1 GTPase activity and increased Adducin phosphorylation levels of phospho-Adducin in day 10 erythroblasts from healthy donors and MDS patient samples (Note: MDS pt.5 from panel D was excluded in this analysis) Data are mean values from four biological replicates. (**, *P* value <0.005, *, *P* value < 0.05, Student's *t* test)

I determined RAC1 GTPase activity (ELISA) in these cells and compared against the activity in cells that were infected with scrambled control shRNAs. These experiments revealed that RAC1 GTPase activity was reduced when *DOCK4* was suppressed; suggesting that actin disruption observed in *DOCK4* deficient cells is at least in part mediated by RAC1 GTPases (Figure 2.6C). I then examined levels of RAC1 GTPase in mature RBCs obtained from blood samples of -7/(del)7q MDS patients who were known to have deletion of one allele of *DOCK4*. I observed significantly lower RAC1 GTPase levels in MDS samples when compared to RBCs from healthy volunteers (Figure 2.6D).

vi) Increased phosphorylation of Adducin in DOCK4 deficient erythroid cells

Adducin is an actin-capping protein that is essential for maintaining the proper length of actin filaments (Kuhlman et al. 1996; Franco and Low 2010). Reduced RAC1 GTPase activity in erythrocytes leads to increased phosphorylation in the MARCKS domain of ADDUCIN (Matsuoka et al. 1996; Matsuoka et al. 1998). In order for actin filaments to be capped at the fast growing-ends, enabling recruitment of Spectrin, Adducin must be dephosphorylated at Ser726. These biochemical alterations occur in the RBC membranes in a dynamic fashion, which is critical for maintaining membrane stability and deformability. Therefore, I investigated whether *DOCK4* suppression in

primary human erythroblasts leads to increased phosphorylation of Adducin. I suppressed *DOCK4* expression by introducing *DOCK4* shRNA into primary human erythroblasts and determined phospho-ADDUCIN levels, which showed that suppression of *DOCK4* expression leads to increased phosphorylation of Adducin (Figure 2.6E, F). I next examined the status of ADDUCIN phosphorylation in erythroblasts from MDS patients and compared the levels to erythroblasts from healthy donors by immunoblot analysis (Figure 2.6G). These studies revealed that -7/(del)7q MDS patient derived erythroblasts had higher levels of Adducin phosphorylation as compared to healthy donor cells (Figure 2.6H).

vii) Reduced terminal differentiation and abnormal erythroid morphology of DOCK4 deficient erythroid cells

In order to determine the functional consequence of *DOCK4* suppression in the erythroid lineage, I examined cells from healthy donors and MDS patients. Human CD34+ cells purified from blood or marrow samples from -7/(del)7q MDS were cultured to promote differentiation along the erythroid lineage. These cultures maintained growth of both healthy and -7/(del)7q cells as confirmed by FISH analysis (Figure 2.7A).

I then used cytospun slides of cultured cells from healthy donors and MDS patient samples to examine the morphology of orthochromatic cells (day 14), which showed large numbers of hyperlobulated and/or cells with frayed cell membrane in -7/(del)7q MDS samples compared to the cells derived from healthy donors (Figure 2.7B). Furthermore, analysis for expression of differentiation markers Glycophorin

A/CD71 in our control and MDS cultures showed reduced levels of Glycophorin A/CD71 expression in MDS samples compared to cells from healthy donors (Figure 2.7B, C). Examination of the extent of enucleation on each of the ten MDS patient samples and comparing them to five healthy donors also showed reduced levels of enucleation, further confirming an impact on terminal differentiation (Figure 2.7D).

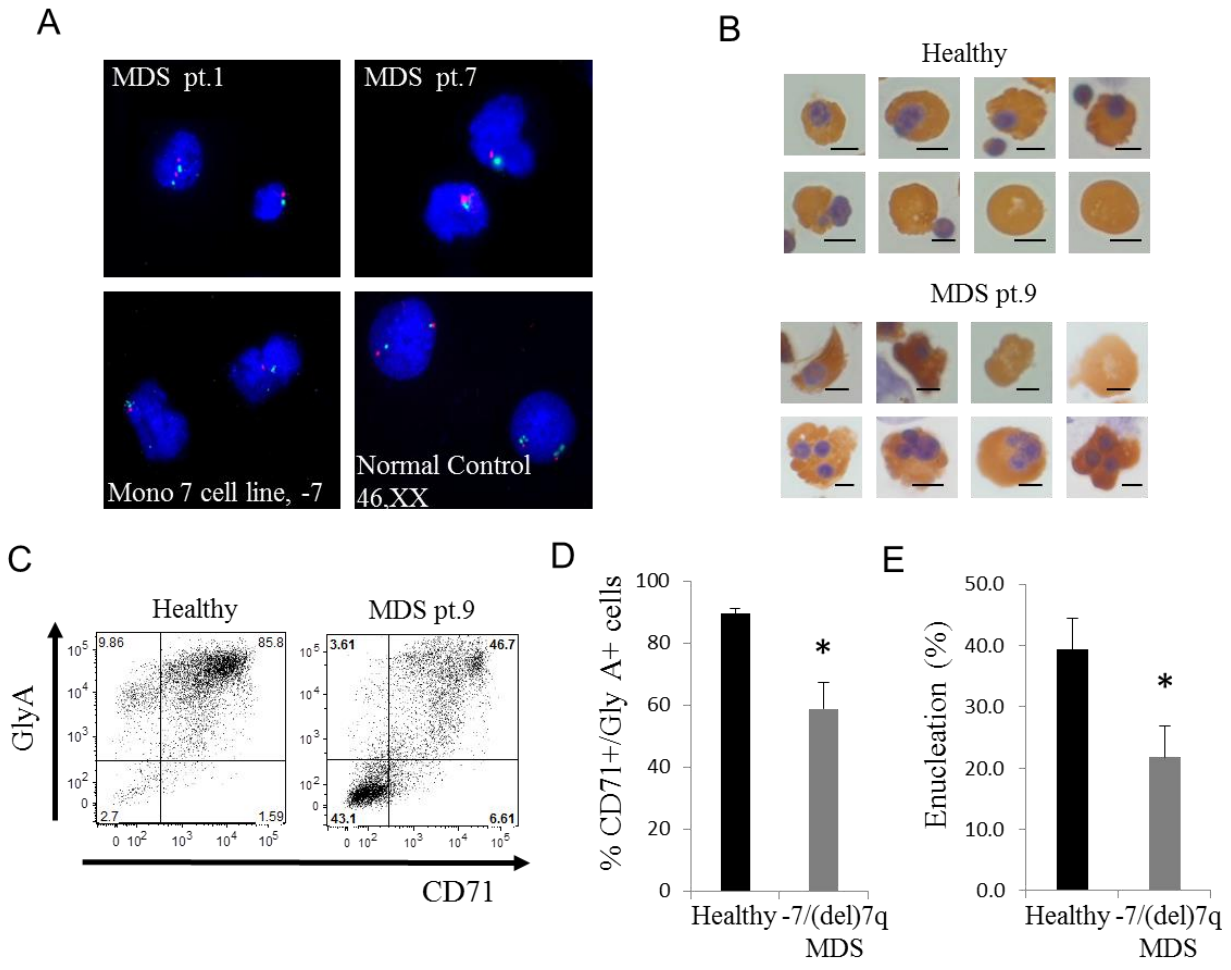

Figure 2.7. Abnormal differentiation in DOCK4 deficient erythroid cells. (A) Photomicrographs of day 10 cultured erythroblasts from MDS patients used for fluorescence in situ hybridization (FISH) that depict clonal malignant cells devoid of an arm of chromosome 7. Mono 7 cell line was used as a positive control and cells from a healthy donor used as a negative control. (B) Photomicrographs of benzidine and hematoxylin stained cells from a healthy donor and a MDS patient showing abnormal erythroid morphology present in erythroblasts derived from MDS CD34+ cells (Scale bar, 5μm). (C) Flow cytometry analysis of erythroid progenitors

Figure 2.7, continued: Abnormal differentiation in DOCK4 deficient erythroid cells. on day 14 of culture to enumerate the percentages of glycophorin A and CD71 expression as a measure of differentiation. (D) Quantitation of percentage of GlyA/CD71 double positive cells on day 14 of culture from healthy donors (n=6) and MDS patients (n=10). (E) Quantitation of percentages of enucleated cells on day 14 of culture using cells from healthy donors (n=5) and MDS patients (n=10) as a measure of terminal differentiation.

I then enumerated the numbers of malignant cells (blast count) on FISH slides and correlated it with size of the erythroid population that was devoid of the late-stage differentiation marker Glycophorin A, which showed that the malignant cells constituted the largest fraction of cells that did not gain positivity for Glycophorin A (Figure 2.8). In Table 1, I have tabulated the clinical features and patient information along with the levels of F-actin disruption that summarize our findings.

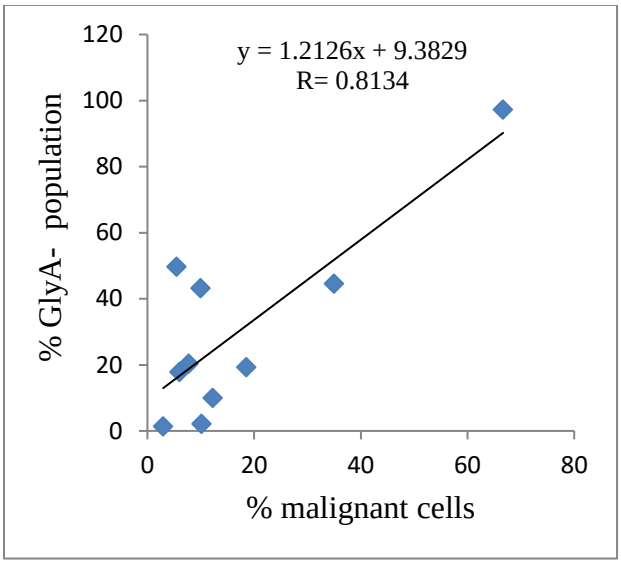

Figure 2.8. Correlation of the extent of erythroid terminal differentiation and the malignant cells in cultured primary MDS erythroblasts. Glycophorin A level were determined by flow cytometry as a measure of terminal differentiation in ten MDS samples along with FISH analysis to enumerate the numbers of malignant cells.

Finally, in order to determine if re-expression of *DOCK4* in -7/(del)7q MDS patient samples can reverse the extent of F-actin disruption I subcloned the *DOCK*4 gene in-frame to the minicircle expression plasmid and transfected CD34+ derived erythroblasts from two -7/(del)7q MDS patients and examined the levels of actin disruption by multispectral flow cytometry. This approach not only allowed us to re-express *DOCK4* in patient samples (Figure 2.9A) but also showed an improvement in the levels of intact actin filaments (Figure 2.9B, C). Furthermore, I found that re-expression of DOCK4 resulted in increased numbers of erythroid colonies (CFU-E) in MDS patient samples (Figure 2.9D).

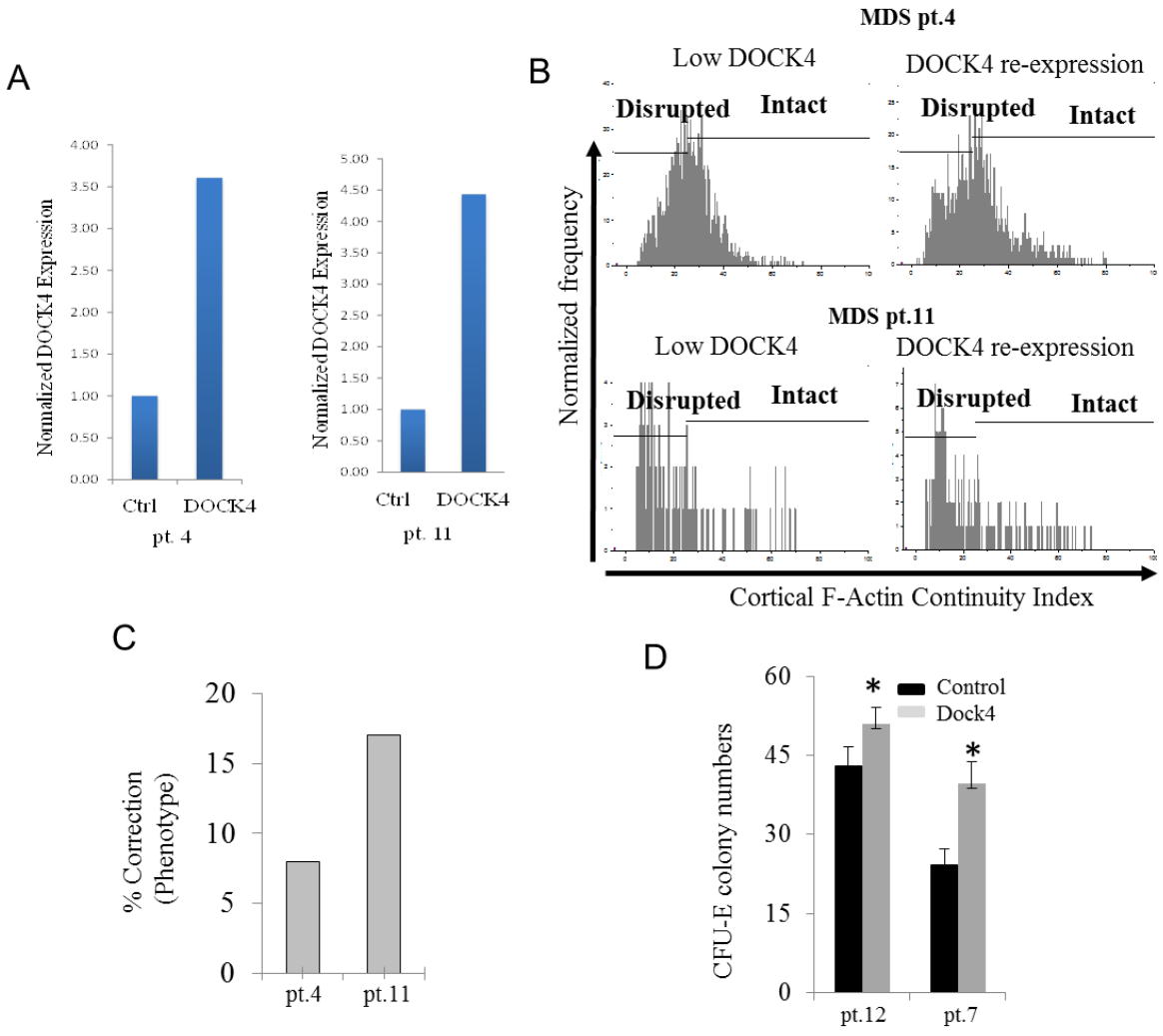

Figure 2.9. Re-expression of DOCK4 in DOCK4 deficient MDS patient samples. (A) Minicircle plasmid carrying *DOCK4* was transfected into CD34+ cell derived day 5 erythroid progenitors from two MDS patients lacking DOCK4 and qPCR was performed on day 10 of erythroblast culture. Normalized levels of *DOCK4* expression is shown compared to untransfected cells. (B) Multispectral flow cytometry analysis for the levels of actin filament disruption in two MDS patient samples before and after re-expression of DOCK in DOCK4 deficient erythroblasts showing longer-length actin filaments as reflected by the higher cortical actin staining index. (C) Percentage of correction of actin filament disruption in the two patients shown in panel E (pt.14, P=0.04; pt.7, P=0.007). (D) Increase in the number of erythroid colony formation after re-expression of DOCK4 in DOCK4 deficient MDS patients.

viii) Reduced DOCK4 expression increases the membrane fragility of erythrocytes

To test the impact of reduced RAC1 activity and subsequent increase in Adducin phosphorylation on the erythroid membrane integrity, I performed osmotic fragility assay. This assay is usually used to determine membrane fragility in mature red blood cells in patients with familial mutations in the cytoskeletal proteins that lead to unstable red blood cell membranes. I performed this assay using mature RBCs from -7/(del)7q MDS patients and compared the results to the healthy controls. The results from these experiments revealed that -7/(del)7q MDS RBCs had reduced erythroid membrane integrity and increased fragility compared to the healthy controls as observed by the right shift of the typical S-curves (Figure 2.10A-D). Taken together, the results from these experiments highlight the importance of actin, RAC1 and Adducin in regulating the RBC membrane integrity.

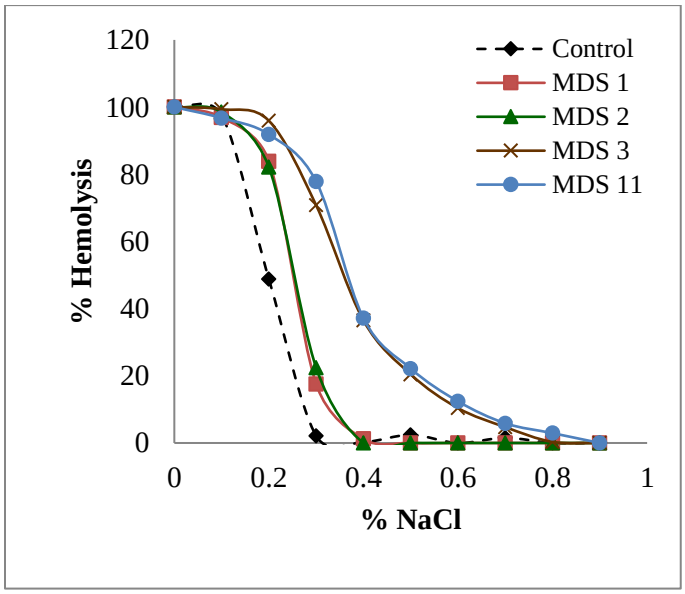

Figure 2.10. Reduced DOCK4 expression increases the membrane fragility of erythrocytes. Osmotic fragility assay was performed using mature RBCs from four different -7/(del)7q MDS patient and compared to healthy control. The right shift of the S-curve compared to the healthy control indicates increased fragility of the RBC membrane. (Unpublished data)

2. d). Conclusion

In a previous study (Zhou et al. 2011b), we had observed that numerous genes, including dedicator of cytokinesis 4 (*DOCK4*), were deleted or epigenetically silenced in MDS, thus prompting an examination of its role in erythropoiesis in the present study. In the present study, I determined the functional role of DOCK4 depletion in RBC formation by using a zebrafish model (Traver et al. 2003) and an *ex vivo* model of human erythropoiesis that recapitulates the erythroid differentiation program. The *ex vivo* model we had developed uses human CD34+ stem/progenitor blood cells in which these cells are induced to commit to the erythroid lineage and then progressively differentiate into reticulocytes over a two week period (Uddin et al. 2004; Kang et al. 2008; Madzo et al. 2014). Using this *ex vivo* model and an established zebrafish model, I demonstrate a critical role of DOCK4 in maintaining the integrity of the erythrocyte cytoskeleton and implicate it as an important pathogenic gene in MDS. I demonstrate that *DOCK4* is under-expressed in MDS bone marrow samples and that the reduced expression is associated with decreased overall survival in patients. I show that depletion of *DOCK4* levels leads to erythroid cells with dysplastic morphology both *in vivo* and *in vitro*. I established a novel single-cell assay to quantify disrupted F-actin filament network in erythroblasts and demonstrate that reduced expression of *DOCK4* leads to disruption of the actin filaments, resulting in erythroid dysplasia that phenocopies the red blood cell (RBC) defects seen in samples from MDS patients. Re-expression of DOCK4 in −7q MDS patient erythroblasts resulted in significant erythropoietic improvements. Mechanisms underlying F-actin disruption revealed that *DOCK4* knockdown reduces RAC1 GTPase activation, leading to increased

phosphorylation of the actin-stabilizing protein Adducin in MDS samples. These data identify *DOCK4* as a putative 7q gene whose reduced expression can lead to erythroid dysplasia. Altogether, our study demonstrated that reduced *DOCK4* expression in -7/(del)7q MDS leads to RAC1 functional deficiency, resulting in aberrant Adducin phosphorylation disrupting proper formation of actin filaments in erythroid cells (Figure 2.11).

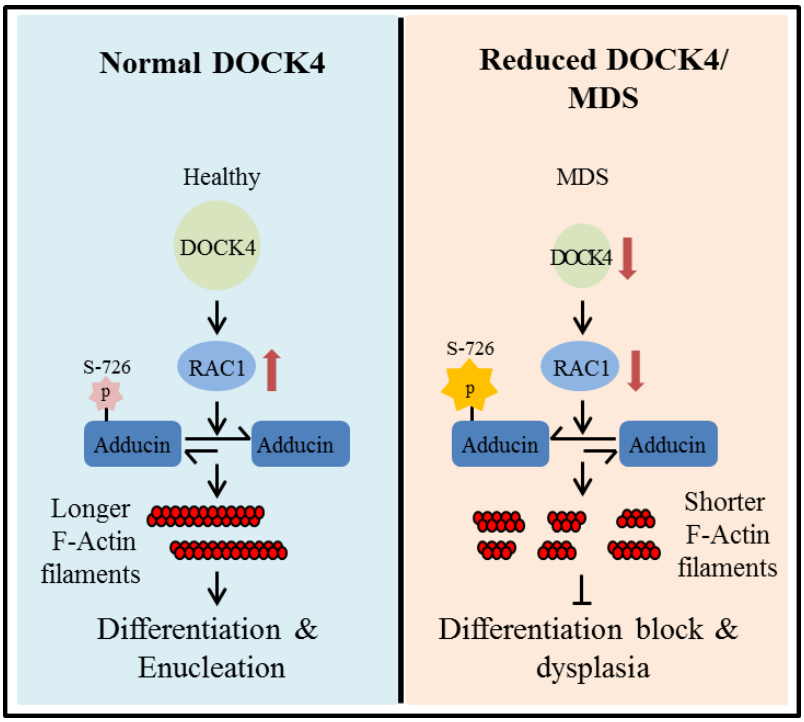

Figure 2.11: Schematic of the DOCK4 signaling pathway in erythroblasts.

Table 1: MDS Patients Characteristics and Summary of Results

Patient	Age (years)	MDS subtype	Karyotype	Hemoglobin (g/dl)	% Clonal cells (FISH)	% Actin disruption	% GlyA (d14)
MDS 1	60	RCMD	-7	6	18.53	91.7	80.67
MDS2	67	RA	-7	8	2.96	77.7	98.7
MDS 3	70	RAEB	-7	6.6	66.67	93	2.7
MDS 4	83	RA	-7	7	12.26	50.2	90
MDS 5	67	RCMD	-7	6.7	10.15	24.9	97.9
MDS 6	77	RCMD	complex -7	11.4	10	82.14	65.6
MDS 7	63	RCMD	complex -7	12.7	35	52.8	55.5
MDS 8	75	RCMD	complex -7	9.8	5.5	77.7	56.7
MDS 9	84	RAEB	complex -7	7.6	6	50.37	59.9
MDS 10	74	RCMD	complex -7	12	7.75	79.6	51

RA – Refractory Anemia; RAEB – Refractory Anemia with Excess Blasts; RCMD – Refractory Cytopenia with Multilineage Dysplasia; FISH – Fluorescence In Situ Hybridization. MDS 11 and 12 were not used for the FISH/actin/GlyA analyses.

Author contributions

I led, designed and performed majority of the experiments performed in this study which was published in PNAS. However, this is a collaborative effort from all the authors. Their contributions are listed below.

Duggan R - Assistance in developing Imagestream assays at the Flow Cytometry Core Facility, University of Chicago.

Bhagat T., Yu Y – Assistance in performing computational analyses at Albert Einstein College of Medicine.

Ebenezer D. L., Liu H – Assistance in DOCK4 siRNA knockdown experiments at University of Chicago.

Bartenstein M., Unnikrishnan M – Assistance in immunohistochemistry experiments performed at Albert Einstein College of Medicine.

Karmakar S – Assistance in cloning DOCK4 plasmids at University of Chicago.

Liu T.-C., Torregroza I., Quenon T – Assistance in *dock4a* knockdown in zebrafish embryos at Weill Cornell Medical College.

Anastasi J., McGraw K. L., Artz A., List A. F – Provided MDS patient samples at University of Chicago. and Moffitt Cancer Center.

Pellagatti A., Boultwood J., Yajnik V., Steidl U – Provided reagents/sequencing datasets at University of Oxford, Massachusetts General hospital and Albert Einstein College of Medicine.

Le Beau M. M – Supervised FISH experiments at University of Chicago.

Evans T – Supervised the zebrafish experiments performed at Weill Cornell Medical College.

Verma A.- Supervised the data analysis performed at Albert Einstein College of Medicine.

Wickrema A – Conceptualized and supervised the overall study.

CHAPTER 3 - LOSS OF FUNCTION OF DOCK4 IN MYELODYSPLASTIC SYNDROMES STEM CELLS IS RESTORED BY INHIBITORS OF DOCK4 SIGNALING NETWORKS

LOSS OF FUNCTION OF DOCK4 IN MYELODYSPLASTIC SYNDROMES STEM CELLS IS RESTORED BY INHIBITORS OF DOCK4 SIGNALING NETWORKS

Majority of the sections of this chapter has been adapted from: Sundaravel, S., Kuo, W., Jeong, J., Choudhary, G., Gordon-Mitchell, S., Liu, H., Bhagat, T., McGraw, K.L., Gurbuxani, S.K., List, A.F., Verma, A., Wickrema, A. Loss of function of DOCK4 in myelodysplastic syndromes stem cells is restored by inhibitors of DOCK4 signaling networks. Clin Cancer Res July 15 2019 **DOI:** 10.1158/1078-0432.CCR-19-0924

3. a). Goals

The key goals of this chapter are to:

- Comprehensively identify DOCK4 regulatory networks in hematopoietic stem cells.
- Define the functions of DOCK4 in HSCs.
- Test the efficacy of modulators of the DOCK4 pathways in reversing erythroid defects in MDS.

3. b). Introduction

Our previous studies have shown that reduced levels of *DOCK4* lead to dysplastic erythropoiesis and restoring *DOCK4* expression in primary MDS erythroblasts improved erythroid differentiation (Zhou et al. 2011b; Sundaravel et al. 2015). Even though *DOCK4* is highly expressed in early-stage stem cells, very little is known with respect to the impact of reduced levels of *DOCK4* expression within the stem cell compartment. Moreover, downstream signaling networks regulated by DOCK4 in pre-lineage committed HSCs are not known.

Because reactivation of DOCK4 pathway in MDS improved erythroid differentiation, I hypothesized that discovering intervention points in the DOCK4 signaling pathway will greatly enhance the probability of developing therapies for patients harboring DOCK4 mutations or low expression. In order to have the maximum impact of any therapeutic intervention it is most desirable to target stem cells as opposed to individual blood cell lineages. In this study, using healthy blood stem cells and blood stem cells expressing reduced levels of *DOCK4,* (as seen in the malignant blood disorder myelodysplastic syndromes), I identified downstream signaling networks regulated by DOCK4 and functional implications of reduced *DOCK4* expression within the blood stem cell compartment.

3. c). RESULTS

i) Reduction of *DOCK4* increases global tyrosine phosphorylation in HSCs

I first confirmed that cells used in our studies were highly enriched for the hematopoietic stem cell phenotype by determining the CD34+/CD90+ expression and cell morphology (Figure 3.1A-C), which showed 84% cells were double positive and greater that 99% were positive for CD34 early stem/progenitor cell marker.

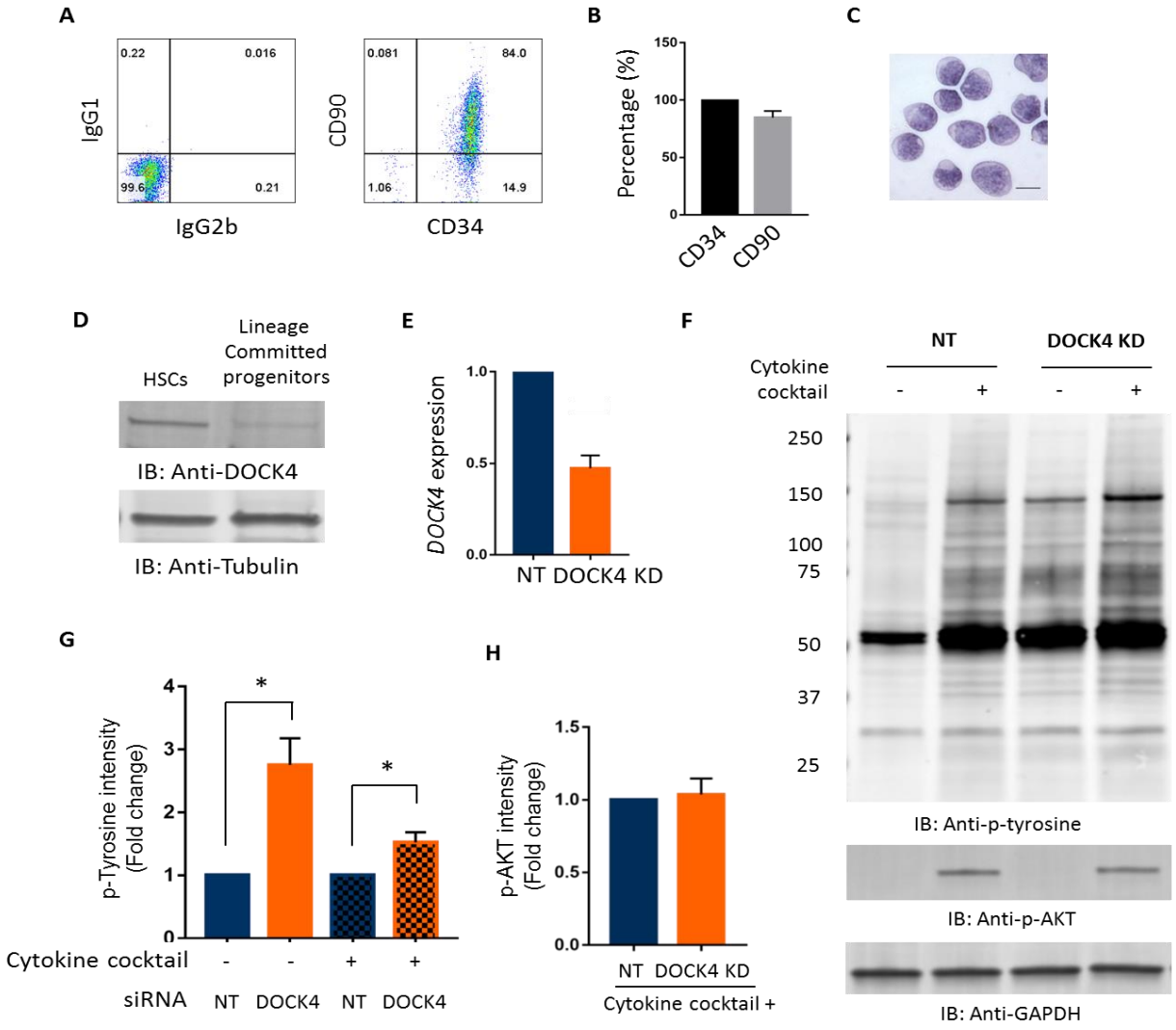

Figure 3.1: Expression of DOCK4 and increased global phosphorylation of proteins in human primary hematopoietic stem cells with reduced DOCK4 levels.

Figure 3.1, continued: Expression of DOCK4 and increased global phosphorylation of proteins in human primary hematopoietic stem cells with reduced DOCK4 levels. (A) Flow cytometry plots showing the levels of CD34 and CD90 following isolation of HSCs. (B) Quantitation of percentages of CD34 and CD90 in HSCs. Data are mean ±SEM from three biological replicates. (C) Photomicrograph of HSCs stained with benzidine-hematoxylin (Scale bar, 10μM). (D) Expression of DOCK4 in CD34+/CD90+ HSCs and in lineage committed progenitors. (E) qPCR analysis for *DOCK4* expression following knockdown of DOCK4 by fifty percent in primary hematopoietic stem cells. The data are 24 hours post-nucleofection. Data are represented as mean ±SEM from six biological replicates (****$P < 0.0005$; Student's *t* test). (F) Immunoblot analysis 24 hrs following DOCK4 knockdown in HSCs with or without exposure to a five-cytokine cocktail (Thrombopoietin (TPO), stem cell factor (SCF), FLT3 ligand, Interleukin-3 (IL-3) and Interleukin-6 (IL-6)) for 15 mins as described in methods. An anti-pan phosphotyrosine antibody was used to detect phosphorylated proteins. The same membrane was stripped and re-probed with an anti-phospho-AKT antibody in order to show activity of signaling in response to cytokine stimulation as a control. GAPDH was used as a loading control. (G) Quantitation of fold change in phospho-tyrosine levels in panel C. Comparisons were made between cells expressing DOCK4 at normal levels and cells expressing DOCK4 at 50% levels with and without cytokine exposure. Data are represented as mean±SEM from four biological replicates (*$P < 0.05$; Student's *t* test). (H) Quantitation of the levels of phospho-AKT in HSCs from control and DOCK4 knockdown samples. Data are represented as mean ±SEM from four biological replicates. NT – Non-targeting control.

I first examined steady state expression levels of DOCK4 in HSCs and in lineage committed progenitors, which showed a relatively high level of expression in HSCs but low levels in committed progenitors (Figure 3.1D). I then knocked down DOCK4 in these cells by siRNA, which enabled us to reduce the levels by fifty percent consistently in multiple primary samples as determined by quantitative PCR (qPCR) (Figure 3.1E). I then determined HSC response to cytokines in cells that are expressing DOCK4 at 50% of their normal levels, by exposing them to a cocktail of stem cell cytokines (TPO, SCF, Flt3L, IL3 and IL6) (Knapp et al. 2017) after a short deprivation of cytokines. I also exposed cells expressing DOCK4 at their normal levels to the same cocktail before harvesting cells and performing immunoblotting against an anti-phospho tyrosine antibody. These experiments revealed increased tyrosine phosphorylation of a large number of proteins in DOCK4 knockdown samples compared to the ones that had

normal levels of DOCK4 expression (Figure 3.1F-H). This increase was observed regardless of cytokine stimulation suggesting DOCK4 levels alone were sufficient to elicit global phosphorylation response. Levels of protein under each condition were equivalent as reflected by no difference in AKT phosphorylation or GAPDH in DOCK4 knockdown cells and non-targeting control cells (Figure 3.1F and H). Collectively, these data demonstrated that reduced levels of DOCK4 increased global tyrosine phosphorylation and suggested that DOCK4 functions as a signaling intermediate downstream of several cytokine receptors in HSCs.

ii) DOCK4 regulates the phosphorylation of kinases and phosphatases

In order to identify the proteins that were impacted in their phosphorylation due to reduced DOCK4 expression, in collaboration with Northwestern University proteomics facility, I performed phosphoproteomic analysis by mass spectrometry. These experiments uncovered a large number of phospho-peptides belonging to mostly kinases and phosphatases that were hyperphosphorylated in cells that expressed low levels of DOCK4. Among them, SHP1, SHIP1 and LYN exhibited greatest increase in tyrosine phosphorylation (Table 1).

I then focused on LYN kinase, and phosphatases SHP1 and SHIP1 for further study since these enzymes have been extensively studied during blood cell development (Harder et al. 2004). I used commercially available phospho-specific antibodies against each of the three proteins to confirm our mass spectrometry results, which showed LYN, SHIP1 and SHP1 proteins were phosphorylated at tyrosine sites

397, 1021 and 536 respectively (Figure 3.2A-D). These results were also confirmed in TF-1 erythroleukemia cells, which are at early phase (CD34+) of blood cell development (supplemental Figure 3.2E-K).

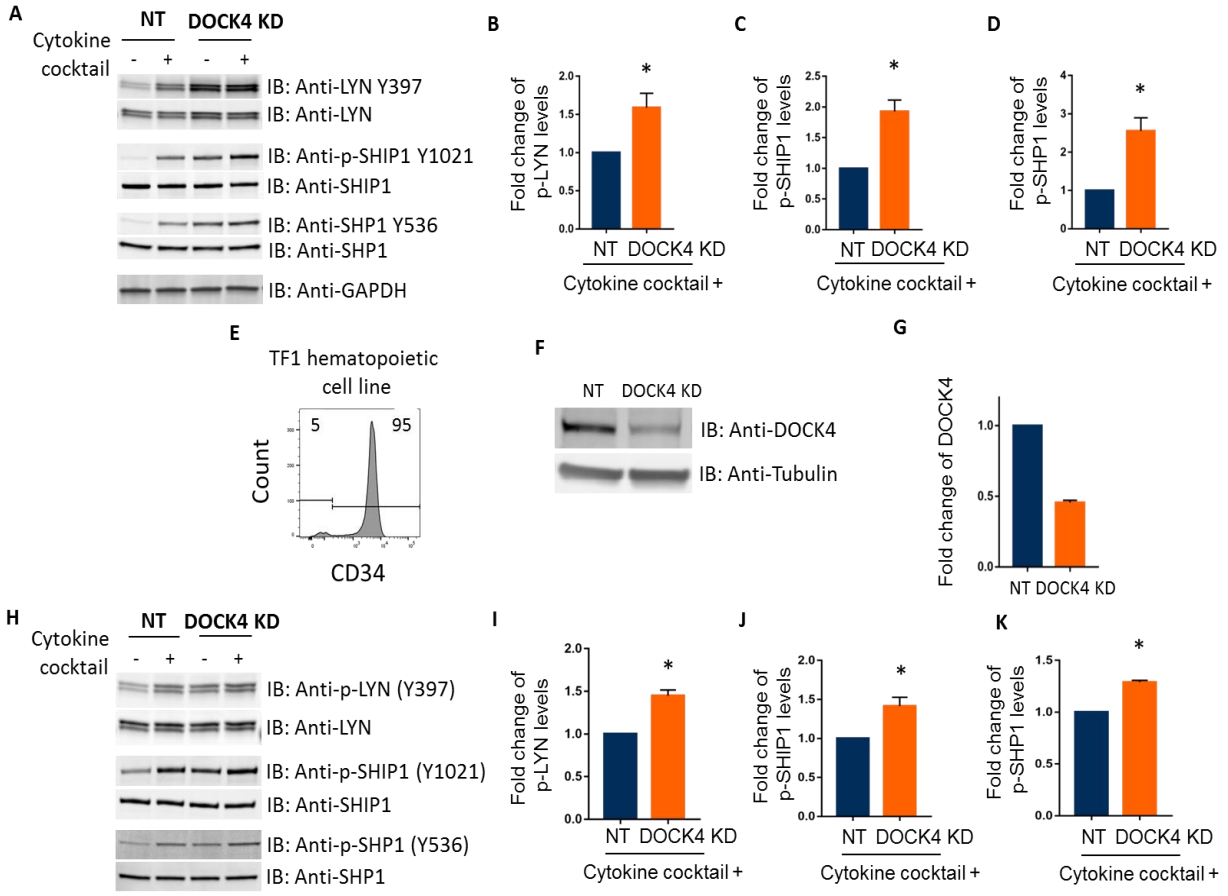

Figure 3.2: Reduced levels of DOCK4 leads to increased phosphorylation of LYN kinase and phosphatases SHIP1 and SHP1. (A) Immunoblot analysis 24 hours following DOCK4 knockdown in HSCs with or without exposure to a five-cytokine cocktail (TPO, SCF, FLT3 ligand, IL-3 and IL-6) for 15 mins as described in methods. An anti-phospho LYN (Y397) antibody, an anti-phospho SHIP1 (Y1021) antibody or an anti-phospho SHP1 (Y536) antibody was used for detection. Same membranes were stripped and re-probed with anti-LYN, SHIP1, SHP1 or anti-GAPDH antibody as protein loading controls. (B, C and D) Quantitation of the levels of phospho-LYN (Y397), phospho-SHIP1 (Y1021) and phospho-SHP1 (Y536) in panel A. Data are represented as mean ±SEM from four biological replicates (*$P < 0.05$; Student's *t* test.). NT– Non-targeting control. (E) Flow cytometry analysis showing that the TF1 erythroleukemia cells express high levels of CD34 marker on their cell surface. (F and G) Twenty four hours post DOCK4 siRNA nucleofection; cells were used for immunoblot analysis for DOCK4 expression. Fold change of DOCK4 was computed by densitometry. Data are mean ±SEM from five independent experiments.

Figure 3.2, continued: Reduced levels of DOCK4 leads to increased phosphorylation of LYN kinase and phosphatases SHIP1 and SHP1. (H) Twenty four hours post DOCK4 knockdown, TF1 cells were briefly deprived of cytokines and then re-exposed to a cytokine cocktail (Stem cell factor (SCF), Interleukin-3 (IL-3) and Granulocyte-Macrophage colony stimulating factor (GM-CSF)) for 15 mins. Samples were resolved by immunoblotting for phospho-LYN (Y397), phospho-SHIP1 (Y1021) and phospho-SHP1 (Y536). Same membranes were probed with total LYN, SHIP1 and SHP1 antibodies as loading controls. (I, J and K) Quantitation of the levels of phospho-LYN (Y397) (N=3), phospho-SHIP1 (Y1021) (N=5) and phospho-SHP1 (Y536) (N=4) respectively in TF1 cells from control and DOCK4 knocked down samples (*$P < 0.05$; Student's *t* test). Data are mean ±SEM from independent experiments as specified.

iii) SHIP1 and SHP1 are substrates for LYN kinase

Next, I wanted to determine whether LYN kinase was directly responsible for phosphorylating the two phosphatases, SHIP1 and SHP1 as a result of LYN Kinase activation due to reduced expression of DOCK4 (Figure 3.3A). In order to determine whether SHIP1 and SHP1 are direct targets of LYN kinase, I designed cell-free *in vitro* kinase assays, where either recombinant full-length SHIP1 protein or recombinant full-length SHP1 protein was incubated with active form of recombinant LYN kinase in a biochemical assay in the presence of a kinase buffer. A parallel assay using the same substrates but recombinant JAK2 as the kinase enzyme was also performed as a control. The reaction products were then analyzed by immunoblotting using an anti-phospho SHIP1 (Y1021) antibody or an anti- phospho SHP1 (Y536) antibody. The results of these experiments showed that LYN kinase phosphorylated SHIP1 at tyrosine 1021 and SHP1 at tyrosine 536 in a dose dependent manner whereas JAK2 kinase did not show such phosphorylation of SHIP1 or SHP1 (Figure 3.3B-E). Furthermore, the presence of the LYN/Src inhibitor, abrogated phosphorylation of both SHIP1 and SHP1, re-enforces the specificity of the *in vitro* kinase assays (Figure 3.3B-E).

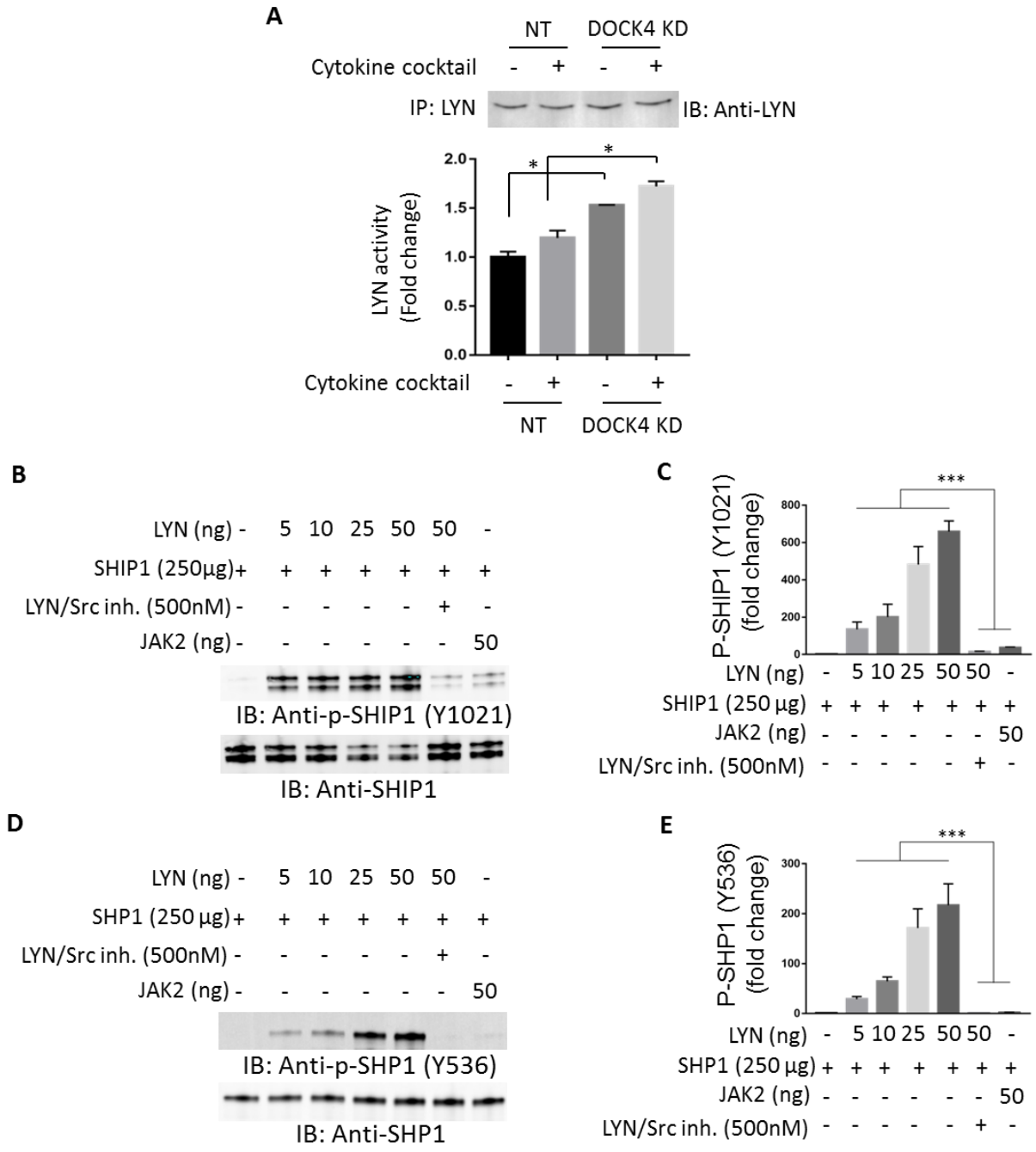

Figure 3.3: Active LYN kinase phosphorylates SHIP1 (Y1021) and SHP1 (Y536). (A) Twenty-four hours post DOCK4 knockdown HSCs were briefly deprived and exposed to 5 cytokine cocktails (TPO, SCF, FLT3 ligand, IL3 and IL6) for 15 mins. Following cytokine exposure, LYN kinase activity assay was performed to examine the endogenous LYN kinase activity in HSCs expressing normal and reduced levels of DOCK4 (*$P < 0.05$; Student's *t* test). Data are represented as mean ±SEM from three technical replicates. (B) An *in vitro* kinase assay was performed using recombinant SHIP1 and increasing concentrations of active LYN kinase under cell-free conditions for ascertaining whether SHIP1 is a direct target for phosphorylation by LYN. JAK2 kinase and LYN/Src inhibitor were used as controls.

Figure 3.3: Active LYN kinase phosphorylates SHIP1 (Y1021) and SHP1 (Y536). *In vitro* kinase reaction products were resolved on SDS-PAGE gel and immunoblot analysis performed using an anti-phospho SHIP1 (Y1021) antibody. The same immunoblots were also probed with anti-SHIP1 antibody as protein loading control. Representative data from three independent experiments are shown. (C) Quantitation of the levels of phospho-SHIP1 (Y1021) in the *in vitro* kinase reaction products (***$P < 0.0005$; One way ANOVA). Data are mean ±SEM from three independent experiments. (D) An *in vitro* kinase experiment as described in panel E was set up to test whether SHP1 is a direct substrate of LYN. *In vitro* kinase reaction products were resolved on a SDS-PAGE gel and immunoblot analysis performed using an anti-phospho SHP1 (Y536) antibody. The same immunoblots were also probed with anti-SHP1 antibody as loading control. Representative data from three independent experiments are shown. (E) Quantitation of the levels of phospho-SHP1 (Y536) in the *in vitro* kinase reaction products (***$P < 0.0005$; One way ANOVA). Data are mean ±SEM from three independent experiments.

In order to determine whether SHIP1 and SHP1 are substrates of LYN kinase in HSCs, I inhibited LYN using the LYN/Src inhibitor in cultured HSCs. Immunoblotting analysis showed that SHIP1 (Y1021) and SHP1 (Y536) phosphorylation decreased in a dose dependent manner when LYN was inhibited (Figure 3.4A-D). Taken together these results demonstrated that reduced expression of DOCK4 initiate a sequential phosphorylation events impacting the signaling cascade involving LYN kinase, SHIP1 and SHP1.

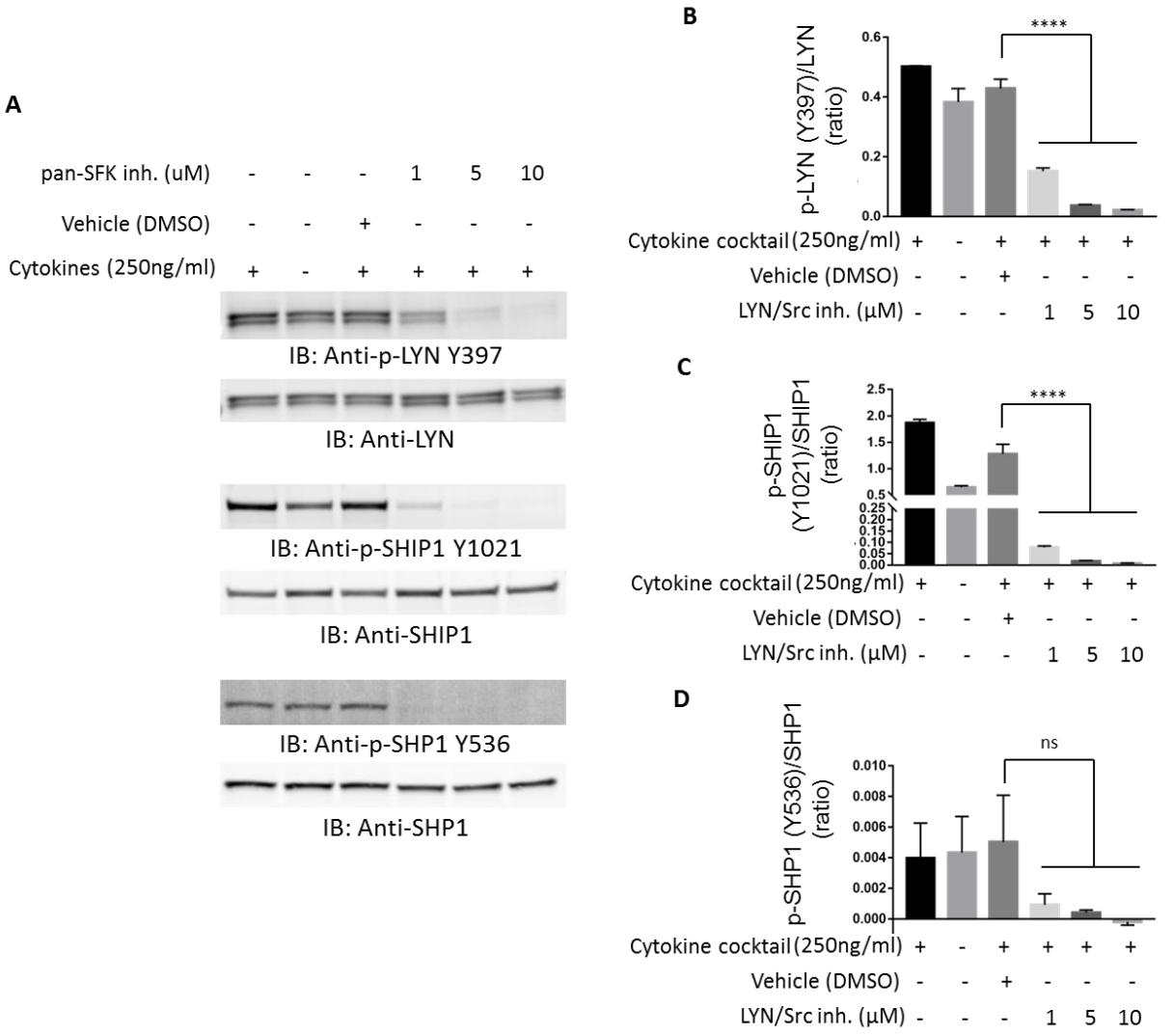

Figure 3.4: SHIP1 and SHP1 are substrates of LYN kinase in HSCs. (A) Cultured HSCs were exposed to increasing doses of LYN/Src inhibitor, RK20449 in the presence or absence of stem cell cytokines. Samples were resolved and immunoblotted for phospho-LYN (Y397), phospho-SHIP1 (Y1021) and phospho-SHP1 (Y536). The same blot was probed with LYN, SHIP1 or SHP1 antibodies as protein loading controls. Representative data from three biological replicates are shown. (B-D) Quantitation of the levels of phospho-LYN (Y397), phospho-SHIP1 (Y1021), and phospho-SHP1 (Y536) respectively in primary human HSCs treated with increasing doses of LYN/Src inhibitor, RK20449. Data are mean ±SEM from three biological replicates (****$P < 0.00005$, One way ANOVA; ns-not significant).

iv) LYN kinase activity is regulated as a result of its interaction with DOCK4

Next, we wanted to ascertain whether DOCK4 directly interacts with LYN kinase as well as SHIP1 and SHP1 phosphatases in addition to whether DOCK4 regulates LYN kinase activity. In order to test this, I ectopically expressed Flag-tagged full length DOCK4 and GFP-tagged full length LYN in HEK293 cells and performed reciprocal co-immunoprecipitation experiments coupled with immunoblot analysis. Immunoprecipitation of Flag-tagged DOCK4 followed by using anti-GFP/LYN antibody for detection as well as immunoprecipitation with GFP-trap beads and immunoblot analysis with anti-FLAG/DOCK4 antibody showed that DOCK4 directly interacted with LYN (Figure 3.5A). Similarly, I ectopically expressed Flag-tagged full length DOCK4 and GFP-tagged full length SHIP1 in HEK293 cells and performed reciprocal co-immunoprecipitation experiments coupled with immunoblot analysis. Immunoprecipitation of Flag-tagged DOCK4 followed by using anti-GFP/SHIP1 antibody for detection as well as immunoprecipitation with GFP-trap beads and immunoblot analysis with anti-FLAG/DOCK4 antibody showed that DOCK4 directly interacted with SHIP1 (Figure 3.5B). However, when similar experiments were performed using GFP-tagged full-length SHP1, I did not detect a direct interaction between DOCK4 and SHP1 suggesting that changes in phosphorylation seen in SHP1 is indirect and most likely only through LYN kinase (Figure 3.5C).

We then determined whether LYN kinase activity is regulated by DOCK4 levels. In order to accomplish this, we set up an in *vitro kinase* assay where varying amounts recombinant DOCK4 protein was incubated with recombinant active form of LYN kinase and measured LYN kinase activity using a commercially available ELISA. These

experiments showed that increasing amounts of DOCK4 protein decreased LYN kinase activity (Figure 3.5E, F). However, when recombinant JAK2 was used as a control no modulation of JAK2 activity was observed when increasing amounts of DOCK4 was used in the assay (Figure 3.5E, F). Experiments where LYN/Src inhibitor was present showed inhibition of LYN kinase activity further reinforcing the specificity of the assay. Taken together these results indicate that DOCK4 is a regulator of Lyn Kinase.

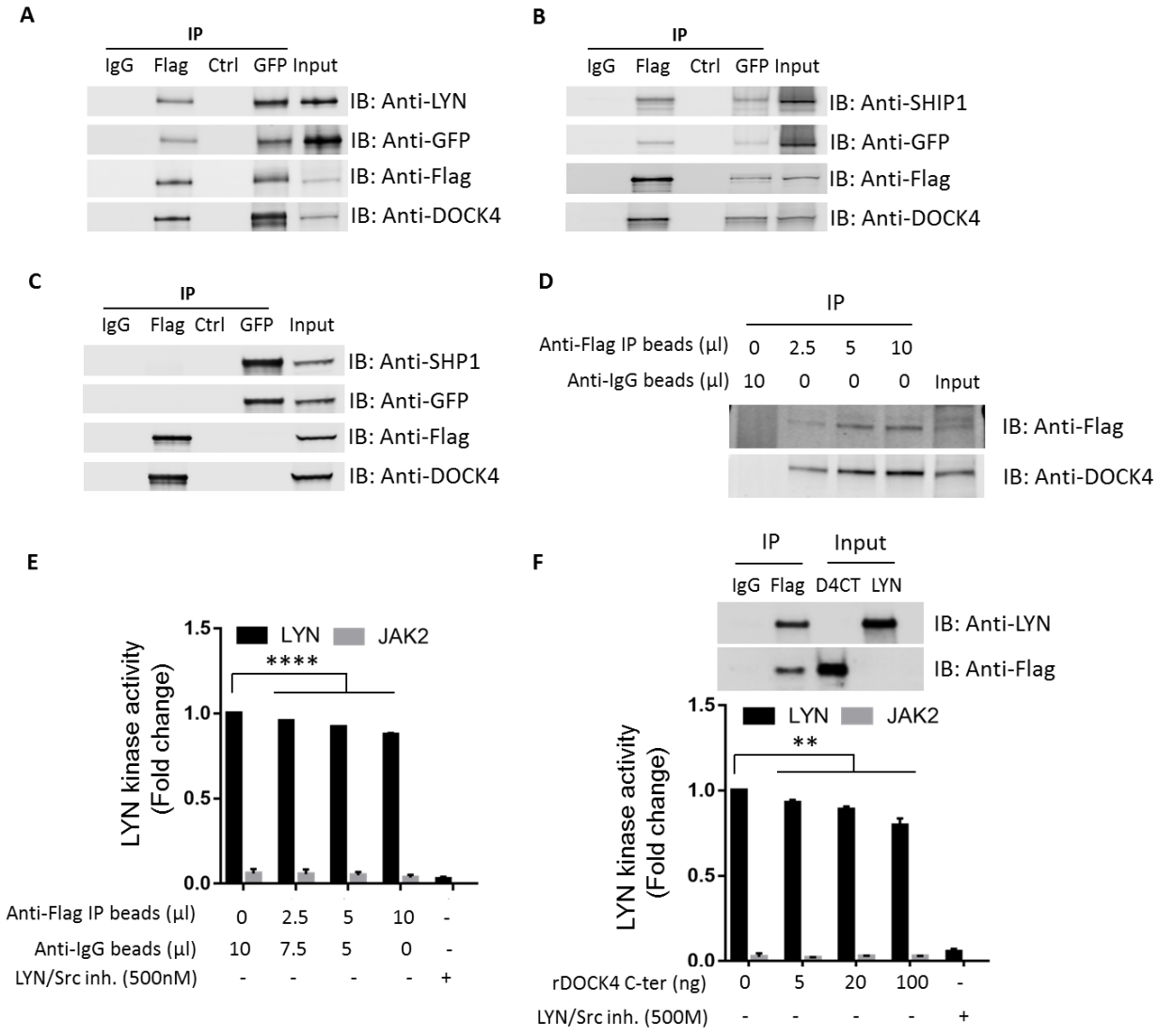

Figure 3.5: LYN kinase and SHIP1 are components of DOCK4 signaling complex.

Figure 3.5, continued: LYN kinase and SHIP1 are components of DOCK4 signaling complex. (A-C) Determination of DOCK4 interaction with LYN, SHIP1 and SHP1. Flag-tagged DOCK4 together with either (A) GFP-tagged LYN or (B) GFP-tagged SHIP1 or (C) GFP-tagged SHP1 was transfected into HEK293 cells and protein lysates were used in reciprocal immunoprecipitation assays. Immunoprecipitations were performed with an anti-Flag antibody followed by immunoblot analysis using either anti-LYN antibody, anti-SHIP1 antibody or anti-SHP1 antibodies. As controls immunoprecipitations were also performed using GFP-trap beads followed by an anti-Flag antibody. Anti-DOCK4 or GFP antibodies were also used as additional controls. D) Flag-tagged DOCK4 was transfected into HEK293 cells and immunoprecipitated with anti-Flag antibody followed by immunoblot analysis using anti-Flag and anti-DOCK4 antibodies with different amounts of DOCK4-flag. E) LYN kinase activity assay was performed using recombinant LYN kinase and increasing amounts of flag-DOCK4 to ascertaining whether DOCK4 controls LYN kinase activity. JAK2 kinase and LYN/Src inhibitor were used as controls. Data are mean ±SEM from three independent experiments. (****$P < 0.00005$; One-way ANOVA). F) An *in vitro* binding assay was performed using flag-tagged DOCK4 C-terminus (D4CT) and recombinant LYN kinase to determine whether LYN kinase interacted with DOCK4-C-terminus (Top). LYN kinase activity assay was performed using recombinant LYN kinase and increasing concentrations of recombinant DOCK4 C-terminus. JAK2 kinase and LYN/Src inhibitor were used as controls (Bottom) Data are mean ±SEM from three independent experiments. (**$P < 0.005$; One-way ANOVA).

v) Decreased *DOCK4* expression leads to increased HSC migration

To identify the functional implications of increased tyrosine signaling in DOCK4 deficient HSCs, I performed *in silico* Database for Annotation Visualization and Integrated Discovery (DAVID) analysis using the list of proteins that were identified by mass spectrometry to be highly phosphorylated (Table 1). This analysis revealed cell migration as one of the highly enriched biological pathways (Figure 3.6A). I tested this prediction experimentally by carrying out transwell migration assays using HSCs expressing normal levels and reduced levels of DOCK4, which showed increased rates of migration of cells expressing reduced levels of DOCK4 (Figure 3.6B). Similar results were also observed in TF1 cells following DOCK4 knockdown (Figure 3.6C). Since F-actin in the cytoskeleton play a key function in cell migration, I examined for changes in the F-actin network in HSCs expressing reduced levels of DOCK4 and compared them

to HSCs expressing normal levels of F-actin. These experiments revealed significantly increased numbers of cells displaying pro-migratory features such as cell spreading and bundled F-actin in the leading edges of the cells (Figure 3.6D). Similar pro-migratory features were also observed in TF1 cells when DOCK4 levels were reduced (Figure 3.6E).

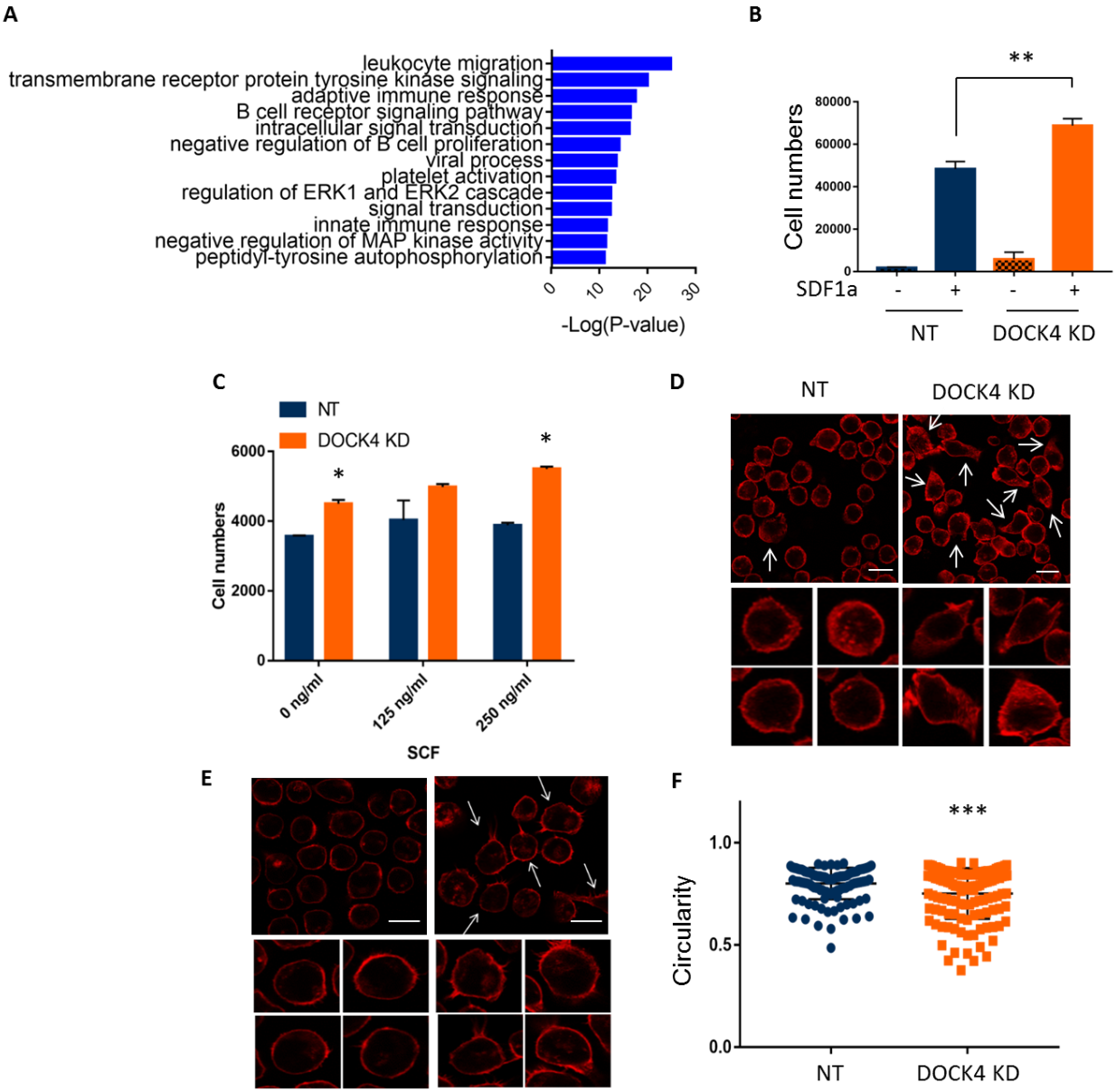

Figure 3.6: Reduced levels of DOCK4 leads to increased cell migration and cell morphology in HSCs.

Figure 3.6, continued: Reduced levels of DOCK4 leads to increased cell migration and cell morphology in HSCs. (A) Differentially phosphorylated proteins displayed in table 1 were used for *in silico* gene ontology pathway analysis to predict functional pathways associated with identified phosphoproteins. Predicted functional pathways are displayed graphically. (B) Transwell cell migration assays performed to compare differences in cell mobility/migration in HSCs expressing normal and reduced levels of DOCK4. Data are represented as mean ±SEM from four biological replicates (**$P < 0.005$; Student's *t* test.). (C) Twenty four hours post DOCK4 siRNA nucleofection into TF1 cells, control and DOCK4 knockdown TF1 cells were subjected to *in vitro* transwell migration assay. Data are represented as mean ±SEM from two technical replicates (*$P < 0.05$; Student's *t* test). Representative data from two independent experiments are shown. (D) Changes in HSC morphology following knockdown of DOCK4 was determined by staining for cytoskeletal F-actin and analyzed by immunofluorescence microscopy. Cells which depicted spread morphology with bundled actin at the leading edges are shown in white arrows (Scale bar, 15μM). Individual cells at high magnification showing pronounced cell spreading and bundled F-actin when DOCK4 levels were reduced. (E) Control and DOCK4 knocked down TF1 cells were stained for actin and analyzed by immunofluorescence microscopy. Cells which depicted spread morphology with bundled actin at the leading edges were marked by white arrows (Scale bar, 15μM). Individual cells at high magnification showing cell spreading and bundled F-actin when DOCK4 levels were reduced. (F) Cell shape/circularity was measured in HSCs expressing normal and reduced levels of DOCK4 using circularity parameter in Fiji image analysis software. A minimum of 100 cells from four random fields were quantified (***$P < 0.0005$; Student's *t* test.). NT – Non-targeting control.

In follow up experiments, I quantified the extent of cell spreading in DOCK4 knocked down (50% knockdown) cells and cells expressing normal levels of DOCK4 by computing circularity values using the built-in circularity feature available in the Fiji software. This quantitation revealed that cell spreading was significantly increased when DOCK4 levels were reduced in HSCs as indicated by the decrease in circularity values (Figure 3.6F).

vi) Reduction of LYN, SHIP1 or SHP1 protein levels or their enzyme activity decreases HSC migration

Given that LYN, SHIP1 and SHP1 are downstream of DOCK4, I next determined whether the LYN kinase and its two down-stream targets SHIP1 and SHP1 were involved in regulating HSC migration. I reduced the expression levels of LYN, SHIP1 or SHP1 in HSCs by 50% or greater by knocking down these proteins using specific siRNAs (Figure 3.7A-C). Using these cells, I performed *in vitro* transwell migration assays and compared their migration to cells that expressed LYN, SHIP1 and SHP1 at normal levels. The results of these experiments revealed that reduced expression of LYN or SHIP1 or SHP1 led to a significant decrease in the migration of HSCs compared to the controls (Figure 3.7D). I extended these studies and performed a series of experiments where I exposed HSCs to increasing concentrations of inhibitors of LYN kinase, SHIP1 and SHP1 and evaluated their migration response. These studies demonstrated a dose dependent decrease in HSC migration (Figure 3.7E-G). Taken together increased migration of HSCs observed in cells expressing reduced levels of DOCK4 seemed to be as a result of each of the three signaling molecules identified in this study.

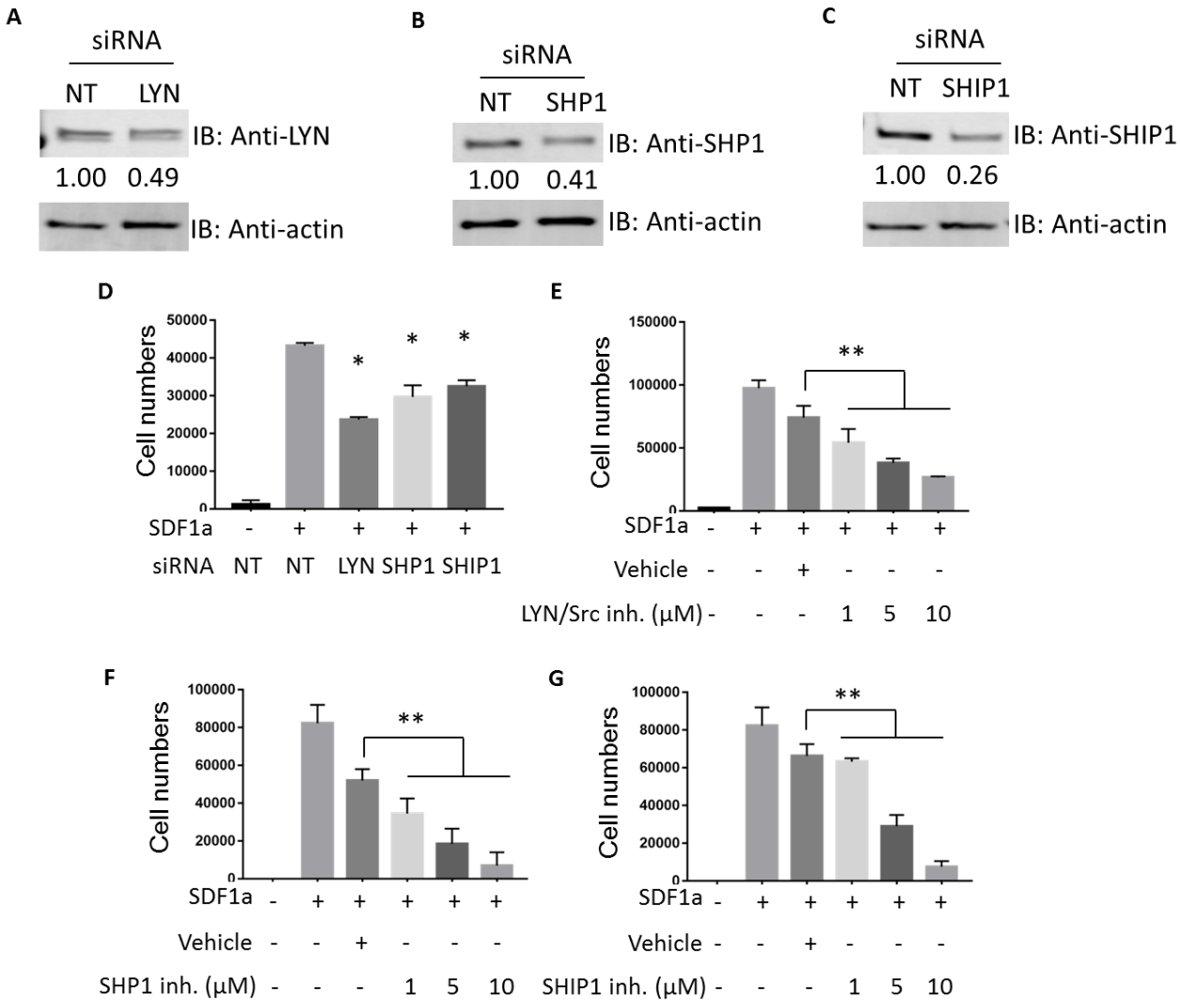

Figure 3.7: LYN kinase, phosphatases SHIP1 and SHP1 regulate HSC migration downstream of DOCK4. Twenty-four hours post siRNA nucleofection immunoblotting analysis was performed to test knockdown of (A) LYN, (B) SHP1 and (C) SHIP1 in primary HSCs. (D) Transwell migration assays performed following knockdown of LYN, SHP1 or SHIP1 by using specific siRNAs in HSCs. Data are represented as mean ±SEM from three technical replicates (*$P < 0.05$; Student's *t* test). Data are representative of three biological replicates. (E, F and G) Transwell migration assays performed on HSCs expressing normal levels of DOCK4 exposed to increasing concentrations of LYN/Src inhibitor (RK20449), SHP1 inhibitor (TPI-1) and SHIP1 inhibitor (3AC) respectively. Data are represented as mean ±SEM from three technical replicates (**$P < 0.005$; One-way ANOVA).

vii) Inhibitors of LYN, SHIP1 and SHP1 restore normal HSC migratory properties in DOCK4 deficient cells

Next, I interrogated whether inhibition of LYN kinase, SHIP1 or SHP1 can reverse the increased migration observed in HSCs expressing reduced levels of DOCK4. I performed *in vitro* transwell migration assays using HSCs expressing normal and reduced levels of DOCK4 in the presence and absence of pharmacological inhibitors of LYN kinase, SHIP1 or SHP1. As expected, in the absence of LYN/Src inhibitor, DOCK4 deficient HSCs exhibited significant increase in transwell migration when compared to the controls (Figure 3.8A). However, in the presence of LYN/Src inhibitor, the increased migration exhibited by the DOCK4 knocked down cells was significantly blunted and returned to migration levels exhibited by DOCK4 intact HSCs (Figure 3.8A). In a similar manner, increased migration exhibited by DOCK4 deficient HSCs was also significantly reduced in the presence of pharmacological inhibitors of SHIP1 and SHP1 (Figure 3.8B, C). Taken together, these studies provide evidence that aberrant migration resulted by reduced DOCK4 levels can be restored to normal levels by pharmacologically targeting its downstream targets LYN or SHIP1 or SHP1.

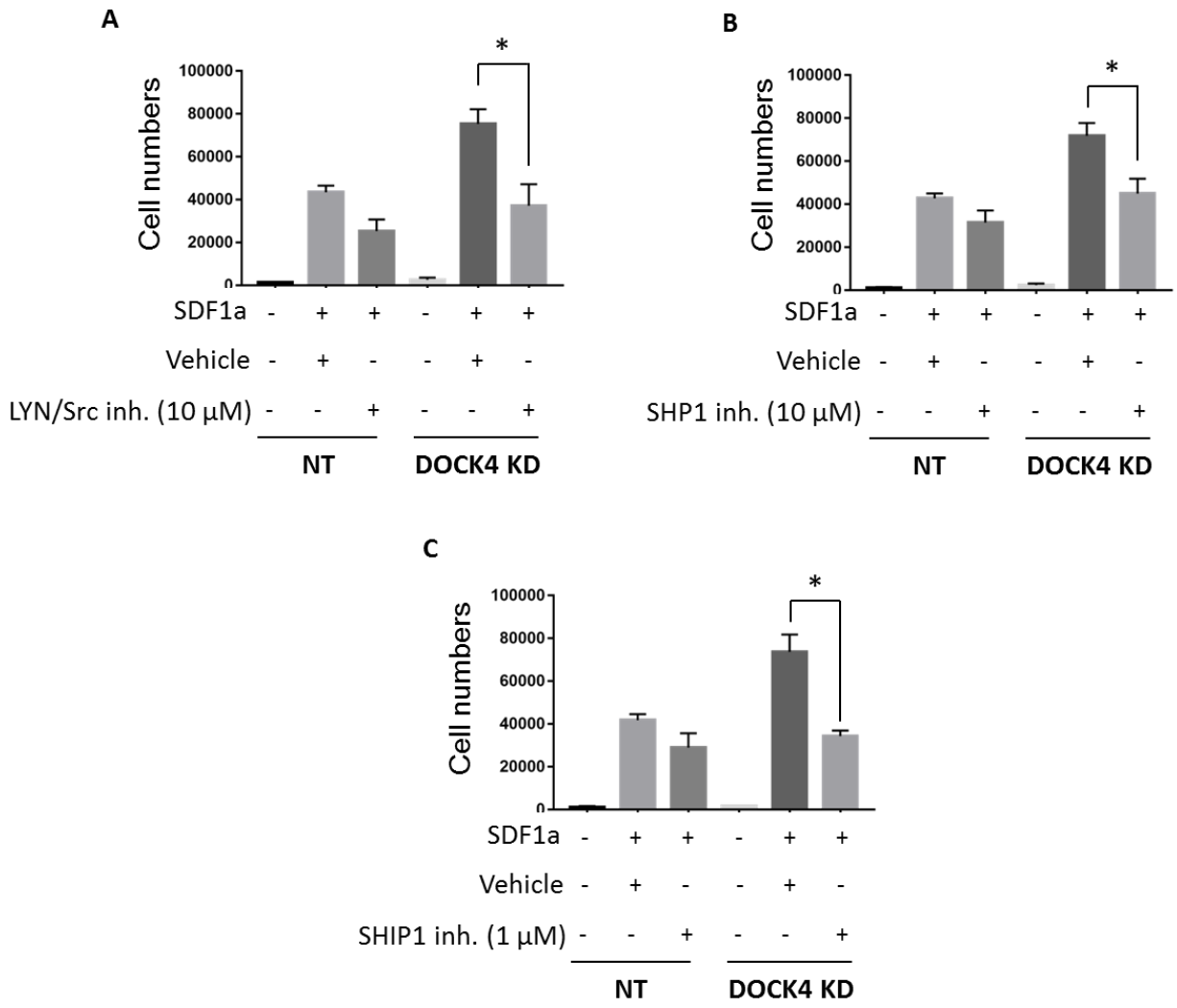

Figure 3.8: Inhibition of LYN or SHP1 or SHIP1 activities reverse increased migration exhibited by DOCK4 deficient HSCs. (A) Transwell migration assays performed on HSCs expressing reduced levels of DOCK4 in the presence or absence of LYN/Src inhibitor (RK20449) (B) SHP1 inhibitor (TPI-1) and (C) SHIP1 inhibitor (3AC). Data are represented as mean ±SEM from three technical replicates (*$P < 0.05$; Student's *t* test). Data are representative of three biological replicates. NT – Non-targeting control.

viii) Inhibition of SHP1 promotes erythroid differentiation in -7/(del)7q MDS samples

Since anemia is central to morbidity and mortality of MDS patients, I investigated whether one or more of the inhibitors of down-stream effectors of DOCK4 are capable

of improving erythroid differentiation. I setup hematopoietic colony assays using MDS HSCs (Table 3) in the presence and absence of inhibitors of LYN/SRC kinase (RK20449), SHIP1 (3AC) and SHP1 (TPI-1) under conditions to promote erythroid colony formations. The results of these experiments revealed that LYN/SRC kinase inhibitors suppressed formation of erythroid colonies, whereas the SHIP1 inhibitor, 3AC, showed no change in colony numbers in -7/(del)7q MDS patient HSCs (data not shown). However, MDS patient samples that were exposed to the SHP1 inhibitor exhibited a 50% increase in erythroid colonies as well as up to five-fold increase in hemoglobin content without suppressing overall colony numbers (Figure 3.9A-D). In agreement with these data morphology of the erythroid colonies was larger, darker red in appearance compared to HSCs from -7/(del)7q MDS patients that were not exposed to the inhibitor. In addition, enumeration of differential colonies showed a shift from myeloid to erythroid under the culture conditions that was used in these experiments.

To test whether pharmacological inhibition of SHP1 under conditions where DOCK4 expression was at 50% will result in improved erythroid differentiation, we performed methyl cellulose colony assays using HSCs that have been treated with DOCK4 siRNAs to reduce DOCK4 expression to haploinsufficient levels in the presence or absence of SHP1 inhibitor. These experiments revealed that exposure of cells expressing reduced levels of DOCK4 to SHP1 inhibitor significantly increased the erythroid colonies, whereas cells expressing normal levels of DOCK4 showed no increase in colony numbers after exposure to the same inhibitor in comparison with the vehicle treated controls (Figure 3.9E).

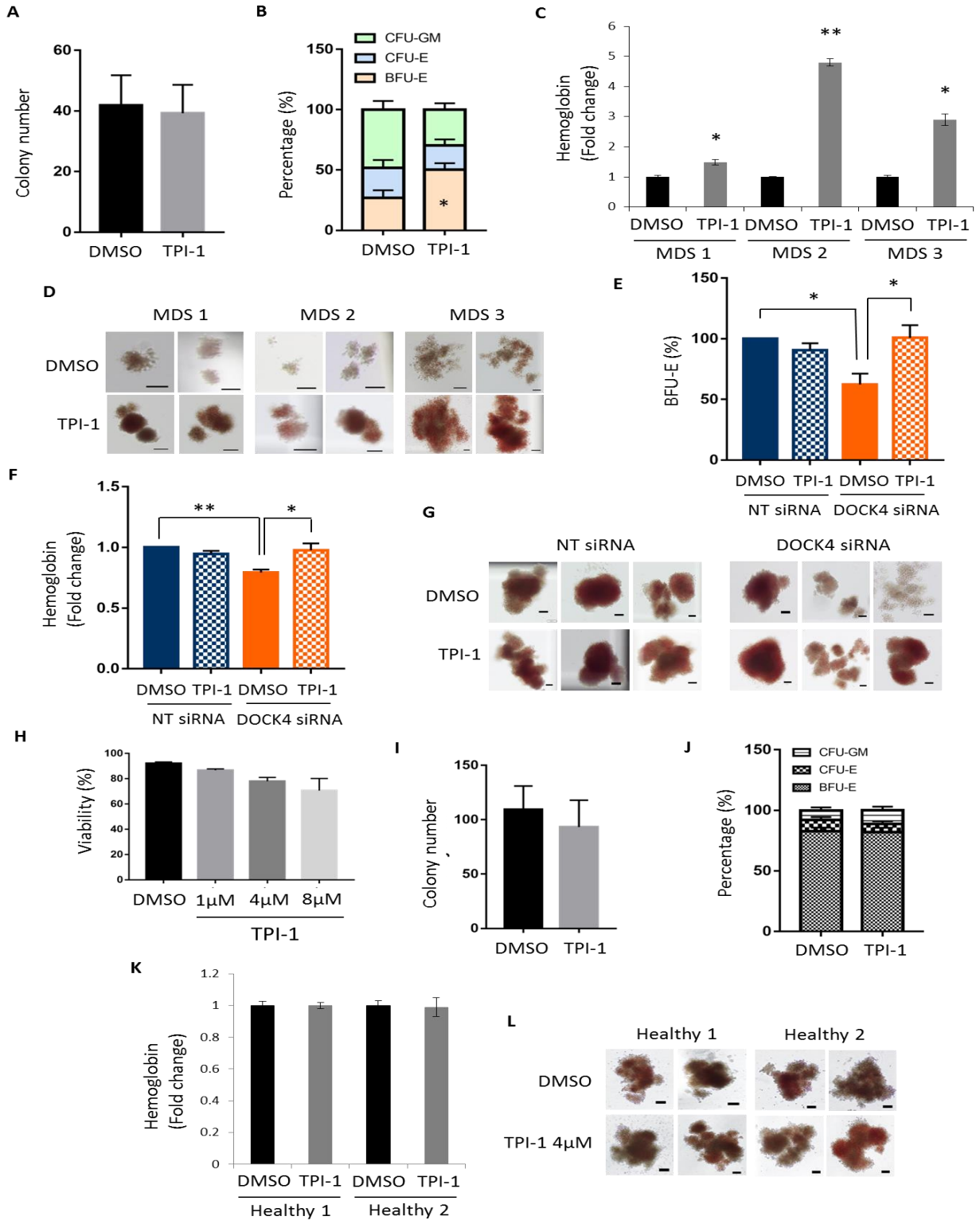

Figure 3.9: Inhibition of SHP1 activity promotes erythroid differentiation in DOCK4 deficient MDS.

Figure 3.9, continued: Inhibition of SHP1 activity promotes erythroid differentiation in DOCK4 deficient MDS.CD34+ stem/progenitor cells were purified from -7/(del)7q MDS patients bone marrow mononucleated cells and methylcellulose colony assays were setup in the presence or absence of SHP1 inhibitor, TPI-1 (4μM). After 14-16 days of culture under differentiation conditions, (A) Total number of colonies enumerated from each arm of the experiment. Data are mean ±SEM from seven different -7/(del)7q MDS patients. (B) Scoring for early erythroid (BFU-E), late erythroid (CFU-E) and myeloid (CFU-GM) (*$P < 0.05$; Student's *t* test.). Data are mean ±SEM from seven different -7/(del)7q MDS patients. (C) ELISA performed to determine beta hemoglobin expression. Data are represented as mean ±SEM from three technical replicates (*$P < 0.05$; **$P < 0.005$; Student's *t* test.). (D) Photomicrographs depicting colony morphology and the extent of hemoglobin after 14-16 days in methylcellulose (Scale bar, 100μM). 24 hrs following DOCK4 knockdown in HSCs, methylcellulose colony assays were setup in the presence or absence of SHP1 inhibitor, TPI-1 (4μM). After 14-16 days of culture under erythroid differentiation conditions, (E) Percentage of erythroid colonies enumerated from each arm of the experiment. Data are mean ±SEM from four biological donors. (*$P < 0.05$; Student's *t* test.). (F) ELISA performed to determine hemoglobin expression. Data are representative of five biological replicates (*$P < 0.05$; ** $P < 0.005$; Student's *t* test.). (G) Photomicrographs depicting colony morphology and the extent of hemoglobin after 14-16 days in methylcellulose (Scale bar, 100μM). (H) Primary HSCs were treated with increasing doses of SHP-1 inhibitor, TPI-1 for 48 hours and viability was analyzed by staining with acridine orange-propidium iodide (AO-PI dye) using Nexcelom automated cell counter. Data are mean ±SEM from four biological replicates. Methylcellulose colony assays were setup using 1500 HSCs from healthy donors in the presence/absence of SHP-1 inhibitor, TPI-1 (4μM). After 14-16 days under differentiation conditions, (I) Number of colonies formed was scored. Data are mean ±SEM from three biological replicates. (J) Frequencies of colonies of different lineages were scored. Data are mean ±SEM from three biological replicates. (K) ELISA was performed to determine beta hemoglobin expression. Data are represented as mean ±SEM from three technical replicates. (L) Colony morphologies were analyzed after 14-16 days in methylcellulose (Scale bar, 100μM).

In addition, SHP1 inhibitor increased the hemoglobin levels and size of the erythroid colonies in the experimental arm of the study compared to the control arm (Figure 3.9F, G). SHP1 inhibition did not have any impact on differentiation of HSCs expressing normal levels of DOCK4 (Figure 3.9E-L). Taken together, these results highlight SHP1 as an attractive therapeutic target in MDS with DOCK4/-7/(del)7q defects.

ix) Increased HSPC mobilization into the peripheral circulation in -7/(del)7q MDS patients

Since increased migration of HSCs within the bone marrow can lead to increased HSPC mobilization, I examined peripheral blood samples from patients that are haplo-insufficient for *DOCK4* (-7/(del)7q) expression. Flow cytometry analysis was performed to determine the percentages of CD34+ sub-population within the CD45+ population using peripheral blood samples from healthy individuals, non -7q MDS patients and -7/(del)7q MDS patients. We found that compared to non -7q MDS samples, percent CD34+ cells in -7/(del)7q MDS samples were approximately 8.8 fold higher (Figure 3.10A-B).

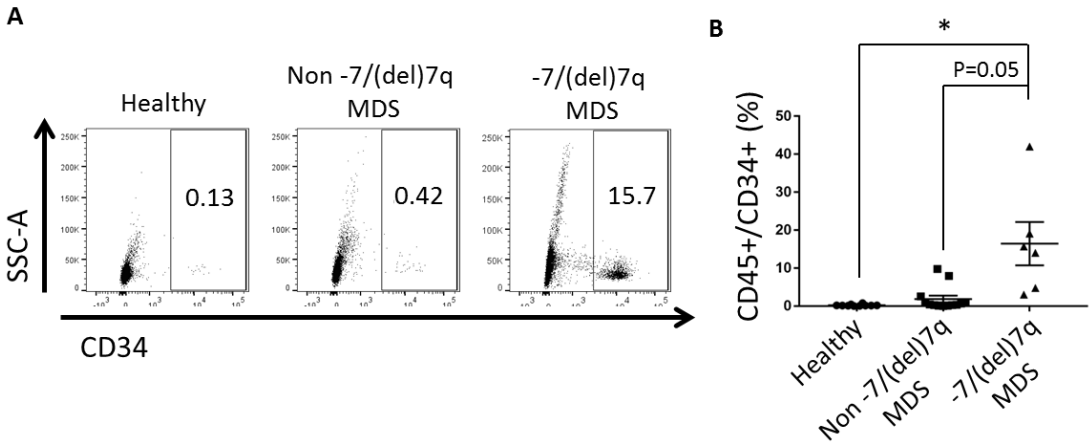

Figure 3.10: Increased HSPC mobilization into the peripheral circulation in -7/(del)7q MDS patients. (A) Peripheral blood mononucleated cells were isolated from healthy, non- -7/(del)7q and -7/(del)7q MDS patient peripheral blood samples and flow cytometry analysis was performed to determine the percentages of CD34+ cells in these samples. Representative flow plot from one individual from each category is depicted. (B) Quantitation of CD34+ cells from healthy (N=10), non- -7/(del)7q (N=13) and -7/(del)7q (N=6) MDS peripheral blood mononuclear cells (*$P < 0.05$; Student's *t* test.).

3. d). Conclusion

In this chapter, I used a population of early-stage human primary hematopoietic stem cells (HSCs), as defined by expression of surface marker proteins CD34 and CD90 to identify downstream signaling networks regulated by DOCK4. Furthermore, I determined the functions of DOCK4 and the consequences of reduced DOCK4 expression in early hematopoietic stem cells. These studies revealed several phosphatases and kinases are regulated by DOCK4. I demonstrate that DOCK4 regulated tyrosine phosphorylation of a large number of signaling proteins resulting in significant increases in global phospho-tyrosine levels. Using mass spectrometry phosphoproteomic approaches, I precisely identified LYN, SHP1 and SHIP1 as most significantly impacted (hyper tyrosine-phosphorylated) proteins. LYN kinase directly phosphorylated phosphatases SHP1 and SHIP1 at tyrosine sites 536 and 1021 respectively. Low DOCK4 levels led to increased stem cell migration, which was blunted in the presence of pharmacological inhibitors of LYN or SHP1 or SHIP1. In DOCK4 deficient MDS patient samples (-7/(del)7q), I observed increased numbers of CD34+/CD45+ cells in circulation. Lastly, I demonstrated that pharmacological inhibition of SHP1 in DOCK4 deficient HSCs from MDS patients can improve erythroid differentiation. Altogether, this study has identified a new signaling network that can be leveraged to potentially overcome the functional defects that arise due to reduced expression of DOCK4 in MDS (Figure 3.11).

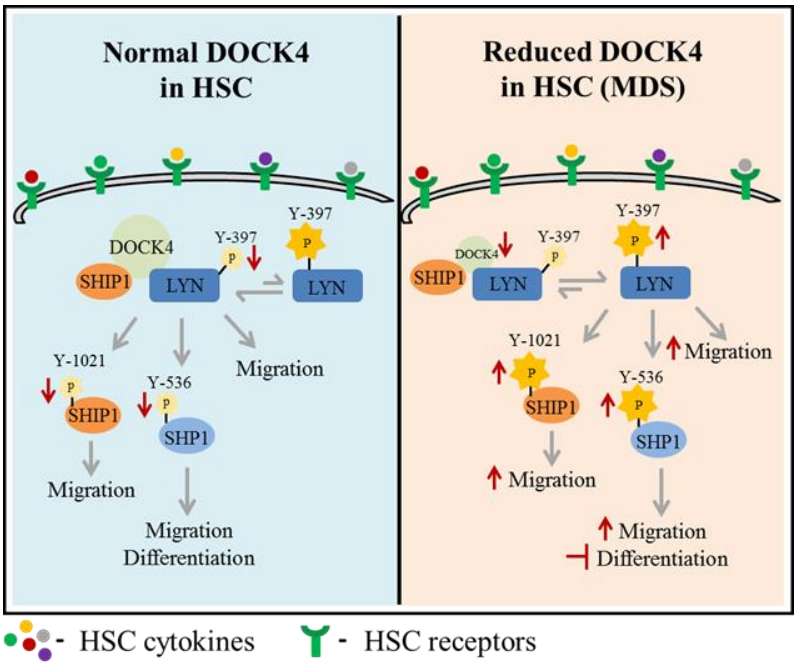

Figure 3.11: Schematic diagram depicting DOCK4 signaling pathway in HSCs.

Table 2: Differentially tyrosine phosphorylated proteins in cells with reduced DOCK4 levels

Protein names	Gene names	Phospho Site	Fold Change (Z-score)
Tyrosine-protein phosphatase non-receptor type 6	*PTPN6* (SHP1)	536	5.43
Phosphatidylinositol 3,4,5-trisphosphate 5-phosphatase 1	*INPP5D* (SHIP1)	865	4.36
Neural Wiskott-Aldrich syndrome protein	*WASL*	256	2.77
Tyrosine-protein kinase Lyn;Tyrosine-protein kinase HCK	*LYN;HCK*	397;411	2.45
Signal transducer and activator of transcription 3	*STAT3*	705	1.76
Glycogen synthase kinase-3 beta;Glycogen synthase kinase-3 alpha	*GSK3B;GSK3A*	216;279	1.58
SHC-transforming protein 1	*SHC1*	427	-2.76
CWF19-like protein 2	*CWF19L2*	201	-2.8
Glucose 1,6-bisphosphate synthase	*PGM2L1*	383	-4.2

Table 3: MDS Patients Characteristics

Patient	Sample source	Age (years)	Sex	MDS subtype	Karyotype	Hemoglobin (g/dL)	IPSS-R
MDS1	BM	74	M	RCMD	Complex -7	12	2
MDS2	BM	65	M	RCMD	-7	6.5	7
MDS 3	BM	47	F	CMML	-7	11.5	NA
MDS	PB	88	F	RA	-7	8.9	2.5
MDS 5	BM	77	F	RCMD	Complex -7	11.4	2
MDS 6	BM	63	M	RCMD	Complex -7	12.7	1
MDS 7	BM	75	M	RCMD	Complex -7	9.8	1

BM – Bone Marrow; PB – Peripheral Blood; RA – Refractory Anemia; RCMD – Refractory Cytopenia with Multilineage Dysplasia; CMML – Chronic Myelo-Monocytic Leukemia.

Author contributions

I conceptualized, led, designed and performed the vast majority of the experiments in this study which is accepted for publication in Clinical Cancer Research. However, this is a collaborative effort from all the authors. Their contributions are listed below.

Kuo, W., Jeong, J., Liu, H – Assistance in performing hemoglobin ELISA, immunoprecipitations, LYN kinase activity assay and siRNA nucleofection experiments respectively at University of Chicago.

Choudhary, G., Gordon-Mitchell, S., Bhagat, T – Assistance in processing MDS patient samples at Albert Einstein College of medicine.

McGraw, K.L., Gurbuxani, S.K., List, A.F., Verma, A – Provided MDS patient samples at Moffitt Cancer Center, Albert Einstein College of medicine and University of Chicago.

Verma, A – Supervised the work at Albert Einstein College of medicine.

Wickrema, A – Conceptualized and supervised the study

CHAPTER 4 - MATERIALS AND METHODS

MATERIALS AND METHODS

4. a). Hematopoietic stem cell culture

CD34+ hematopoietic stem/progenitor cells were purified from G-mobilized peripheral blood of healthy donors purchased from All Cells Inc or Key biologicals, Inc using the CliniMACS instrument. Purified cells were cultured in Isocove's modified Dulbecco's medium (IMDM, Lonza) containing 15% FBS (Life Technologies), 15% human serum and supplemented with 2 units/ml Erythropoietin (EPO), 50 ng/ml Stem Cell Factor (SCF) and 10 ng/ml Interleukin-3 (IL3). Throughout the entire 17 day culture duration a strict cytokine feeding regimen was followed as described previously to promote lineage commitment and terminal differentiation (Kang et al. 2008; Madzo et al. 2014).

In experiments where CD34+ cells from peripheral blood or bone marrow samples from MDS patients were used, mononuclear cells (MNC) were obtained by ficoll-hypaque separation and CD34+ cells were purified using EasySep CD34 positive selection kit (Stemcell Technologies, Inc.) according to the manufacturer's protocol. In experiments where cryopreserved patient samples were used, initially thawed MNCs were cultured under short-term expansion conditions (IMDM with 20% FBS, 20ng/mL TPO, 20ng/mL FLT3-L, 50ng/mL SCF, and 50ng/mL IL-6) for two days prior to CD34+ purification using the EasySep CD34 selection kit, and subsequently cultured under erythroid differentiation conditions.

Flow cytometry analysis and cytospun slides of cells were prepared on-days 3, 7, 10, 13 and 17 for monitoring of terminal differentiation during the erythroid program. Benzidine and hematoxylin staining of cytospun slides were performed as described previously (Wickrema et al. 1992).

In the experiments involving HSCs, purified cells were cultured in Stemspan SFEM II (Stemcell technologies Inc.) supplemented with 50 ng/ml thrombopoietin (TPO), 50ng/ml stem cell factor (SCF), 50 ng/ml Fms-related tyrosine kinase-3 ligand (FLT3-L), 50 ng/ml interleukin-3 (IL3), and 50 ng/ml interleukin-6 (IL-6). Benzidine-hematoxylin staining of the cytospun HSCs were performed as previously described (Wickrema et al. 1992). In the experiments involving cytokine deprivation and exposure, HSCs were washed twice to get rid of cytokines and cultured in IMDM containing 1% (v/v) BSA fraction V (Fisher Scientific) for 3 hours. Following this, the cells were exposed to cytokines for 15 minutes at a concentration of 250 ng/ml. Specific cytokines and cytokine cocktail used in experiments are described in figure legends appropriately.

TF1 erythroleukemia cells were purchased from ATCC and cultured in Roswell Park Memorial Institute (RPMI; Gibco) containing 10% (v/v) FBS, supplemented with 4 ng/ml granulocyte-macrophage colony stimulating factor (GM-CSF). HEK293 cells were cultured in Dulbecco's modified Eagle medium (DMEM; Gibco) containing 10% (v/v) FBS. All the cytokines were purchased from R&D systems.

All the MDS patient samples were obtained after informed consent and approval from the Institutional Review Boards of University of Chicago, Albert Einstein College of Medicine and Moffitt cancer center.

4. b). Zebrafish *dock4a* analysis

Wild-type (AB/TU hybrid) and transgenic zebrafish were maintained at 28.5°C and staged as described (Kimmel et al. 1995). The Tg(*gata1:dsRed)* reporter line was used to examine red blood cell circulation (Traver et al. 2003). Morpholino oligomers (MOs) were purchased from Gene Tools (Philomath). Two distinct MOs were designed to target around the *dock4a* initiation ATG (5'-GTACCATCCTTCACATTTTT) or across the exon2-intron2 splice site (5'- AATAAAACAGCGATTACCTTCACAT). Blast analysis indicated the MOs are specific for *dock4a.* All morphants were compared to stage matched embryos that were injected with a control morpholino (Genetools, standard control MO). Each MO was titrated by injection into 1-4 cell fertilized embryos to determine a minimal dose for the reproducible phenotype. Microinjection of MOs was performed using a PLI-100 Pico-Injector (Harvard Apparatus). Semi-quantitative RT-PCR was used to measure the efficacy of the splice-blocking MO, using primers: F, 5'-TCGAGGAATGGTTCAGCATGGACT; R, 5'- TCTCTCCGTGGGACCAAATCCAAA. The same primers were used to generate a PCR fragment that was cloned into pCR-BluntII-TOPO plasmid (Life Technologies) as a clone used for generating the in situ hybridization probe, following digestion with Not1 and RNA synthesis using SP6 polymerase. Whole-mount in situ hybridization was performed as described (Alexander et al. 1998). Embryos were treated with 0.003% phenylthiourea (PTU; Sigma) to block pigmentation. Following fixation in 4% paraformaldehyde (Sigma), embryos were treated with 10 μg/mL proteinase K (Roche). Hybridization was performed at 68°C in 57% formamide buffer (Roche) with digoxigenin-labeled RNA probes (Roche).

4. c). O-dianisidine staining

Embryos were treated with PTU at 24 hpf. Embryos were dechorionated at 48 hpf and stained for 20 minutes in the dark in 0.6 mg/ml o-dianisidine (Sigma), 0.01M sodium acetate (pH 4.5), 0.65% H_2O_2 and 40% (v/v) ethanol. Embryos were washed with dH_2O three times and post-fixed in 4% paraformaldehyde for 1hour at 4C and rinsed in PBST. Embryos were transferred from 1X PBST into 25%, 50%, and 75% glycerol/PBST for microscopy.

4. d). Harvesting cells from zebrafish embryos

For each experiment, approximately 200 *dock4a* morphant tg (*gata1:dsred*) -or control embryos were dechorionated at 48 hpf and placed into 1.5 ml tubes. Embryos were dissociated by manual agitation with a pellet pestle (Fisher) and trypsinized with pre-warmed TrypLE (Life Technologies) at 32^{o} C for 20-30 minutes on a rotator. Trypsinized samples were pipetted through a 35 µm cell strainer into a 5 ml tube, trypsin was inhibited by addition of 4 ml FACS buffer (L-15 medium supplemented with 1% heat inactivated FBS, 0.8 mM $CaCl_2$, 50 U/ml penicillin, and 0.05 mg/ml streptomycin) followed by addition of FBS to 7.5% final concentration. Cells were pelleted at 300 RCF for 5 min and then washed with FACS buffer. Dissociated embryonic cells were resuspended in 1ml of FACS buffer. FACS was performed on a Vantage cell sorter (BD) into PBS. Alternatively, the cells were washed one more time and resuspended in PBS before analyzing with ImageStreamX^{TM}.

4. e). siRNA and lentiviral transductions

In experiments where *DOCK4* knockdown by siRNA was carried out for immunofluorescence microscopy studies, day 5 cells were plated at a density of 0.5x10^6 cells/ml of erythroid culture media in a 12-well plate and incubated at 37 ^{o}C for 30 minutes. The transfection cocktail solution required per well was prepared in a 1.5ml micro-centrifuge tube by mixing 50 µl of X-vivo 15 (Lonza) with 3 µl of TransIT-siQUEST transfection reagent (Mirus) and 50nM siRNA (scrambled control and *DOCK4* siRNA, purchased from Thermo Scientific Inc.). Each cocktail was mixed well and incubated at room temperature for 15 minutes. The mixture was added to the 12 well plate and mixed gently. After incubating for 48 hours, the cells were collected for immunofluorescence microscopy and RNA isolation.

Custom-made high titer (1 X 10^9) lentiviral particles expressing shRNAs (control and *DOCK4*) were purchased commercially (Systems BioSciences Inc). The control and *DOCK4* shRNA (5' CTCAGTATTTGCAGATATA 3') sequences were cloned into the pGreenPuro shRNA expression lentivector (Systems Biosciences Inc) with the H1 promoter driving shRNA and the EF1 promoter driving the GFP. Lentiviral transductions were carried out on 24-well plates coated with retronectin (Takara Bio Inc). Day 0 CD34+ cells were thawed and pre stimulated in X-vivo 10 base media (Lonza) supplemented with SCF (10 µg/ml), TPO (5 µg/ml), IL3 (10 µg/ml), FLT3L (10 µg/ml) for 48 hours (Millington et al. 2009). On the day of infection, an appropriate amounts of viral soup (both control and *DOCK4* shRNA) to infect 100,000 cells at MOI 20 was added to 0.25 ml of complete X-vivo 10 media. This mixture was added to the retronectin coated well and incubated for 90 minutes. The plate with the virus was then centrifuged for 25

minutes at 4ºC at 800x*g*. 100,000 cells were then added to each well along with polybrene at a concentration of 5 µg/ml and the final volume was made up to 0.5 ml with the X-vivo 10 complete media. The virus-cells-polybrene mixture was incubated for 30 minutes at 37ºC and the plate was centrifuged for 25 minutes at 27ºC at 400x*g*. The plate was incubated for 20 hours at 37ºC. The following day (day 1) cultures were centrifuged and media containing polybrene and virus was removed prior to re-culture in erythroid culture media. The following day puromycin was added at 2 µg/ml concentration to select for transduced cells. On day 6 cells were collected for RAC activity assays, western blotting, and RNA isolation. In addition flow cytometry and cytospun cells were carried out to ascertain the extent of terminal differentiation in cells lacking DOCK4.

4. f). Immunofluorescence Microscopy

CD34+ stem/progenitor cell derived erythroblasts from healthy donors and MDS patients were immobilized on Alcian blue coated cover slips and fixed with 2% formaldehyde solution as previously described (Kang et al. 2008). Briefly, cells were permeabilized with PBS containing 0.5% Triton-X100 for 5 minutes and the cover slips were washed once with PBS for 5 minutes and then blocked with 1% BSA for 20 minutes. Cells were subsequently stained for actin with Phalloidin-Texas Red (dilution 1:160, Life Technologies) for 30 minutes in a humidifying chamber. Following multiple washes with PBS the actin-stained cells on cover slips were mounted onto slides using Prolong gold antifade™ reagent (Life Technologies).

Similarly, control and DOCK4 knockdown HSCs were immobilized on Alcian blue-coated coverslips and stained for actin with Phalloidin. Images were captured using Leica STED-SP5 confocal microscope using a 63x oil immersion lens. Fiji Image J software was used to quantify the promigratory cells using the circularity feature. At least 100 cells from 4 random fields were analyzed.

4. g). Flow cytometry

Cells were stained with antibodies for transferrin receptor, CD71 (BD biosciences) and Glycophorin A (eBioscience) at various time points to monitor the erythroid differentiation program.

HSCs were by staining with antibodies for CD34 (BD biosciences), CD90 (eBioscience). In the experiments involving peripheral blood samples from MDS patients, the samples were stained with CD45 (BD biosciences), CD34 and ghost red 780 (Tonbo biosciences Inc.) dye. Samples were analyzed using LSR-Fortessa flow cytometers (BD biosciences) available in the University of Chicago Cytometry and Antibody Technology Facility. FlowJo software was used to analyze the flow cytometry data. TF1 cells were stained with the CD34 antibody and analyzed. Unstained cells and Isotype specific antibody stained cells were used as controls to set gates.

4. h). Multispectral flow cytometry (ImageStreamX^{TM} analysis)

i) Actin disruption quantitation

An ImageStreamX^{TM} (EMD-Millipore/Amnis) multispectral imaging flow cytometer was used to quantify the extent of actin filament disruption in erythroblasts derived from culturing CD34+ stem/progenitor cells (Comparing healthy and MDS patient samples). Erythroblasts treated with Cytochalasin D (5 µg/ml for 5 hours, Sigma) and Rac1 inhibitor (100 µM for 5 hours, Calbiochem) were used as positive controls. Cells were fixed, permeabilized and stained for F-actin using fluorescently labeled (Texas Red) phalloidin as described previously (Wickrema et al. 1994).

Acquisition of cellular images was performed on an ImageStreamX using 50mW of 561nm laser light and an emission filter range of 594nm – 660nm. Both brightfield (B.F.) and fluorescence images were acquired at 60x magnification. A cell classifier was set on B.F. area to exclude small debris and system focus beads. Up to 10,000 events per sample were acquired.

Analysis to determine populations of cells with intact actin filaments and populations with disrupted actin was performed using the IDEAS 6.0 software package available through Amnis, Inc (www.amnis.com). Intact, single cells that were suitably in focus were gated utilizing a hierarchical gating strategy starting with bright field. Area and B.F. “Aspect Ratio” (single cells of appropriate size) and then by the B.F. “Gradient Root Mean Square” feature (cells in focus). Lastly, cells with no F-Actin fluorescence were excluded from the downstream analysis (typically less than 10%). I employed an algorithm available in the software package that enabled discrimination of defined

fluorescence staining of the F-actin filaments together with quantitation of the length (in microns) of the longest undisrupted actin filament staining seen by the custom-defined “Mask” function of the software. The “Mask” was defined utilizing the built in Spot Mask function. This option obtains bright regions from an image regardless of the intensity differences from one cell to another. The ability to extract bright objects is achieved using an image processing step that erodes the image and leaves only the bright areas. Once the mask properly captured the F-actin filament staining, the “Length” feature was utilized to measure the longest part of the object defined by the mask, wherein cells with intact F-actin filaments would have a long length and cells with disrupted F-actin filaments would have a short length. A sample from a healthy donor for cells with intact F-actin and a Cytochalasin D treated control with disrupted F-actin were used to set the cut-off level on the “Length” parameter defining intact versus disrupted F-actin based on fluorescent staining. The following sequential steps were taken in the analysis of populations from each of the samples that allowed us to develop the cortical F-actin staining index. a) Excluded aggregates and debris by gating cells with moderate B.F. area and high B.F. aspect ratio. b) Selected a level of B.F. “Gradient RMS” to achieve well focused cells (RMS value > 50). c) Gated cells with any level of F-actin staining. d) Applied “Spot Mask” to final subset. e) Plotted the “Length” feature based on the F-Actin “Spot Mask (Intact/Disrupted cut-off value set at a unit of 25).

ii) Quantifying circular/irregular shaped erythroid cells in zebrafish embryos

ImageStreamX^{TM} was also used for quantifying the ratio of circular/irregular cells in the erythroid (Gata1-expressing RFP cells) compartment of control and *dock4a* knockdown zebrafish embryos. A similar strategy as described above was used to eliminate the aggregates and debris. Well focused RFP positive single cells were used in subsequent analysis. Using the built-in 'Erode Mask", a continuous mask was created on the periphery of the cell in both the Brightfield channel and the RFP channel to define the shape of the cell. An IDEAS 6.0 built-in feature called circularity was then used to differentiate between the circular and irregular shaped cells. This feature measures the degree of the mask's deviation from a circle. This measurement is based on the average distance of the object boundary from its center divided by the variation of this distance. Thus, the closer the object to a circle, the smaller the variation and therefore the feature value will be high. On the other hand the more the shape deviates from a circle, the higher the variation and therefore the "Circularity" value will be low. The following sequential steps were taken in the analysis of populations from each of the samples: a) Excluded aggregates and debris by gating cells with moderate B.F. area and high B.F. "Aspect Ratio". b) Selected a level of B.F. "Gradient RMS" to achieve well focused cells (RMS value > 50). c) Gated cells with RFP signal. d) Applied "Erode Mask" to final subset. e) Plotted a graph between the circularity features based on the B.F "Erode Mask" and "RFP Erode Mask" and gates were applied to separate out "Circular" and "Irregular" cells.

4. i). RAC1 G-LISA

Levels of active GTP bound RAC1 were quantified using the G-LISA RAC1 activation assay Biochem Kit (Cytoskeleton, Inc) according to the manufacturer's protocol. In experiments where RBC ghosts or erythroblasts were used, frozen pellets from each preparation was lysed using reagents provided in the RAC1 activation kit.

4. j). RBC ghost preparation

Fresh peripheral blood samples were collected from healthy volunteers and MDS patients with approval from the institutional review board (IRB). RBC ghosts were prepared according to published protocols (Andrews et al. 2002) with minor modifications. Briefly, washed RBCs (devoid of the buffy coat) were suspended at 40% hematocrit containing hypotonic buffer (5 mM Tris-HCl, 5 mM KCl, pH 7.4). Cells were centrifuged at 20,000x*g* for 5 min at 4°C. The pellet obtained (white ghost) was washed two more times in hypotonic buffer. After washing, cells were transferred to micro-centrifuge tubes and centrifuged at 14,000x*g* for 10 minutes at 4°C. The pellets consisting of erythroid ghosts were flash frozen after discarding the supernatant and stored at -80°C until subsequent use in the RAC1 activity assay.

4. k). Immunoblot analysis

In experiments to determine phospho-Adducin levels, cell lysates were prepared (M-PER, lysis reagent Thermoscientific) from day 10 (polychromatic erythroblasts) cells derived from purification and culture of CD34+ cells obtained from healthy donors or

MDS patients. Protein concentrations were determined by the Lowry-Bradford method using a commercially available reagent (Bio-Rad). Electrophoresis was performed in a 4-16% gradient precast SDS gel (Bio-Rad) at 70-100 V using a gel electrophoresis kit (Bio-Rad). The gel was then electro-blotted onto a nitrocellulose membrane (Millipore) in a Semi-dry blot electrophoretic transfer unit (Bio-Rad) using transfer buffer (10mM CAPS + 10% Methanol, pH-11). The nitrocellulose membrane was then incubated in blocking buffer (Li-Cor Biosciences) for 1 hour at room temperature. The membrane was incubated with mouse anti-human phospho-adducin (Ser 726) antibody (dilution 1:1000, Upstate) overnight on a shaker at 4^{o}C. After three PBS-T washes, the membrane was incubated with IRDye 680RD goat anti-mouse IgG (dilution 1:3000, li-cor) for 2 hours on a shaker at room temperature. The membranes were washed three times (5 minutes each) with PBS scanned on the blot scanner (Odyssey CLx, Li-Cor). The blot was probed with an anti-tubulin antibody (dilution 1:2000, Neomarkers) as loading control.

In experiments involving HSCs, cell lysis was performed using phosphorylation lysis buffer comprising 50 mM Hepes (pH 7.3), 150 mM sodium chloride, 1 mM EDTA, 1.5 mM magnesium chloride, 100 mM sodium fluoride, 10 mM sodium pyrophosphate, 200 μM sodium orthovanadate, 10% glycerol, 0.5% Triton X-100, and 1 mM phenylmethylsulfonyl fluoride (Wickrema et al. 1999b). The antibodies used in these experiments are listed here: rabbit polyclonal anti-DOCK4 (dilution 1:500, Proteintech), mouse monoclonal anti-phospho-tyrosine 4G10 (dilution 1:1000, Millipore), rabbit monoclonal anti-phospho-AKT S473 (dilution 1:1000, Cell Signaling), rabbit polyclonal anti-GAPDH (dilution 1:1000, Santa Cruz), rabbit polyclonal anti-phospho-LYN (Y397)

(dilution 1:1000, GeneTex), rabbit polyclonal anti-phospho-SHIP1 (Y1021) (dilution 1:1000, Assay biotechnology), rabbit polyclonal anti- phospho-SHP1 (Y536) (dilution 1:1000, Assay biotechnology), mouse monoclonal anti-LYN (dilution 1:1000, Santa Cruz), mouse monoclonal anti-SHIP1 (dilution 1:1000, Santa Cruz), mouse monoclonal anti-SHP1 (dilution 1:1000, Santa Cruz), rabbit polyclonal anti-GFP (dilution 1:1000, Chromotek), mouse monoclonal anti-Flag (dilution 1:3000, Sigma), mouse monoclonal anti-actin (dilution 1:10000, Neomarkers). Densitometric analyses of bands were performed in Odyssey V3.0 analysis software. The target band intensities were normalized to the band intensities of the loading controls as indicated.

4. l). Fluorescence In-situ hybridization (FISH)

To quantify numbers of clonal malignant cells after *in vitro* culture, day 10 erythroblasts from MDS patients were cytospun (1000-10,000 cells) for further analysis. Cells from the Mono7 cell line (Fujisaki et al. 2002) were used as a positive control. FISH was performed according to the manufacturers' instructions using the dual color Vysis probe D7S486/CEP 7 (7q31 S.O./7p11.1-q11.1 Alpha Satellite DNA S. G.) (Abbott Molecular Inc.) enabling us to detect and quantify cells with loss of 7q. Analysis was performed using a Zeiss Axioplan Epifluorescence microscope.

4. m). QPCR

To quantify DOCK4 expression levels, total RNA was isolated from erythroblasts at different stages of differentiation using the RNeasy Mini Kit (Qiagen) following the

manufacturer's instructions. Isolated RNA was quantified and cDNA synthesized using SuperScript VILO cDNA synthesis kit (Invitrogen). Control samples were prepared without RT enzyme or RNA template. Specific *DOCK4* primers were used (FP: 5' GACCCACACACAGACTGCTTCA 3' and RP: 5' GAGAGGGGGTGAAAGACTGC 3') and the gene expression was quantified using the delta delta CT method using fast SYBR green/Rox real time PCR master mix (Invitrogen). 18S Ribosomal RNA was used as the normalizing control. Primer specificity was verified using melting curve analysis.

In experiments involving HSCs, total RNA was isolated from control and DOCK4 knockdown HSCs 24 hours post siRNA nucleofection using RNeasy Mini kit (Qiagen). Following the extraction, the RNA was quantified and cDNA was synthesized using high capacity RNA to cDNA synthesis kit (Applied Biosystems). qPCR for DOCK4 was performed using human DOCK4 Taqman primers in viia7 thermocycler (Applied Biosystems) using built-in Taqman programs. GAPDH was used as a normalizing control.

4. n). Restoration of DOCK4 expression in MDS patient samples

In order to re-express DOCK4 in MDS patient samples lacking DOCK4 expression, I subcloned the full-length *DOCK4* cDNA (5,901 bp) into the minicircle (System Biosciences) plasmid. The subcloned sequence was verified by DNA sequencing. The minicircle (MC) technology allows expression of large genes efficiently by only containing the circular DNA elements minimally required for sustained

expression in cells once transfected into cells. The production of custom MC DNA was carried out by SBI, Inc (Mountain View), using engineered *E. coli* strain (ZYCY10P3S2T) that allows the production of the minicircles. The minicircle DNA are conditionally produced by an expression of inducible integrase via intramolecular (cis)-recombination. Transfection of minicircles into CD34+ patient derived erythroid progenitors were performed on day 5 of culture and re-expression of DOCK4 was verified by qPCR on day 10 of culture from the same sample that was used in assaying for the restoration of F-actin filament length and cell shape. CFU-E colony forming assays were done by plating 50,000 cells on day 7 following DOCK4 minicircle plasmid transfection on day 5. Enumeration of colonies was carried out on day 14.

4. o). Osmotic fragility assay

Peripheral blood from healthy volunteers and -7/(del7q) MDS patients was Collected and centrifuged al 1,200x*g* to remove the plasma and buffy coat. RBCs were washed thrice with PBS and centrifuged consecutively at 800, 600 and 500x*g* to remove any residual leukocytes. Ten samples of 10% hematocrit (in 100µl volume) were prepared for each blood sample. After that, samples are immediately plunged on ice and 100 µL of cell suspensions are added to 400 µL of buffer of varying NaCl percentages (0, 0.1, 0.2, 0.3, 0.4, 0.5, 0.6, 0.7, 0.8, 0.9 and 1 %). The samples are incubated at 4°C for 20 min and then centrifuged at 1,000x*g* for 10 min. The supernatants are transferred into cuvettes and the absorbance at 540 nm is recorded by a spectrophotometer. Complete hemolysis of RBCs in water is normalized to 100%.

4. p). Nucleofection of CD34+ HSCs

Control (#D-001810-10, Dharmacon Inc. CO, USA) or DOCK4 siRNA (Dharmacon Inc.) was nucleofected into CD34+ HSCs using CD34+ cells nucleofection kit (Lonza) according to manufacturer's protocol. Briefly, 2.5x10^6 cells were nucleofected with 300nM siRNA using the U-08 program in the Nucleofector II machine. Following nucleofection, cells were cultured in Stemspan SFEM II supplemented with 50 ng/ml TPO, 50ng/ml SCF, 50 ng/ml FLT3-L, 50 ng/ml IL3, and 50 ng/ml IL-6 until used for subsequent experiments. Similarly, in the experiments involving knockdown of LYN, SHIP1 or SHP1, respective smartpool siRNA (Dharmacon Inc.) were used. In the experiments involving TF1 cells, control or DOCK4 siRNA was nucleofected using nucleofection kit T (Lonza) according to manufacturer's protocol.

4. q). siRNA sequences

DOCK4 siRNA: GGAGAAAAUUGCACGAUUA. Non-targeting siRNA target sequence 1: UGGUUUACAUGUCGACUAA; target sequence 2: UGGUUUACAUGUUGUGUGA; target sequence 3: UGGUUUACAUGUUUUCUGA; target sequence 4: UGGUUUACAUGUUUUCCUA. LYN siRNA target sequence 1: GCGACAUGAUUAAACAUUA; target sequence 2: GUGAUGUUAUUAAGCACUA; target sequence 3: GAGAUCCAACGUCCAAUAA; target sequence 4: UUACAUCUCUCCACGAAUC. SHIP1 siRNA target sequence 1: CGACAGGGAUGAAGUACAA; target sequence 2: GAAUUGCGUUUACACUUAC; target sequence 3: GCAUUGCCCUUCGGUUAGA; target sequence 4:

UGACAGCGACGAAUCCUAU. SHP1 siRNA target sequence 1: GGAACAAAUGCGUCCCAUA; target sequence 2: AUACAAACUCCGUACCUUA; target sequence 3: UAUGAGAACCUGCACACUA; target sequence 4: GCUCCGAUCCCACUAGUGA.

4. r). Mass spectrometry phosphoproteomics

HSCs that were briefly cultured for three hours were used to knockdown DOCK4 and re-cultured for twenty four hours prior to lysing both DOCK4 knockdown (50%) and DOCK4 intact cells using phosphorylation lysis buffer as described previously (Wickrema et al. 1999b). Protein concentration in the supernatants was determined by a BCA assay. 450 µg of total protein for each of the two samples were reduced and alkylated prior to trypsin digestion. Phosphopeptides from the digests were enriched using TiO2 beads and fractionated them by high pH reverse phase into four fractions each (Yue and Hummon 2013). Each fraction was desalted prior to LC-MS analysis. Nano LC-MS/MS analyses were performed with a 75 µm x 10.5 cm PicoChip column packed with 3 µm Reprosil C18 beads with Dionex UltiMate 3000 Rapid Separation nanoLC coupled to a Q Exactive™ HF Hybrid Quadrupole-Orbitrap™ Mass Spectrometer (Thermo Fisher Scientific Inc, San Jose, CA). A 150 µm x 3 cm trap packed with 3um beads was installed in-line. Peptides were separated in 120min gradient. Data was acquired in data-dependent MS/MS mode with a top-15 method. Dynamic exclusion was set to 20 s and charge 1+ ions were excluded. MS1 scans were collected from 300-2000 m/z with resolving power equal to 60,000. The MS1 automatic gain control (AGC) was set to 3x106. Precursors were isolated with a 2.0 m/z isolation

width, and the HCD normalized collision energy was set to 30%. The MS2 AGC was set to 1x105 with the resolving power set at 30,000. Phosphopeptides in which the phosphorylation sites that can be assigned to a single amino acid with 75% probability or better in at least one sample were filtered. Robust z-scores were computed from the log2 –fold changes to compare knocked down cells vs. control cells and defined a z-score of >= 1.5 as up-regulated and <= -1.5 as down-regulated.

4. s). Plasmid transfection and Immunoprecipitation

Flag-tagged full length DOCK4 plasmid (Yu et al. 2015) (gift from Dr. Linda Van Aelst, CSHL) was co-transfected along with GFP-tagged LYN plasmid (Yoo et al. 2011) (Addgene) or GFP-tagged SHIP1 plasmid (Pauls et al. 2016) (gift from Dr. Aaron Marshall, University of Manitoba, CN) or GFP-tagged SHP1 plasmid (Liu et al. 2007) (Addgene) using Lipofectamine 2000 reagent (ThermoScientific) according to manufacturer's protocol. 24 hours later cells were harvested, lysed and protein concentration was calculated using Lowry-Bradford assay. Protein G dynabeads (ThermoScientific) were coated with indicated antibodies and immunoprecipitation was carried out according to the manufacturer's protocol. GFP-trap beads (Chromotek Inc.) were used to immunoprecipitate GFP-tagged proteins. The eluted samples after immunoprecipitation were analyzed by immunoblotting as described earlier.

4. t). LYN kinase activity assay (endogenous)

LYN kinase activities in DOCK4 knocked down HSCs were measured using the universal tyrosine kinase activity assay kit (Takara) according to the manufacturer's guidelines. Briefly, cytokines deprived and exposed control and DOCK4 knockdown HSCs (1.5 million cells/assay) were lysed using the extraction buffer from the kit and LYN kinase was immunoprecipitated from these samples using 5µg anti-LYN antibody and used in the activity assay. Immunoprecipitation using anti-IgG antibody was used as controls. Elute from the immunoprecipitation was immunoblotted to normalize the LYN activity data.

4. u). LYN kinase activity assay (*in vitro*)

LYN kinase activities in the presence of flag-tagged DOCK4 or recombinant DOCK4 C-terminus were measured using the universal tyrosine kinase activity assay kit (Takara) according to the manufacturer's guidelines. In experiments involving flag-tagged DOCK4, we ectopically expressed Flag-tagged full length DOCK4 in HEK293 cells and immunoprecipitated flag-tagged DOCK4 using anti-Flag coated protein G dynabeads (ThermoFisher) according to the manufacturer's protocol. Following this, increasing amounts of immunoprecipitated flag-tagged DOCK4 as indicated was incubated with 20ng of active recombinant LYN kinase or active recombinant JAK2 kinase. Similarly, in experiments involving recombinant DOCK4 C-terminus, increasing concentration of DOCK4 C-terminus (Proteintech) as indicated was incubated with 20ng of active recombinant LYN kinase or active recombinant JAK2 kinase.

4. v). *In vitro* binding assay

Flag-tagged recombinant DOCK4 C-terminus was generated by cloning DOCK4 C-terminus using primers DOCK4 C-terminus forward primer - 5'-GGTGCCATGGGCCACCATCACCACCATCATCACCACCATCACCCTTTGTTGTCTGACAAACACAC and DOCK4 C-terminus reverse primer - 5'-CACCCTCGAGTCACTTGTCGTCATCGTCTTTGTAGTCTAACTGAGAGACCTTGCGG into pET15b plasmid purchased from Novagen. Following cloning, we produced recombinant flag-tagged DOCK4-C-terminus according to the manufacturer's protocol. 100ng recombinant LYN and 400ng of flag-tagged recombinant DOCK4 C-terminus was incubated overnight along with anti-IgG or anti-Flag coated magnetic beads in a rotating shaker at 4^{o}C. Immunoprecipitation followed by immunoblot analysis was performed as described earlier.

4. w). *In vitro* kinase assays

Multiple doses of recombinant active LYN kinase (SignalChem) were incubated along with 250ng recombinant active SHIP1 (SignalChem) or recombinant SHP1 (SignalChem) in the presence of ATP at a final concentration of 100uM. The total volume of each in vitro reaction was 25µl using kinase dilution buffer I (SignalChem) and deionized water. The samples were incubated in a 30^{o}C water bath for 15 minutes. The kinase reaction was stopped by adding 8.3µl 4X laemlii buffer (Bio-Rad) and boiling the samples for 5 minutes. The samples were then analyzed by immunoblotting. In the

samples where inhibitor was added, the LYN/Src inhibitor, RK20449 (Selleck Inc.) was added to a final concentration of 500nM.

4. x). Transwell migration assays

HSC migration assays were performed using transwells. Briefly, 150,000 HSCs were suspended in 100µl of starvation media (IMDM containing 1% (vol/vol) BSA fract V) and was added to the upper chamber of the 5-µm-pore transwell insert (24-well plate format transwell, Corning). 0.5ml of starvation media with various concentrations (0-100ng/ml) of chemokine stromal derived factor-1 alpha (SDF-1α) was added to the bottom chamber. The transwell plates were incubated for 4 hours in a 37°C 5% CO_2. The transwell inserts were carefully removed and the migrated cells in the bottom chamber were resuspended. Samples were obtained from the bottom chamber and stained with acridine orange and propidium iodide nuclear dyes (AO-PI dye, Nexcelom). The stained samples were enumerated using Nexcelom auto 2000 cell counter (Nexcelom). All the migration experiments were performed in triplicates. In the experiments involving inhibitor treatments (LYN/Src inh. – RK20449 (Selleck Inc.), SHIP1 inh. – 3AC (EMD Millipore Inc.) and SHP1 inh. – TPI-1 (Cayman Inc.)), the cells were exposed to inhibitors for 1 hour in IMDM containing 1% BSA media prior to adding to the top chamber of the transwell. Migration assays with TF1 cells were performed as described previously (Prebet et al. 2010).

4. y). Database for Annotation Visualization and Integrated Discovery (DAVID) analysis

Proteins that were hyper-tyrosine phosphorylated greater that 1.5 fold and tyrosine phosphorylated proteins identified only in DOCK4 knockdown samples were subjected to functional annotation analysis available in the DAVID website (http://david.abcc.ncifcrf.gov/) Gene ontology option GOTERM_BP_ALL was selected and a functional annotation chart generated.

4. z). Methylcellulose colony assays and hemoglobin ELISA

1500 HSCs from healthy or MDS patients were cultured in methylcellulose (Stemcell technologies Inc. #H4434) supplemented with 2 Units/ml erythropoietin for 14-16 days in the presence/absence of SHP1 inhibitor, 4μM TPI-1 (Cayman Inc.). DMSO was used as a vehicle control. After 14-16 days, the colonies were enumerated and imaged. Images of the colonies were captured using Olympus microscope at 10X magnification. Following colony enumeration, cells were collected from the methylcellulose plates and hemoglobin levels were quantitated using hemoglobin ELISA kit (Abcam) according to the manufacturer's guidelines.

4. aa). Statistical analysis

The error bars are computed as mean ± SE. Paired Student's t tests were performed to determine the statistical significance between the samples. In experiments involving dose responses, one-way ANOVA test was performed to determine statistical

significance. Experiments were from three biological replicates, and values with $P < 0.05$ were considered statistically significant. Multivariate analysis for survival and DOCK4 expression was performed by adjusting for IPSS scores using SAS software.

CHAPTER 5 - DISCUSSION AND PERSPECTIVES

DISCUSSION AND PERSPECTIVES

5. a). Discussion

Anemia and dysplastic erythropoiesis are predominant clinical manifestations of myelodysplasia. Deletion of chromosome 7/7q is a common cytogenetic alteration in MDS and is associated with a poor prognosis (Cazzola et al. 2013). The commonly deleted segment contains a large number of genes, and studies have not identified the genes whose haplo-insufficiency can lead to myelodysplastic phenotypes. Two recent studies identified *CUX1* and *MLL3* as 7q genes that can act as tumor suppressors in MDS, but these and others have not been implicated in erythropoietic defects that are a hallmark of MDS (McNerney et al. 2013; Chen et al. 2014). Another recent study using iPS cells generated from -7/(del)7q MDS implicated reduced expression of *HIPK2*, *ATP6V0E2*, *LUC7L2* and *EZH2* in aberrant early hematopoiesis, but did not specifically evaluate their role in erythropoiesis (Kotini et al. 2015). My work has identified *DOCK4* as a candidate 7q pathogenic gene by demonstrating that it is reduced in MDS stem and progenitor cells and that its reduced expression leads to dysplastic erythropoiesis *in vivo* and *in vitro.*

Human Red cells are characterized by a biconcave shape that is essential for their functionality. These cells require the coordinate formation of actin cytoskeleton that relies on activation of RAC1 GTPases during erythropoiesis. My work revealed that low *DOCK4* expression in -7/(del)7q MDS RBCs, or in normal erythroblasts depleted of *DOCK4*, leads to diminished RAC1 GTPase activity resulting in disruption of actin

filaments and hyperphosphorylation of ADDUCIN, an actin protofilament stabilizing protein. These changes in the erythroid membrane skeleton have a profound impact on the overall integrity of the cell, as seen by an inability to complete the terminal differentiation program and increase in hemolysis of erythrocytes. Previous studies have shown that *Rac1*$^{-/-}$*/Rac2*$^{-/-}$ mice have impairment of skeletal stability and increased phosphorylation of ADDUCIN in the erythroid compartment (Kalfa et al. 2006). The significance of increased ADDUCIN phosphorylation at Ser-726 has far reaching implications because this biochemical modification allows cleavage of ADDUCIN by caspase, yielding a 74-kDA fragment that does not dissociate from the cytoskeleton (van de Water et al. 2000). Furthermore the Ser-726 is in the MARCKS domain, which acts as a substrate for protein kinase A (PKA) and protein kinase C (PKC) and therefore potentially providing us an opportunity to intervene and reverse hyperphosphorylation of ADDUCIN in -7/(del)7q MDS (Matsuoka et al. 1996; Matsuoka et al. 1998). The findings in this study provide mechanistic insight into how chromosomal deletion or epigenetic silencing of a signaling intermediate (DOCK4) can have far reaching implications for cellular morphology and cell membrane stability leading to dysplasia in the erythroid lineage, with possible therapeutic implications.

Previous work from our group has shown that DOCK4 can also be transcriptionally regulated by DNA methylation and aberrant hypermethylation of the promoter can be seen in some cases of MDS (Zhou et al. 2011b). In fact, some of the samples examined by me without deletion of chromosome 7 did show that reduced expression of DOCK4. The expression of DOCK4 increases during erythroid differentiation and in our studies, we observed a major role for DOCK4 is in the post-

lineage commitment phase. Additionally, since DOCK4 can be epigenetically silenced (Zhou et al. 2011b) and numerous epigenetic marks are preserved between HSCs and differentiated cells (Figueroa et al. 2009; Polo et al. 2010), it is possible that lower levels of DOCK4 in HSCs is a potential predictor of lower levels in differentiated cells in those samples, thus accounting for the higher red cell transfusion requirements in these cases. Erythroid cells generated from these samples also demonstrated dysplastic actin filament disruption further demonstrating the important role played by DOCK4 in myelodysplasia. Pathogenesis of MDS is multifactorial and studies have shown that cooperative effects of different mutations and deletions can lead to abnormal stem cell cycling, differentiation and malignant clone expansions seen in this disease (Malcovati et al. 2007; Will et al. 2012). Since deleted segments of 7q contain large numbers of genes with *DOCK4* being one of them, our data suggests that reduction of this gene can contribute to erythroid dysplasia and contribute to the anemia phenotype seen in MDS.

Myelodysplastic syndromes are one of the most common blood malignancies in the elderly and usually present as low blood counts in this population. Dysplasia is challenging to quantify and is often based on a subjective histological assessment. Our demonstration of F-actin network disruption in MDS erythroblasts together with the development of a new approach to quantify the extent of disruption in the F-actin network (multispectral flow cytometry) raises the possibility that one could use this approach as a quantifiable measure of erythroid dysplasia.

Re-expression of DOCK4 in -7/(del)7q MDS led to a significant improvement in erythroid differentiation. This suggests that reactivation of DOCK4 pathway can alleviate anemia in MDS. Due to its large size, lack of complete structural information and

absence of enzyme-like domain, pharmacological targeting of DOCK4 directly for activation presents as a challenging task. To overcome this pitfall, I identified key signaling pathways/intervention points regulated by the adaptor protein DOCK4. As a classical adaptor protein DOCK4 lacks catalytic activity but provide multiple docking sites for other signaling elements and regulate their catalytic activities or stabilities via protein-protein interaction. Using HSCs, I showed that reduced levels of DOCK4 results in global increase in tyrosine phosphorylation both with and without exposure to hematopoietic cytokines. Among the tyrosine phosphorylated proteins LYN kinase, phosphatases SHIP1 and SHP1 were quite prominent.

Although activation of phosphatases, SHP1 and SHIP1 leads to de-phosphorylation of their targets, overall reduced expression of DOCK4 resulted in phosphorylation of a large number of proteins due to activation of kinases. As result, I observed a net gain in global phosphorylation when DOCK4 levels were low. Overall, the mechanism of action of DOCK4 is to act as a negative regulator of protein phosphorylation. LYN kinase, SHP1 and SHIP1 identified in this study are examples of downstream targets of DOCK4.

Increased cell migration and morphological changes I observed when DOCK4 levels were low are consistent with functions that have been ascribed to LYN kinase based on previously published work (O'Laughlin-Bunner et al. 2001; Nakata et al. 2006; Orschell et al. 2008; Wheeler et al. 2012; Röselová et al. 2018). Previous studies have also shown that increased HSC migration was consistent with increase in HSC mobilization (Borneo et al. 2007; Gur-Cohen et al. 2015), which I also observed in -7/(del)7q MDS patient blood samples. My current work seemed to suggest that

increased HSC mobilization is specifically associated with -7/(del)7q MDS since MDS samples with other chromosomal abnormalities did not exhibit increased HSC mobilization. Furthermore, my current findings showing increased phosphorylation/activation of SHIP1 and SHP1 is also consistent with previous findings showing both these phosphatases are substrates for LYN kinase (Baran et al. 2003; Mkaddem et al. 2017). In fact, *Lyn* deficient mice exhibit similar phenotypic characteristics to mice lacking *Ship1* and *Shp1* (Harder et al. 2004). Based on these data I show DOCK4, LYN kinase, SHIP1 and SHP1 are all part of the same signaling cascade and because deficiency of DOCK4 in HSCs impacts all three enzymes one could target this pathway to reverse functional deficiency observed in these HSCs.

In fact, when I evaluated for terminal differentiation of MDS patient derived CD34+ cells under culture conditions that was permissive for erythroid differentiation, cells that were exposed to the SHP1 inhibitor (TPI-1) showed pro-differentiation characteristics (increased BFU-Es and hemoglobinization). These results were in agreement with previous studies using healthy cells, which had demonstrated that SHP1 phosphatase is a negative regulator of erythroid differentiation (Sharlow et al. 1997; Bittorf et al. 1999; Wickrema et al. 1999a). Therefore, by blocking SHP1 activity one can potentially reverse anemia in -7/(del)7q MDS patients. Recent work by Taolin Yi and colleagues (Kundu et al. 2010) have demonstrated that TPI-1 and its analogues are non-toxic when administered to mice and is effective in reducing the melanoma tumor burden in mice (Kundu et al. 2010). In another study it was shown that mice lacking *Shp1* do not respond to TGF-beta (Jiang et al. 2018). Since previous work by us and others have shown that in MDS TGF-beta signaling is overactive and inhibiting this

pathway can restore hematopoiesis in MDS (Zhou et al. 2008; Zhou et al. 2011a; Shastri et al. 2017), my current work identifying SHP1 inhibition leads to terminal erythroid differentiation provides a unique opportunity to develop inhibitors of SHP1 that might be effective in treating MDS patients.

Kinase inhibitors such as midostaurin are effective in high-risk Flt3 mutated MDS/AML patients, whereas pro-erythroid differentiation agents such as luspatercept and erythropoietin are effective in low-risk MDS patients. My findings in this dissertation highlight the potential use of SHP1 inhibitor as a pro-erythroid differentiation agent in intermediate/high risk MDS patients with chromosome 7 deletions. Future investigation of SHP1 inhibitor as single agent and in combination with luspatercept or 5-azacytidine/decitabine as a treatment strategy in -7/del(7q) MDS is warranted.

In summary, my work provides the first mechanistic basis of erythroid dysplasia due to reduced expression of a gene identified on chromosome 7q and demonstrates that disrupted F-actin filaments can be seen at the single-cell level in MDS. In addition, my work has uncovered novel functions and signaling networks regulated by DOCK4 that can be targeted to reverse the aberrant phenotypes arising due to reduced expression of DOCK4 in hematopoietic cells.

5. b). Future directions

The following sub-topics in this section highlight the far-reaching implications of the findings presented here, in the context of MDS. Although these are very exciting avenues to pursue, these directions are beyond the scope of my tenure as a graduate student. These studies will be performed by other current/new members of the Wickrema research group.

i) Delineate the function of DOCK4 in HSC differentiation, localization and mobilization *in vivo*

My studies show that *DOCK4* expression is reduced in CD34+ HSPCs in MDS and AML patient samples. However, there is no information about the significance and roles of DOCK4 in the hematopoietic stem cells (HSC) compartment. In my preliminary studies, knockdown of *DOCK4* in human HSCs aberrantly increased the migration of HSCs. Furthermore, we observed increased mobilization of HSCs in MDS patients with chromosome 7 deletions. Therefore, in order to uncover the role/s of DOCK4 in regulating key functions associated with HSCs, we will determine the functional consequences of reduced levels of DOCK4 expression on a) overall HSC maintenance and differentiation, b) niche localization of HSCs in the bone marrow and c) mobilization of HSCs into peripheral circulation. These experiments will be performed *in vivo* using our recently generated conditional *Dock4* knockout mouse model. In order to overcome the early embryonic lethality of homozygous deletion of Dock4(Abraham et al. 2015) and to completely dissect the role of Dock4 in hematopoietic stem cell maintenance and

function, we generated a conditional Dock4 knockout mouse to induce full deletion of Dock4 in a tissue-specific and time-dependent manner. The mouse was generated by targeting exon 39 using CRISPR/Cas9 technology. Exon 39 codes for a region of DHR2 which is involved in actin regulation and other signaling processes(Upadhyay et al. 2008; Carnell and Insall 2011). We bred the Dock4 flox/flox (f/f) mice with mice that express a *Vav-Cre* to generate the line *Vav-Cre; Dock4 f/f. Vav-Cre* enables Dock4 knock down only in the hematopoietic cells. We are currently in the process of performing the proposed experiments using this mouse model.

ii) Identify the molecular mechanisms by which DOCK4 regulates LYN/SHIP1/SHP1 signaling axis

DOCK4 is a signaling intermediate that is known to participate in multiple signaling cascades. In this thesis, I have shown DOCK4 acts as a guanine exchange factor which activates RAC1 GTPase to maintain F-actin homeostasis in differentiating erythroblasts. In addition, DOCK4 also acts as a receptor scaffolding protein in HSCs by regulating the activities of kinase LYN, phosphatases SHIP1 and SHP1 downstream of HSC receptors. Preliminary data from my experiments have revealed that DOCK4 is phosphorylated in hematopoietic cells (Figure 5.1). Even though I have identified the signaling pathways downstream of DOCK4, the precise mechanisms by which DOCK4 is activated and how it regulates the activities of downstream kinases and phosphatases are not known.

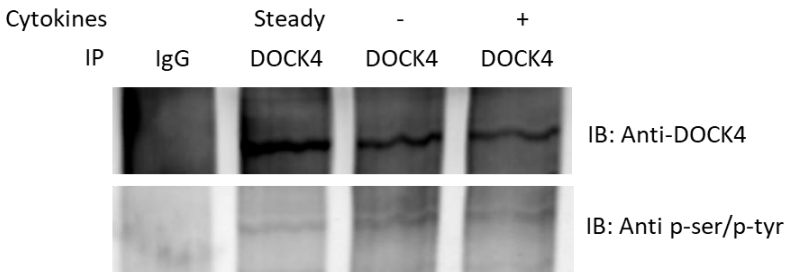

Figure 5.1: DOCK4 is phosphorylated in hematopoietic cells. TF1 hematopoietic cell line was maintained under steady-state, cytokine deprived or cytokine exposed conditions. Total cell lysates from these samples were used to immunoprecipitate DOCK4 with anti DOCK4 antibody followed by immunoblotting. DOCK4 phosphorylation was determined using a pan phospho-serine/tyrosine antibody. Subsequently the anti-DOCK4 antibody was used to confirm the band phosphorylated on the Western blot correspond to the molecular size of DOCK4. Cytokines used were SCF, IL3 and GM-CSF.

To identify the specific receptor which activates DOCK4, we will expose DOCK4 reduced HSCs to each of the HSC cytokines (TPO, SCF, FLT3, IL3 and IL6) individually and perform immunoblotting using anti-phospho-tyrosine antibody. The results from these experiments will enable us to pinpoint the specific receptor tyrosine kinases that activate DOCK4. In order to investigate upstream mediators of DOCK4 activation we will focus on two candidates which are known to regulate DOCK4 phosphorylation directly and/or known downstream targets of DOCK4 in other systems. A recent study demonstrated that DOCK4 is phosphorylated at serine/threonine site/s by Glycogen synthase kinase 3 (GSK3) (Upadhyay et al. 2008). In another independent study it was shown DOCK4 is also phosphorylated by RhoG (Hiramoto et al. 2006). To test whether these two kinases regulate the phosphorylation of DOCK4 in HSCs, we will determine if DOCK4 phosphorylation is abolished by GSK3 and RhoG inhibition using commercially available inhibitors. Total cell lysates will be immunoprecipitated with anti DOCK4 antibody and immunocomplexes will be separated by SDS-PAGE electrophoresis. DOCK4 phosphorylation will be determined using a pan phospho-serine/theronine

antibody. In addition, we will test other candidate kinases which are important in HSCs such as JAK2, SYK, LYN kinase. If we observe that DOCK4 phosphorylation is regulated by these upstream kinases, we will determine the functional role of these kinases in HSCs. This will elucidate the exact upstream pathways that are involved in DOCK4 mediated events in erythropoiesis. Furthermore, we will identify the specific sites phosphorylated on DOCK4 by performing mass spectrometry phosphoproteomics.

To delineate the mechanism by which DOCK4 regulates the activities of downstream proteins, we will identify the specific regions within the DOCK4 protein that a) interacts with its downstream proteins and b) regulates the activities of downstream kinases and phosphatases.

iii) Determine the involvement SHP1 in the pathogenesis of anemia associated with DOCK4 reduced MDS

My recent studies have shown that reduced levels of DOCK4 resulted in increased phosphorylation of SHP1. However, the specific contributions of SHP1 in the pathogenesis of anemia in MDS are not known. The results from my preliminary studies indicated that pharmacological inhibition of SHP1 improved erythroid differentiation of DOCK4 reduced MDS HSCs *in vitro*. Although our studies clearly demonstrate the involvement of SHP1 in erythroid differentiation, the underlying molecular mechanisms as well as the status of SHP1 in MDS are unknown.

Firstly, we will delineate the status of SHP1 in MDS and uncover the mechanisms of SHP1 alterations in MDS. These will involve mutational analysis,

promoter DNA methylation analysis and copy number analysis using bone marrow mononucleated cells in a large cohort of MDS samples. Specifically, we will analyze the phosphorylation status of SHP1 in these samples by performing phosphor-flow cytometry analysis using anti-SHP1 Y536 antibody and the expression of SHP1 by performing QPCR for SHP1 in CD34+ HSCs enriched from MDS samples. We will also analyze previously published sequencing datasets of MDS patients to explore the status of SHP1. We will correlate the levels of SHP1 in MDS to overall survival and clinical characteristics of anemia in these patients.

To elucidate the molecular mechanisms by which SHP1 controls HSC differentiation into erythroid lineage, we will perform the following experiments in parallel. Firstly, we will perform immunoprecipitation coupled with mass spectrometry to precisely identify the proteins which are directly regulated by SHP1 through direct interactions. Indeed, preliminary results from my experiments clearly demonstrate that SHP1 interacts with many proteins in primary human HSCs (Figure 5.2). To identify the molecular pathways regulated by SHP1, we will perform parallel mass spectrometry phosphoproteomics and RNA sequencing using our CD34+ primary human HSC differentiation model in which we will either reduce or increase the expression of SHP1 using lentivirus. Following this we will perform DAVID pathway analysis to specifically pinpoint the mechanisms regulated by SHP1. We are in the process of acquiring the SHP1 knockdown and expression lentiviral particles.

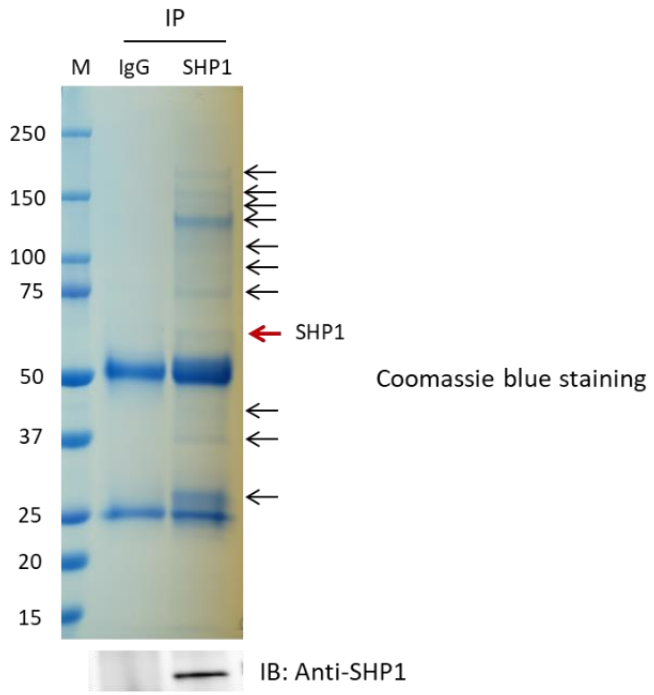

Figure 5.2: SHP1 interacts with multiple proteins in HSCs. (Top) Detection of SHP1-multiprotein complex following SHP1 immuno-precipitation using anti-SHP1 antibody in HSCs by Coomassie staining. (Bottom) Detection of SHP1following SHP1 immuno-precipitation using anti-SHP1 antibody in HSCs by immunoblotting. Red arrow – SHP1, Black arrows – SHP1-interacting proteins.

Finally, we will test the efficacy of the pharmacological SHP1 inhibitor to improve erythroid differentiation *in vivo.* We will perform these experiments by xenografting primary MDS samples into MISTRG (M-CSF$^{h/h}$ IL-3/GM-CSF$^{h/h}$ SIRPa$^{h/h}$ TPO$^{h/h}$ RAG2$^{-/-}$ IL2Rg$^{-/-}$) humanized mice which is capable of promoting erythroid differentiation of MDS samples *in vivo* (Song et al. 2019). Following xenografting, we will test the efficacy of SHP1 inhibitor as a single agent as well as in combination in the current standard of care, decitabine.

iv) Develop multispectral flow cytometry (Imagestream) actin disruption assay as an early prediction/diagnostic tool for MDS

In this study, we used Imagestream multispectral imaging to develop strategies to quantify morphological changes in erythroid cells. Specifically, we quantitated the changes in cell shape and the extent of actin disruption in these cells. Our results in this study highlight the potential of multispectral flow cytometry in not only improving the diagnosis of erythroid dysplasia but also detecting MDS early.

Existing flow cytometry based erythroid dysplasia diagnosis strategies are reliable; however, these strategies are solely based on protein expression levels and completely ignore morphological changes observed by visualization of the BM sections (Della Porta et al. 2006). Dysplastic cells are characterized by several morphological abnormalities such as i) larger size, ii) irregular shapes, iii) multi-nucleated/nuclear dysplasia and iv) increased cytoplasm to nuclear ratio (Invernizzi et al. 2015). Here, we have shown that Imagestream can be utilized to quantify cell shape and size changes. Furthermore, nuclear morphologies and cytoplasm-nuclear ratio can also be analyzed by staining the cells with cell permeable nuclear stain such as DRAQ5. Imagestream can enable the amalgamation of existing flow cytometry-based strategies and morphological analyses to diagnose erythroid dysplasia which can make the diagnosis powerful and reliable.

MDS patients with reduced levels of DOCK4 exhibited a significant increase in disruption of F-actin organization in erythroid cells. In addition, we observed actin disruption in some patients with unexplained anemia who also had reduced levels of DOCK4. Unexplained anemia (UA) is a condition in elderly in which anemia couldn’t be

attributed to nutritional deficiency, inflammatory disease or renal insufficiency(Makipour et al. 2008). Recent studies have shown that approximately 23% of MDS patients had unexplained anemia prior to MDS progression(Goldberg et al. 2008). We hypothesize that analyzing for F-actin disruption might identify the group of patients who will progress to MDS earlier. This is a valid hypothesis because we observed F-actin disruption in 2 out of the 3 UA patients in this study. Stratification of UA patients based on actin disruption would allow the physicians to monitor/treat these patients closely for any signs of MDS. For this purpose, we will perform F-actin disruption analysis using multispectral flow cytometry using primary differentiating erythroblasts derived from CD34+ HSCs of UA patients. We will correlate the results from these experiments to MDS progression from UA and DOCK4 expression levels.

REFERENCES

Abraham S, Scarcia M, Bagshaw RD, McMahon K, Grant G, Harvey T, Yeo M, Esteves FOG, Thygesen HH, Jones PF, Speirs V, Hanby AM, Selby PJ, Lorger M, Dear TN, Pawson T, Marshall CJ, Mavria G (2015) A Rac/Cdc42 exchange factor complex promotes formation of lateral filopodia and blood vessel lumen morphogenesis. Nat Commun 6:7286 . doi: 10.1038/ncomms8286

Alexander J, Stainier DY, Yelon D (1998) Screening mosaic F1 females for mutations affecting zebrafish heart induction and patterning. Dev Genet 22:288–99 . doi: 10.1002/(SICI)1520-6408(1998)22:3<288::AID-DVG10>3.0.CO;2-2

Alvarez-Dominguez JR, Hu W, Yuan B, Shi J, Park SS, Gromatzky AA, van Oudenaarden A, Lodish HF (2014) Global discovery of erythroid long noncoding RNAs reveals novel regulators of red cell maturation. Blood 123:570–81 . doi: 10.1182/blood-2013-10-530683

Andrews DA, Yang L, Low PS (2002) Phorbol ester stimulates a protein kinase C-mediated agatoxin-TK-sensitive calcium permeability pathway in human red blood cells. Blood 100:3392–9 . doi: 10.1182/blood.V100.9.3392

Athanassiou G, Symeonidis A, Kourakli A, Missirlis YF, Zoumbos NC (1992) Deformability of the Erythrocyte Membrane in Patients with Myelodysplastic Syndromes. Acta Haematol 87:169–172 . doi: 10.1159/000204753

Baran CP, Tridandapani S, Helgason CD, Humphries RK, Krystal G, Marsh CB (2003) The inositol 5'-phosphatase SHIP-1 and the Src kinase Lyn negatively regulate macrophage colony-stimulating factor-induced Akt activity. J Biol Chem 278:38628–36 . doi: 10.1074/jbc.M305021200

Bejar R, KE S, BA C, Abdel-Wahab O, DP S, Galili N, Raza A, Kantarjian H, RL L, Neuberg D, Garcia-Manero G, BL. E (2012) Validation of a prognostic model and the impact of mutations in patients with lower-risk myelodysplastic syndromes. J Clin Oncol 30:3376–3382

Bejar R, Levine R, Ebert BL (2011a) Unraveling the molecular pathophysiology of myelodysplastic syndromes. J Clin Oncol 29:504–15 . doi: 10.1200/JCO.2010.31.1175

Bejar R, Steensma DP (2014) Recent developments in myelodysplastic syndromes. Blood 124:2793–2803 . doi: 10.1182/blood-2014-04-522136

Bejar R, Stevenson K, Abdel-Wahab O, Galili N, Nilsson B, Garcia-Manero G, Kantarjian H, Raza A, Levine RL, Neuberg D, Ebert BL (2011b) Clinical effect of point mutations in myelodysplastic syndromes. N Engl J Med 364:2496–506 . doi: 10.1056/NEJMoa1013343

Bittorf T, Seiler J, Zhang Z, Jaster R, Brock J (1999) SHP1 Protein Tyrosine Phosphatase Negatively Modulates Erythroid Differentiation and Suppression of Apoptosis in J2E Erythroleukemic Cells. Biol Chem 380:1201–1209 . doi: 10.1515/BC.1999.152

Borneo J, Munugalavadla V, Sims EC, Vemula S, Orschell CM, Yoder M, Kapur R (2007) Src family kinase–mediated negative regulation of hematopoietic stem cell mobilization involves both intrinsic and microenvironmental factors. Exp Hematol 35:1026–1037 . doi: 10.1016/J.EXPHEM.2007.03.017

Carnell MJ, Insall RH (2011) Actin on disease--studying the pathobiology of cell motility using Dictyostelium discoideum. Semin Cell Dev Biol 22:82–8 . doi: 10.1016/j.semcdb.2010.12.003

Cazzola M, Della Porta MG, Malcovati L (2013) The genetic basis of myelodysplasia and its clinical relevance. Blood 122:4021–34 . doi: 10.1182/blood-2013-09-381665

Challen GA, Boles N, Lin KK, Goodell MA (2009) Mouse Hematopoietic Stem Cell Identification And Analysis. Cytometry A 75:14 . doi: 10.1002/CYTO.A.20674

Challen GA, Sun D, Jeong M, Luo M, Jelinek J, Berg JS, Bock C, Vasanthakumar A, Gu H, Xi Y, Liang S, Lu Y, Darlington GJ, Meissner A, Issa J-PJ, Godley LA, Li W, Goodell MA (2012) Dnmt3a is essential for hematopoietic stem cell differentiation. Nat Genet 44:23–31 . doi: 10.1038/ng.1009

Chen C, Liu Y, Rappaport AR, Kitzing T, Schultz N, Zhao Z, Shroff AS, Dickins RA, Vakoc CR, Bradner JE, Stock W, LeBeau MM, Shannon KM, Kogan S, Zuber J, Lowe SW (2014) MLL3 Is a Haploinsufficient 7q Tumor Suppressor in Acute Myeloid Leukemia. Cancer Cell 25:652–665 . doi: 10.1016/j.ccr.2014.03.016

Cimmino L, Dolgalev I, Wang Y, Yoshimi A, Martin GH, Wang J, Ng V, Xia B, Witkowski MT, Mitchell-Flack M, Grillo I, Bakogianni S, Ndiaye-Lobry D, Martín MT, Guillamot M, Banh RS, Xu M, Figueroa ME, Dickins RA, Abdel-Wahab O, Park CY, Tsirigos A, Neel BG, Aifantis I (2017) Restoration of TET2 Function Blocks Aberrant Self-Renewal and Leukemia Progression. Cell 170:1079–1095.e20 . doi: 10.1016/J.CELL.2017.07.032

Côté J-F, Vuori K (2002) Identification of an evolutionarily conserved superfamily of DOCK180-related proteins with guanine nucleotide exchange activity. J Cell Sci 115:4901–13

Debruyne DN, Turchi L, Burel-Vandenbos F, Fareh M, Almairac F, Virolle V, Figarella-Branger D, Baeza-Kallee N, Lagadec P, kubiniek V, Paquis P, Fontaine D, Junier M-P, Chneiweiss H, Virolle T (2018) DOCK4 promotes loss of proliferation in glioblastoma progenitor cells through nuclear beta-catenin accumulation and subsequent miR-302-367 cluster expression. Oncogene 37:241–254 . doi: 10.1038/onc.2017.323

Della Porta M, Malcovati L, Invernizzi R, Travaglino E, Pascutto C, Maffioli M, Gallí A, Boggi S, Pietra D, Vanelli L, Marseglia C, Levi S, Arosio P, Lazzarino M, Cazzola M (2006) Flow cytometry evaluation of erythroid dysplasia in patients with myelodysplastic syndrome. Leukemia 20:549–555 . doi: 10.1038/sj.leu.2404142

Dzierzak E, Philipsen S (2013) Erythropoiesis: development and differentiation. Cold Spring Harb Perspect Med 3:a011601 . doi: 10.1101/cshperspect.a011601

Ebert BL, Pretz J, Bosco J, Chang CY, Tamayo P, Galili N, Raza A, Root DE, Attar E, Ellis SR, Golub TR (2008) Identification of RPS14 as a 5q- syndrome gene by RNA interference screen. Nature 451:335–9 . doi: 10.1038/nature06494

Eidenschink Brodersen L, Menssen AJ, Wangen JR, Stephenson CF, de Baca ME, Zehentner BK, Wells DA, Loken MR (2015) Assessment of erythroid dysplasia by “Difference from normal” in routine clinical flow cytometry workup. Cytom Part B Clin Cytom 88:125–135 . doi: 10.1002/cyto.b.21199

Erdem-Eraslan L, Gao Y, Kloosterhof NK, Atlasi Y, Demmers J, Sacchetti A, Kros JM, Sillevis Smitt P, Aerts J, French PJ (2015) Mutation specific functions of EGFR result in a mutation-specific downstream pathway activation. Eur J Cancer 51:893–903 . doi: 10.1016/j.ejca.2015.02.006

Figueroa ME, Skrabanek L, Li Y, Jiemjit A, Fandy TE, Paietta E, Fernandez H, Tallman

MS, Greally JM, Carraway H, Licht JD, Gore SD, Melnick A (2009) MDS and secondary AML display unique patterns and abundance of aberrant DNA methylation. Blood 114:3448–58 . doi: 10.1182/blood-2009-01-200519

Franco T, Low PS (2010) Erythrocyte adducin: a structural regulator of the red blood cell membrane. Transfus Clin Biol 17:87–94 . doi: 10.1016/j.tracli.2010.05.008

Fujisaki H, Takai K, Akihisa S, Tokimasa S, Matsuda Y, Ohta H, Osugi Y, Kim JY, Hosoi G, Sako M, Hara J (2002) Establishment of a monosomy 7 leukemia cell line, MONO-7, with a ras gene mutation. Int J Hematol 75:72–7

Garcia-Manero G ANNUAL CLINICAL UPDATES IN HEMATOLOGICAL MALIGNANCIES: A CONTINUING MEDICAL EDUCATION SERIES Myelodysplastic syndromes: 2011 update on diagnosis, risk-stratification, and management. doi: 10.1002/ajh.22047

Goldberg SL, Mody-Patel N, Chen ER (2008) Clinical and Economic Consequences of Myelodysplastic Syndromes in the United States: An Analysis of the Medicare Database. Blood 112:

Gur-Cohen S, Itkin T, Chakrabarty S, Graf C, Kollet O, Ludin A, Golan K, Kalinkovich A, Ledergor G, Wong E, Niemeyer E, Porat Z, Erez A, Sagi I, Esmon CT, Ruf W, Lapidot T (2015) PAR1 signaling regulates the retention and recruitment of EPCR-expressing bone marrow hematopoietic stem cells. Nat Med 21:1307–1317 . doi: 10.1038/nm.3960

Harder KW, Quilici C, Naik E, Inglese M, Kountouri N, Turner A, Zlatic K, Tarlinton DM, Hibbs ML (2004) Perturbed myelo/erythropoiesis in Lyn-deficient mice is similar to that in mice lacking the inhibitory phosphatases SHP-1 and SHIP-1. Blood 104:3901–10 . doi: 10.1182/blood-2003-12-4396

Hasegawa H, Kiyokawa E, Tanaka S, Nagashima K, Gotoh N, Shibuya M, Kurata T, Matsuda M (1996) DOCK180, a major CRK-binding protein, alters cell morphology upon translocation to the cell membrane. Mol Cell Biol 16:1770–6

Hattangadi SM, Wong P, Zhang L, Flygare J, Lodish HF (2011) From stem cell to red cell: regulation of erythropoiesis at multiple levels by multiple proteins, RNAs, and chromatin modifications. Blood 118:6258–6268 . doi: 10.1182/blood-2011-07-356006

Heaney ML, Golde DW (1999) Myelodysplasia. N Engl J Med 340:1649–60 . doi: 10.1056/NEJM199905273402107

Higgins JM (2015) Red blood cell population dynamics. Clin Lab Med 35:43–57 . doi: 10.1016/j.cll.2014.10.002

Hiramoto K, Negishi M, Katoh H (2006) Dock4 is regulated by RhoG and promotes Rac-dependent cell migration. Exp Cell Res 312:4205–4216 . doi: 10.1016/j.yexcr.2006.09.006

Ichikawa M, Yoshimi A, Nakagawa M, Nishimoto N, Watanabe-Okochi N, Kurokawa M (2013) A role for RUNX1 in hematopoiesis and myeloid leukemia. Int J Hematol 97:726–734 . doi: 10.1007/s12185-013-1347-3

Inaba T, Honda H, Matsui H (2018) The enigma of monosomy 7. Blood 131:2891–2898 . doi: 10.1182/blood-2017-12-822262

Invernizzi R, Quaglia F, Porta MG Della (2015) Importance of classical morphology in the diagnosis of myelodysplastic syndrome. Mediterr J Hematol Infect Dis 7:e2015035 . doi: 10.4084/MJHID.2015.035

Jagannathan-Bogdan M, Zon LI (2013) Hematopoiesis. Development 140:2463–7 . doi: 10.1242/dev.083147

Jeong JJ, Gu X, Nie J, Sundaravel S, Liu H, Kuo W-L, Bhagat TD, Pradhan K, Cao J, Nischal S, McGraw KL, Bhattacharyya S, Bishop MR, Artz A, Thirman MJ, Moliterno A, Ji P, Levine RL, Godley LA, Steidl U, Bieker J, List AF, Sauntharajah Y, He C, Verma A, Wickrema A (2019) Cytokine regulated phosphorylation and activation of TET2 by JAK2 in hematopoiesis. Cancer Discov CD-18-1138 . doi: 10.1158/2159-8290.CD-18-1138

Ji P, Jayapal SR, Lodish HF (2008) Enucleation of cultured mouse fetal erythroblasts requires Rac GTPases and mDia2. Nat Cell Biol 10:314–21 . doi: 10.1038/ncb1693

Jiang L, Han X, Wang J, Wang C, Sun X, Xie J, Wu G, Phan H, Liu Z, Zhang C, Zhao M, Kang X, Kang X (2018) SHP-1 regulates hematopoietic stem cell quiescence by coordinating TGF-β signaling. J Exp Med 215:1337–1347 . doi: 10.1084/jem.20171477

Kalfa TA, Pushkaran S, Mohandas N, Hartwig JH, Fowler VM, Johnson JF, Joiner CH, Williams DA, Zheng Y (2006) Rac GTPases regulate the morphology and deformability of the erythrocyte cytoskeleton. Blood 108:3637–45 . doi: 10.1182/blood-2006-03-005942

Kang J-A, Zhou Y, Weis TL, Liu H, Ulaszek J, Satgurunathan N, Zhou L, van Besien K, Crispino J, Verma A, Low PS, Wickrema A (2008) Osteopontin regulates actin cytoskeleton and contributes to cell proliferation in primary erythroblasts. J Biol Chem 283:6997–7006 . doi: 10.1074/jbc.M706712200

Kawada K, Upadhyay G, Ferandon S, Janarthanan S, Hall M, Vilardaga J-P, Yajnik V (2009) Cell migration is regulated by platelet-derived growth factor receptor endocytosis. Mol Cell Biol 29:4508–18 . doi: 10.1128/MCB.00015-09

Kennedy JA, Ebert BL (2017) JOURNAL OF CLINICAL ONCOLOGY Clinical Implications of Genetic Mutations in Myelodysplastic Syndrome. doi: 10.1200/JCO.2016.71.0806

Kimmel CB, Ballard WW, Kimmel SR, Ullmann B, Schilling TF (1995) Stages of embryonic development of the zebrafish. Dev Dyn 203:253–310 . doi: 10.1002/aja.1002030302

Kjeldsen E, Veigaard C (2013) DOCK4 deletion at 7q31.1 in a de novo acute myeloid leukemia with a normal karyotype. Cell Oncol 36:395–403 . doi: 10.1007/s13402-013-0145-5

Knapp DJHF, Hammond CA, Aghaeepour N, Miller PH, Pellacani D, Beer PA, Sachs K, Qiao W, Wang W, Humphries RK, Sauvageau G, Zandstra PW, Bendall SC, Nolan GP, Hansen C, Eaves CJ (2017) Distinct signaling programs control human hematopoietic stem cell survival and proliferation. doi: 10.1182/blood

Konstantinidis DG, Pushkaran S, Johnson JF, Cancelas JA, Manganaris S, Harris CE, Williams DA, Zheng Y, Kalfa TA (2012) Signaling and cytoskeletal requirements in erythroblast enucleation. Blood 119:6118–27 . doi: 10.1182/blood-2011-09-379263

Kotini AG, Chang C-J, Boussaad I, Delrow JJ, Dolezal EK, Nagulapally AB, Perna F, Fishbein GA, Klimek VM, Hawkins RD, Huangfu D, Murry CE, Graubert T, Nimer SD, Papapetrou EP (2015) Functional analysis of a chromosomal deletion associated with myelodysplastic syndromes using isogenic human induced pluripotent stem cells. Nat

Biotechnol 33:646–55 . doi: 10.1038/nbt.3178

Kuhlman PA, Hughes CA, Bennett V, Fowler VM (1996) A new function for adducin. Calcium/calmodulin-regulated capping of the barbed ends of actin filaments. J Biol Chem 271:7986–91

Kuhrt D, Wojchowski DM (2015) Emerging EPO and EPO receptor regulators and signal transducers. Blood 125:3536–41 . doi: 10.1182/blood-2014-11-575357

Kundu S, Fan K, Cao M, Lindner DJ, Zhao ZJ, Borden E, Yi T (2010) Novel SHP-1 Inhibitors Tyrosine Phosphatase Inhibitor-1 and Analogs with Preclinical Anti-Tumor Activities as Tolerated Oral Agents. J Immunol 184:6529–6536 . doi: 10.4049/jimmunol.0903562

Laurin M, Côté J-F (2014) Insights into the biological functions of Dock family guanine nucleotide exchange factors. Genes Dev 28:533–47 . doi: 10.1101/gad.236349.113

Li W, Ren Y, Si Y, Wang F, Yu J (2018) Long non-coding RNAs in hematopoietic regulation. Cell Regen 7:27–32 . doi: 10.1016/J.CR.2018.08.001

Liu Y, Kruhlak MJ, Hao J-J, Shaw S (2007) Rapid T cell receptor-mediated SHP-1 S591 phosphorylation regulates SHP-1 cellular localization and phosphatase activity. J Leukoc Biol 82:742–751 . doi: 10.1189/jlb.1206736

Lodish H, Flygare J, Chou S (2010) From stem cell to erythroblast: regulation of red cell production at multiple levels by multiple hormones. IUBMB Life 62:492–6 . doi: 10.1002/iub.322

Madzo J, Liu H, Rodriguez A, Vasanthakumar A, Sundaravel S, Caces DBD, Looney TJ, Zhang L, Lepore JB, Macrae T, Duszynski R, Shih AH, Song C-X, Yu M, Yu Y, Grossman R, Raumann B, Verma A, He C, Levine RL, Lavelle D, Lahn BT, Wickrema A, Godley LA (2014) Hydroxymethylation at Gene Regulatory Regions Directs Stem/Early Progenitor Cell Commitment during Erythropoiesis. Cell Rep 6:231–44 . doi: 10.1016/j.celrep.2013.11.044

Makipour S, Kanapuru B, Ershler WB (2008) Unexplained anemia in the elderly. Semin Hematol 45:250–4 . doi: 10.1053/j.seminhematol.2008.06.003

Malcovati L, Germing U, Kuendgen A, Della Porta MG, Pascutto C, Invernizzi R, Giagounidis A, Hildebrandt B, Bernasconi P, Knipp S, Strupp C, Lazzarino M, Aul C, Cazzola M (2007) Time-dependent prognostic scoring system for predicting survival and leukemic evolution in myelodysplastic syndromes. J Clin Oncol 25:3503–10 . doi: 10.1200/JCO.2006.08.5696

Matsuoka Y, Hughes CA, Bennett V (1996) Adducin regulation. Definition of the calmodulin-binding domain and sites of phosphorylation by protein kinases A and C. J Biol Chem 271:25157–66

Matsuoka Y, Li X, Bennett V (1998) Adducin is an in vivo substrate for protein kinase C: phosphorylation in the MARCKS-related domain inhibits activity in promoting spectrin-actin complexes and occurs in many cells, including dendritic spines of neurons. J Cell Biol 142:485–97

McGrath KE, Bushnell TP, Palis J (2008) Multispectral imaging of hematopoietic cells: where flow meets morphology. J Immunol Methods 336:91–7 . doi: 10.1016/j.jim.2008.04.012

McNerney ME, Brown CD, Wang X, Bartom ET, Karmakar S, Bandlamudi C, Yu S, Ko J, Sandall BP, Stricker T, Anastasi J, Grossman RL, Cunningham JM, Le Beau MM, White KP (2013) CUX1 is a haploinsufficient tumor suppressor gene on chromosome 7 frequently inactivated in acute myeloid leukemia. Blood 121:975–83 . doi: 10.1182/blood-2012-04-426965

McNerney ME, Godley LA, Le Beau MM (2017) Therapy-related myeloid neoplasms: when genetics and environment collide. Nat Rev Cancer 17:513–527 . doi: 10.1038/nrc.2017.60

Millington M, Arndt A, Boyd M, Applegate T, Shen S (2009) Towards a clinically relevant lentiviral transduction protocol for primary human CD34 hematopoietic stem/progenitor cells. PLoS One 4:e6461 . doi: 10.1371/journal.pone.0006461

Mkaddem S Ben, Murua A, Flament H, Titeca-Beauport D, Bounaix C, Danelli L, Launay P, Benhamou M, Blank U, Daugas E, Charles N, Monteiro RC (2017) Lyn and Fyn function as molecular switches that control immunoreceptors to direct homeostasis or inflammation. Nat Commun 8:246 . doi: 10.1038/s41467-017-00294-0

Moran-Crusio K, Reavie L, Shih A, Abdel-Wahab O, Ndiaye-Lobry D, Lobry C, Figueroa

ME, Vasanthakumar A, Patel J, Zhao X, Perna F, Pandey S, Madzo J, Song C, Dai Q, He C, Ibrahim S, Beran M, Zavadil J, Nimer SD, Melnick A, Godley LA, Aifantis I, Levine RL (2011) Tet2 Loss Leads to Increased Hematopoietic Stem Cell Self-Renewal and Myeloid Transformation. Cancer Cell 20:11–24 . doi: 10.1016/j.ccr.2011.06.001

Morrison SJ, Scadden DT (2014) The bone marrow niche for haematopoietic stem cells. Nature 505:327–334 . doi: 10.1038/nature12984

Nagase R, Inoue D, Pastore A, Fujino T, Hou H-A, Yamasaki N, Goyama S, Saika M, Kanai A, Sera Y, Horikawa S, Ota Y, Asada S, Hayashi Y, Kawabata KC, Takeda R, Tien H-F, Honda H, Abdel-Wahab O, Kitamura T (2018) Expression of mutant Asxl1 perturbs hematopoiesis and promotes susceptibility to leukemic transformation. J Exp Med 215:1729–1747 . doi: 10.1084/jem.20171151

Nakata Y, Tomkowicz B, Gewirtz AM, Ptasznik A (2006) Integrin inhibition through Lyn-dependent cross talk from CXCR4 chemokine receptors in normal human CD34 marrow cells. doi: 10.1182/blood-2005-08-3343

Ng AP, Alexander WS (2017) Haematopoietic stem cells: past, present and future. Cell Death Discov 3:17002 . doi: 10.1038/cddiscovery.2017.2

Nolan KM, Barrett K, Lu Y, Hu KQ, Vincent S, Settleman J (1998) Myoblast city, the Drosophila homolog of DOCK180/CED-5, is required in a Rac signaling pathway utilized for multiple developmental processes. Genes Dev 12:3337–42

O'Laughlin-Bunner B, Radosevic N, Taylor ML, Shivakrupa, DeBerry C, Metcalfe DD, Zhou M, Lowell C, Linnekin D (2001) Lyn is required for normal stem cell factor-induced proliferation and chemotaxis of primary hematopoietic cells. Blood 98:343–50

Obeng EA, Chappell RJ, Seiler M, Wu CJ, Fleming MD, Ebert BL (2016) Physiologic Expression of Sf3b1 K700E Causes Impaired Erythropoiesis, Aberrant Splicing, and Sensitivity to Therapeutic Spliceosome Modulation. doi: 10.1016/j.ccell.2016.08.006

Orkin SH, Zon LI (2008) Hematopoiesis: an evolving paradigm for stem cell biology. Cell 132:631–44 . doi: 10.1016/j.cell.2008.01.025

Orschell CM, Borneo J, Munugalavadla V, Ma P, Sims E, Ramdas B, Yoder MC, Kapur R (2008) Deficiency of Src family kinases compromises the repopulating ability of

hematopoietic stem cells. Exp Hematol 36:655–666 . doi: 10.1016/J.EXPHEM.2008.01.002

Pauls SD, Ray A, Hou S, Vaughan AT, Cragg MS, Marshall AJ (2016) FcγRIIB-Independent Mechanisms Controlling Membrane Localization of the Inhibitory Phosphatase SHIP in Human B Cells. J Immunol 197:1587–1596 . doi: 10.4049/jimmunol.1600105

Pellagatti A, Cazzola M, Giagounidis A, Perry J, Malcovati L, Della Porta MG, Jädersten M, Killick S, Verma A, Norbury CJ, Hellström-Lindberg E, Wainscoat JS, Boultwood J (2010) Deregulated gene expression pathways in myelodysplastic syndrome hematopoietic stem cells. Leukemia 24:756–64 . doi: 10.1038/leu.2010.31

Polo JM, Liu S, Figueroa ME, Kulalert W, Eminli S, Tan KY, Apostolou E, Stadtfeld M, Li Y, Shioda T, Natesan S, Wagers AJ, Melnick A, Evans T, Hochedlinger K (2010) Cell type of origin influences the molecular and functional properties of mouse induced pluripotent stem cells. Nat Biotechnol 28:848–855 . doi: 10.1038/nbt.1667

Prebet T, Lhoumeau A-C, Arnoulet C, Aulas A, Marchetto S, phane Audebert S, Puppo F, Chabannon C, Sainty D, Santoni M-J, Sebbagh M, Summerour V, Huon Y, Shin W-S, Lee S-T, Esterni B, Vey N, Borg J-P (2010) The cell polarity PTK7 receptor acts as a modulator of the chemotherapeutic response in acute myeloid leukemia and impairs clinical outcome. doi: 10.1182/blood-2010-01-262352

Röselová P, Obr A, Holoubek A, Grebeňová D, Kuželová K (2018) Adhesion structures in leukemia cells and their regulation by Src family kinases. Cell Adh Migr 12:286–298 . doi: 10.1080/19336918.2017.1344796

Seita J, Weissman IL (2010) Hematopoietic stem cell: self-renewal versus differentiation. Wiley Interdiscip Rev Syst Biol Med 2:640–53 . doi: 10.1002/wsbm.86

Sekeres MA, Gerds AT (2014) Established and novel agents for myelodysplastic syndromes. Hematology Am Soc Hematol Educ Program 2014:82–9 . doi: 10.1182/asheducation-2014.1.82

Sharlow ER, Pacifici R, Crouse J, Batac J, Todokoro K, Wojchowski DM (1997) Hematopoietic cell phosphatase negatively regulates erythropoietin-induced hemoglobinization in erythroleukemic SKT6 cells. Blood 90:2175–87

Shastri A, Will B, Steidl U, Verma A (2017) Stem and progenitor cell alterations in myelodysplastic syndromes. Blood 129:1586–1594 . doi: 10.1182/blood-2016-10-696062

Song Y, Rongvaux A, Taylor A, Jiang T, Tebaldi T, Balasubramanian K, Bagale A, Terzi YK, Gbyli R, Wang X, Fu X, Gao Y, Zhao J, Podoltsev N, Xu M, Neparidze N, Wong E, Torres R, Bruscia EM, Kluger Y, Manz MG, Flavell RA, Halene S (2019) A highly efficient and faithful MDS patient-derived xenotransplantation model for pre-clinical studies. Nat Commun 10:366 . doi: 10.1038/s41467-018-08166-x

Sundaravel S, Duggan R, Bhagat T, Ebenezer DL, Liu H, Yu Y, Bartenstein M, Unnikrishnan M, Karmakar S, Liu T-C, Torregroza I, Quenon T, Anastasi J, McGraw KL, Pellagatti A, Boultwood J, Yajnik V, Artz A, Le Beau MM, Steidl U, List AF, Evans T, Verma A, Wickrema A (2015) Reduced DOCK4 expression leads to erythroid dysplasia in myelodysplastic syndromes. Proc Natl Acad Sci U S A 112:E6359-68 . doi: 10.1073/pnas.1516394112

Traver D, Paw BH, Poss KD, Penberthy WT, Lin S, Zon LI (2003) Transplantation and in vivo imaging of multilineage engraftment in zebrafish bloodless mutants. Nat Immunol 4:1238–46 . doi: 10.1038/ni1007

Uddin S, Ah-Kang J, Ulaszek J, Mahmud D, Wickrema A (2004) Differentiation stage-specific activation of p38 mitogen-activated protein kinase isoforms in primary human erythroid cells. Proc Natl Acad Sci U S A 101:147–52 . doi: 10.1073/pnas.0307075101

Upadhyay G, Goessling W, North TE, Xavier R, Zon LI, Yajnik V (2008) Molecular association between beta-catenin degradation complex and Rac guanine exchange factor DOCK4 is essential for Wnt/beta-catenin signaling. Oncogene 27:5845–55 . doi: 10.1038/onc.2008.202

van de Water B, Tijdens IB, Verbrugge A, Huigsloot M, Dihal AA, Stevens JL, Jaken S, Mulder GJ (2000) Cleavage of the actin-capping protein alpha -adducin at Asp-Asp-Ser-Asp633-Ala by caspase-3 is preceded by its phosphorylation on serine 726 in cisplatin-induced apoptosis of renal epithelial cells. J Biol Chem 275:25805–13 . doi: 10.1074/jbc.M001680200

van Galen P, Kreso A, Mbong N, Kent DG, Fitzmaurice T, Chambers JE, Xie S, Laurenti E, Hermans K, Eppert K, Marciniak SJ, Goodall JC, Green AR, Wouters BG, Wienholds E, Dick JE (2014) The unfolded protein response governs integrity of the haematopoietic stem-cell pool during stress. Nature 510:268–272 . doi:

10.1038/nature13228

Westers TM, Cremers EMP, Oelschlaegel U, Johansson U, Bettelheim P, Matarraz S, Orfao A, Moshaver B, Brodersen LE, Loken MR, Wells DA, Subirá D, Cullen M, Te Marvelde JG, van der Velden VHJ, Preijers FWMB, Chu S-C, Feuillard J, Guérin E, Psarra K, Porwit A, Saft L, Ireland R, Milne T, Béné MC, Witte BI, Della Porta MG, Kern W, van de Loosdrecht AA, IMDSFlow Working Group (2017) Immunophenotypic analysis of erythroid dysplasia in myelodysplastic syndromes. A report from the IMDSFlow working group. Haematologica 102:308–319 . doi: 10.3324/haematol.2016.147835

Wheeler SE, Morariu EM, Bednash JS, Otte CG, Seethala RR, Chiosea SI, Grandis JR (2012) Lyn Kinase Mediates Cell Motility and Tumor Growth in EGFRvIII-Expressing Head and Neck Cancer. Clin Cancer Res 18:2850–2860 . doi: 10.1158/1078-0432.CCR-11-2486

Wickrema A, Chen F, Namin F, Yi T, Ahmad S, Uddin S, Chen YH, Feldman L, Stock W, Hoffman R, Platanias LC (1999a) Defective expression of the SHP-1 phosphatase in polycythemia vera. Exp Hematol 27:1124–32

Wickrema A, Crispino JD (2007) Erythroid and megakaryocytic transformation. Oncogene 26:6803–6815 . doi: 10.1038/sj.onc.1210763

Wickrema A, Kee B (eds) (2009) Molecular Basis of Hematopoiesis. Springer New York, New York, NY

Wickrema A, Koury ST, Dai CH, Krantz SB (1994) Changes in cytoskeletal proteins and their mRNAs during maturation of human erythroid progenitor cells. J Cell Physiol 160:417–26 . doi: 10.1002/jcp.1041600304

Wickrema A, Krantz SB, Winkelmann JC, Bondurant MC (1992) Differentiation and erythropoietin receptor gene expression in human erythroid progenitor cells. Blood 80:1940–9

Wickrema A, Uddin S, Sharma A, Chen F, Alsayed Y, Ahmad S, Sawyer ST, Krystal G, Yi T, Nishada K, Hibi M, Hirano T, Platanias LC (1999b) Engagement of Gab1 and Gab2 in erythropoietin signaling. J Biol Chem 274:24469–74 . doi: 10.1074/JBC.274.35.24469

Will B, Zhou L, Vogler TO, Ben-Neriah S, Schinke C, Tamari R, Yu Y, Bhagat TD, Bhattacharyya S, Barreyro L, Heuck C, Mo Y, Parekh S, McMahon C, Pellagatti A, Boultwood J, Montagna C, Silverman L, Maciejewski J, Greally JM, Ye BH, List AF, Steidl C, Steidl U, Verma A (2012) Stem and progenitor cells in myelodysplastic syndromes show aberrant stage-specific expansion and harbor genetic and epigenetic alterations. Blood 120:2076–86 . doi: 10.1182/blood-2011-12-399683

Wu YC, Horvitz HR (1998) C. elegans phagocytosis and cell-migration protein CED-5 is similar to human DOCK180. Nature 392:501–4 . doi: 10.1038/33163

Yajnik V, Paulding C, Sordella R, McClatchey AI, Saito M, Wahrer DCR, Reynolds P, Bell DW, Lake R, van den Heuvel S, Settleman J, Haber DA (2003) DOCK4, a GTPase activator, is disrupted during tumorigenesis. Cell 112:673–84

Yoo SK, Starnes TW, Deng Q, Huttenlocher A (2011) Lyn is a redox sensor that mediates leukocyte wound attraction in vivo. Nature 480:109–112 . doi: 10.1038/nature10632

Yoshimura A, Arai K (1996) Physician Education: The Erythropoietin Receptor and Signal Transduction. Oncologist 1:337–339

Yu J-R, Tai Y, Jin Y, Hammell MC, Wilkinson JE, Roe J-S, Vakoc CR, Van Aelst L (2015) TGF-β/Smad signaling through DOCK4 facilitates lung adenocarcinoma metastasis. Genes Dev 29:250–261 . doi: 10.1101/gad.248963.114

Yu Y, Mo Y, Ebenezer D, Bhattacharyya S, Liu H, Sundaravel S, Giricz O, Wontakal S, Cartier J, Caces B, Artz A, Nischal S, Bhagat T, Bathon K, Maqbool S, Gligich O, Suzuki M, Steidl U, Godley L, Skoultchi A, Greally J, Wickrema A, Verma A (2013) High resolution methylome analysis reveals widespread functional hypomethylation during adult human erythropoiesis. J Biol Chem 288:8805–14 . doi: 10.1074/jbc.M112.423756

Yue X-S, Hummon AB (2013) Combination of Multistep IMAC Enrichment with High-pH Reverse Phase Separation for In-Depth Phosphoproteomic Profiling. J Proteome Res 12:4176–4186 . doi: 10.1021/pr4005234

Zhang CC, Lodish HF (2008) Cytokines regulating hematopoietic stem cell function. Curr Opin Hematol 15:307–11 . doi: 10.1097/MOH.0b013e3283007db5

Zhang L, Sankaran VG, Lodish HF (2012) MicroRNAs in erythroid and megakaryocytic differentiation and megakaryocyte–erythroid progenitor lineage commitment. Leukemia 26:2310–2316 . doi: 10.1038/leu.2012.137

Zhang X, Hu W (2016) Long noncoding RNAs in hematopoiesis. F1000Research 5: . doi: 10.12688/f1000research.8349.1

Zhao G, Yu D, Weiss MJ (2010) MicroRNAs in erythropoiesis. Curr Opin Hematol 17:1 . doi: 10.1097/MOH.0b013e328337ba6c

Zhou L, McMahon C, Bhagat T, Alencar C, Yu Y, Fazzari M, Sohal D, Heuck C, Gundabolu K, Ng C, Mo Y, Shen W, Wickrema A, Kong G, Friedman E, Sokol L, Mantzaris G, Pellagatti A, Boultwood J, Platanias LC, Steidl U, Yan L, Yingling JM, Lahn MM, List A, Bitzer M, Verma A, Verma A (2011a) Reduced SMAD7 Leads to Overactivation of TGF- Signaling in MDS that Can Be Reversed by a Specific Inhibitor of TGF- Receptor I Kinase. Cancer Res 71:955–963 . doi: 10.1158/0008-5472.CAN-10-2933

Zhou L, Nguyen AN, Sohal D, Ying Ma J, Pahanish P, Gundabolu K, Hayman J, Chubak A, Mo Y, Bhagat TD, Das B, Kapoun AM, Navas TA, Parmar S, Kambhampati S, Pellagatti A, Braunchweig I, Zhang Y, Wickrema A, Medicherla S, Boultwood J, Platanias LC, Higgins LS, List AF, Bitzer M, Verma A (2008) Inhibition of the TGF- receptor I kinase promotes hematopoiesis in MDS. Blood 112:3434–3443 . doi: 10.1182/blood-2008-02-139824

Zhou L, Opalinska J, Sohal D, Yu Y, Mo Y, Bhagat T, Abdel-Wahab O, Fazzari M, Figueroa M, Alencar C, Zhang J, Kambhampati S, Parmar S, Nischal S, Hueck C, Suzuki M, Freidman E, Pellagatti A, Boultwood J, Steidl U, Sautharajah Y, Yajnik V, McMahon C, Gore SD, Platanias LC, Levine R, Melnick A, Wickrema A, Greally JM, Verma A (2011b) Aberrant epigenetic and genetic marks are seen in myelodysplastic leukocytes and reveal Dock4 as a candidate pathogenic gene on chromosome 7q. J Biol Chem 286:25211–23 . doi: 10.1074/jbc.M111.235028

Zhu J, Emerson SG (2002) Hematopoietic cytokines, transcription factors and lineage commitment. Oncogene 21:3295–3313 . doi: 10.1038/sj.onc.1205318

Zini G (2017) Diagnostics and Prognostication of Myelodysplastic Syndromes. Ann Lab Med 37:465–474 . doi: 10.3343/alm.2017.37.6.465

Zon LI (2008) Intrinsic and extrinsic control of haematopoietic stem-cell self-renewal. Nature 453:306–313 . doi: 10.1038/nature07038

Zuba-Surma EK, Kucia M, Abdel-Latif A, Lillard JW, Ratajczak MZ (2007) The ImageStream System: a key step to a new era in imaging. Folia Histochem Cytobiol 45:279–90

Zuba-Surma EK, Ratajczak MZ (2011) Analytical Capabilities of the ImageStream Cytometer. In: Methods in cell biology. pp 207–230